

PSEUDO-ANOSOV MAPS AND GENUS-TWO L-SPACE KNOTS

Braeden Reinoso

A dissertation submitted to the Faculty of the
Department of Mathematics in partial fulfillment of the
requirements for the degree of Doctor of Philosophy

Boston College
Morrissey College of Arts and Sciences
Graduate School

March, 2024

Pseudo-Anosov maps and genus-two L-space knots

Braeden Reinoso

Advisor: John A. Baldwin, Ph.D.

We classify genus-two L-space knots in S^3 and the Poincaré homology sphere. This leads to the first and to-date only detection results in knot Floer homology for knots of genus greater than one. Our proofs interweave Floer-homological properties of L-space knots, the geometry of pseudo-Anosov maps, and the theory of train tracks and folding automata for braids. The crux of our argument is a complete classification of fixed-point-free pseudo-Anosov maps in all but one stratum on the genus-two surface with one boundary component. To facilitate our classification, we exhibit a small family of train tracks carrying all pseudo-Anosov maps in most strata on the marked disk. As a consequence of our proof technique, we almost completely classify genus-two, hyperbolic, fibered knots with knot Floer homology of rank 1 in their next-to-top grading in any 3-manifold. Several corollaries follow, regarding the Floer homology of cyclic branched covers, $SU(2)$ -abelian Dehn surgeries, Khovanov and annular Khovanov homology, and instanton Floer homology.

Contents

Contents	i
List of Figures	iii
Acknowledgements	v
1 Introduction	1
1.1 Context	1
1.2 Summary of results	2
1.2.1 Applications to the Floer homology of branched covers	6
1.2.2 Applications to instanton Floer theory	7
1.2.3 Applications to Khovanov homology	7
1.3 Outline	8
1.3.1 Reducing Theorem B into Theorems B1 — B4	9
1.3.2 The case $(6; \emptyset; \emptyset)$	10
1.3.3 The remaining three singularity cases	11
1.3.4 The main idea of Chapter 6	12
2 Background and setup	14
2.1 Pseudo-Anosov maps, three manifolds, fibered knots, and Floer theory	14
2.1.1 Mapping classes, pseudo-Anosovs, and singularity types	15
2.1.2 Fibered knots and fractional Dehn twists	17

2.1.3	Floer theory, and Theorem A from Theorem B	19
2.2	Train tracks and maps, and standard tracks	21
2.2.1	Train tracks carrying mapping classes	21
2.2.2	Real and infinitesimal edges	24
2.2.3	Standard and jointless tracks, and a carrying theorem	25
2.3	Branched covers and lifting train track maps	26
2.3.1	Braids and the Birman–Hilden correspondence	26
2.3.2	Lifting standard tracks, and the trace lemma	28
3	The stratum $(6; \emptyset; \emptyset)$	32
4	The strata $(2; \emptyset; 4^2)$ and $(4; \emptyset; 3^2)$	38
4.1	The stratum $(2; \emptyset; 4^2)$	38
4.2	The stratum $(4; \emptyset; 3^2)$	42
4.2.1	A family of braids lifting to fixed-point-free maps	43
4.2.2	Train track maps on the Peacock	47
5	The stratum $(2; \emptyset; 3^4)$	57
5.1	Analyzing the candidate braids	60
5.2	Setup for the case analysis	62
5.3	Cases B, C, D	66
5.4	Case A	70
6	The tight splitting	74
6.1	Splitting standardly embedded tracks	74
6.2	Switch rigidity	86
6.3	The proofs of Theorems 4.2.1, 1.2.6, and C	90

List of Figures

2.1	Allowable singularities in the invariant foliations of a pseudo-Anosov .	14
2.2	An example illustrating the fractional part of the FDTC	18
2.3	An example fibered neighborhood, and transversality of a train tack map	21
2.4	Examples of standard and jointless train tracks in the stratum $(1; 1^5; 4)$	25
2.5	Lifting a train track and train track map via the hyperelliptic involution	29
2.6	Smoothing infinitesimal polygons near a marked point in a lifted track	30
4.1	The jellyfish track and map notation	39
4.2	Visual aids for the proof of Lemma 4.1.2.	40
4.3	Visual aids for the proof of Lemma 4.1.3.	41
4.4	The two train track classes with no joints in the stratum $(2; 1^5; 3)$. . .	42
4.5	The Peacock track and map notation	43
4.6	The train track map for β_n	44
4.7	Isotopies of $\widehat{\Delta^2\beta_n^{-1}}$ to $P(3, 3 - n, -2)$	46
4.8	An edge absorbed into a vertex	48
4.9	Cases for the proof of Lemma 4.2.7.	49
4.10	Cases for the proof of Lemma 4.2.8.	50
4.11	Cases for the proof of Proposition 4.2.3.	53
5.1	The folding automaton for the stratum $(1; 1^5; 3^2)$ on D_5	58
5.2	The two pairs of jointless tracks in the stratum $(1; 1^5; 3^2)$	59

5.3	The Camel track and notation	60
5.4	The images $\beta_i(\tau)$ before collapsing back onto τ	61
5.5	Visual aids for the proof of Lemma 5.3.1.	64
5.6	Visual aids for the proof of Lemma 5.3.2.	64
5.7	Visual aids for the proof of Lemma 5.3.3.	64
5.8	Visual aids for the proof of Lemma 5.3.4.	64
5.9	Visual aids for the proof of Lemma 5.3.5.	65
5.10	Visual aids for the proof of Lemma 5.4.1	69
5.11	Visual aid for the proof of Lemma 5.4.2.	70
5.12	Visual aids for the proof of Lemma 5.4.3	70
5.13	Visual aids for the proof of Lemma 5.4.4.	70
6.1	An example of an elementary folding map	75
6.2	Tight splitting to the right (r -splitting)	78
6.3	Tight splitting at a monogon	78
6.4	A series of t -splits on an example	83
6.5	A rigid switch	87

Acknowledgments

Thank you to my advisor, John Baldwin, for all of his support and encouragement over the past 5 years, and for introducing me to a new way to see the world. Thank you to all of my friends within and outside of math, especially: Alex, Augie, Caroline, Chris, Clayton, Emily, Ethan, Finn, Jacob, Jee Uhn, Laura, Martha, Nick, Stella, and Tyler. I am so lucky to be surrounded with such insight and joy each day. And thank you, most of all, to my loving family: Mom, Dad, Loren, Nana, Val. What more can I hope for, than to make something beautiful for the people I love?

*Here, what's made, these braids, unmakes
itself in time, and must be made
again, within and against time...
And though what's made does not abide,
my making is steadfast, and, besides, there is a making
of which this making-in-time is just a part,
a making which abides
beyond the hands that rise in the combing,
the hands which fall in the braiding,
trailing hair in each stage of its unbraiding.*

—Li-Young Lee

Chapter 1

Introduction

1.1 Context

Heegaard Floer homology, defined by Ozsváth–Szabó in [OS04d], is a package of algebraic invariants for 3-manifolds and knots/links inside of them. Structural properties of the invariants are often closely related to geometric properties of 3-manifolds and knots/links. For example, Heegaard Floer homology has proven exceptionally useful for understanding Dehn surgery relations between 3-manifolds (see any of [OS04a] [OS04c] [Han23] [NW15] [BS22] [Gre13] [Cau23], among many others).

A 3-manifold with very simple Heegaard Floer homology is called an *L-space*: S^3 , the Poincaré homology sphere \mathcal{P} , and lens spaces are all L-spaces. A knot K which admits a non-trivial surgery to an L-space is called an *L-space knot*: the unknot, torus knots, and the pretzel knot $P(-2, 3, 7)$ are L-space knots in S^3 . The study of L-space knots is intimately related to much recent progress on the Berge conjecture ([Gre13] [Cau23]), the cosmetic surgery conjecture ([Han23] [NW15]), and several other deep conjectures in 3-manifold topology and knot theory.

The geometry of L-space knots in S^3 (or, more generally, integer homology sphere L-spaces, like \mathcal{P}) is known to be tightly constrained. For example, any L-space knot

is fibered and strongly quasipositive, and the coefficients of its Alexander polynomial each lie in the set $\{-1, 0, 1\}$ ([Ni07] [Ghi08] [OS04a] [Hed10] [Tan11]). These properties together immediately lead to a classification of L-space knots in S^3 with Seifert genus at most one: the unknot and the trefoil are the only such knots. However, classification of L-space knots of genus two or more remained elusive for the next decade-and-a-half, or so.

Recent work of Baldwin–Hu–Sivek [BHS21], Ni [Ni22], and Ghiggini–Spano [GS22] connects the structure of the Floer homology of a fibered knot (including all L-space knots) to fixed-point properties of a corresponding surface map (the return map of the fibration of the knot complement). This connection allows us to use tools from surface dynamics to study L-space knots.

When K is a hyperbolic L-space knot, the corresponding surface map is *pseudo-Anosov* (see Chapter 2 for a definition). In this case, we may count fixed points of the map combinatorially, using the construction of *train tracks* originally due to Thurston [Thu88], and later developed by Bestvina–Handel [BH95] and Penner–Harer [PH22], by Ko–Los–Song [KLS02] and Ham–Song [HS07] on the marked disk, and by many others. In other words, we can use structural properties of train tracks and their corresponding maps to prove results about L-space knots. The aim of this thesis is to do just that: we classify genus-two L-space knots in S^3 and \mathcal{P} , obtained by studying train tracks and fixed points of surface maps.

1.2 Summary of results

Here, we include a brief summary of our main results, and some applications. Much of the work in the rest of this document is taken directly from the papers [FRW22] and [Rei23], the first of which represents joint work with Ethan Farber and Luya Wang.

As stated in the previous section, our main goal is to classify L-space knots in genus two. Here is what we will prove:

Theorem A. The torus knot $T(2, 5)$ is the only genus-two L-space knot in S^3 . The order-three Seifert-fiber $\mathcal{K} \subset \mathcal{P}$ (considering \mathcal{P} as a small Seifert-fibered space) and the torus knot $T(2, 5) \subset B^3 \subset \mathcal{P}$ are the only genus-two L-space knots in \mathcal{P} .

As mentioned in the previous section, we prove Theorem A by counting fixed points of surface maps in genus two. The following definition captures the key connection:

Definition 1.2.1. Let K be a hyperbolic, fibered knot in a 3-manifold Y . The fibration of the exterior of K is described by an open book decomposition (S, h) , where S is a compact surface with one boundary component, and $h : S \rightarrow S$ is freely isotopic to a pseudo-Anosov map ψ_h . We say that K is *fixed-point-free* (FPF for short) if ψ_h has no fixed points in the interior of S .

By work of Baldwin–Hu–Sivek [BHS21], Ni [Ni22], and Ghiggini–Spano [GS22], we know that hyperbolic L-space knots are FPF. By work of [Hed10] and [Tan11], we know that L-space knots in S^3 and \mathcal{P} have non-zero fractional Dehn twist coefficient: $c(K) \neq 0$. So, we will show:

Theorem B. Let K be a hyperbolic, genus-two, fibered knot in S^3 or \mathcal{P} . If the fractional Dehn twist coefficient $c(K) \neq 0$, then K is not FPF.

Corollary 1.2.2. There are no genus-two hyperbolic L-space knots in S^3 or \mathcal{P} .

Theorem A follows quickly from Corollary 1.2.2, by examining the geometry of the knot exterior of any candidate genus-two L-space knots. Corollary 1.2.2 in turn follows quickly from Theorem B after applying the relevant Floer-theoretic results. Both of these proofs are carried out in subsection 2.1.3. The proof of Theorem B, on the other hand, is much more involved, and takes up the bulk of this thesis.

In the process of proving Theorem B, we obtain the following classification of *all* FPF maps in genus two, in most strata:

Theorem 1.2.3. Let $h : S \rightarrow S$ be a pseudo-Anosov mapping class on the genus-two surface with one boundary component. If the pseudo-Anosov representative ψ_h has no interior fixed points, then one of the following is true:

- The invariant foliations of ψ_h have 1-pronged or 6-pronged boundary
- h or h^{-1} is conjugate to the lift of $\Delta^{4k+2}\sigma_1^{n+2}\sigma_2\sigma_3\sigma_4\sigma_1\sigma_2\sigma_3\sigma_4^2$ for $n \geq 0, k \in \mathbb{Z}$
- h or h^{-1} is conjugate to the lift of $\Delta^{4k+2}(\sigma_4\sigma_3)^2(\sigma_2\sigma_1)^{-2}$ for $k \in \mathbb{Z}$
- h or h^{-1} is conjugate to the lift of $\Delta^{4k+2}\sigma_1^{-3}\sigma_2^{-1}\sigma_3^{-1}\sigma_2(\sigma_3\sigma_4)^2$ for $k \in \mathbb{Z}$
- h or h^{-1} is conjugate to the lift of $\Delta^{4k+2}(\sigma_4\sigma_3\sigma_1^{-1}\sigma_2^{-1})^2$ for $k \in \mathbb{Z}$

This fixed point classification represents significant progress toward the general “botany problem” of knot Floer homology in genus two, in any 3-manifold. Combining the previous stated results with [Ni20] and some of the work from Chapter 3, we have:

Corollary 1.2.4. Let K be a null-homologous knot of genus-two in a 3-manifold Y . Suppose that the exterior of K is hyperbolic, and denote by S a genus-two Seifert surface for K . If $\text{rk } \widehat{HFK}(K, [S], a) = 1$ for $a = 1, 2$ then K is fibered, and either:

- The invariant foliations of its monodromy have 6-pronged boundary, and the dilatation of its monodromy is a root of $\Delta_K(t) = t^4 - t^3 \pm |H_1(Y)|t^2 - t + 1$
- The monodromy of K is conjugate to one of the maps in Theorem 1.2.3

The same techniques we use in this paper can surely be applied to study the 6-pronged boundary case, to complete the aforementioned botany problem. In the special cases of S^3 and \mathcal{P} , this almost-complete solution to the botany problem can be summarized as a “detection result” for knot Floer homology:

Corollary 1.2.5. Each of the knots in Theorem A is detected by knot Floer homology, in the following sense: if K is one of the knots from Theorem A, and K' is any knot in S^3 or \mathcal{P} with $\widehat{HFK}(K'; \mathbb{Z}/2\mathbb{Z}) \cong \widehat{HFK}(K; \mathbb{Z}/2\mathbb{Z})$, then in fact $K' = K$.

One of the central tools in the proof of Theorem B is the theory of train tracks for pseudo-Anosov braids, including a theory of *tight splitting* developed in Chapter 6. Roughly, we find canonical train tracks that carry all pseudo-Anosovs with certain singularity data, which allows us to simplify our fixed point analysis significantly. We believe these techniques are broadly applicable elsewhere in the study of surface dynamics. For example:

Theorem 1.2.6 (cf. Theorem 4.2.1). Let ψ be a pseudo-Anosov map with singularity type $(4; \emptyset; 3^2)$ (see Chapter 2 for singularity type conventions). Then, ψ is conjugate to a map carried by the lift of the Peacock train track depicted on the left in Figure 4.4. A similar statement holds for the closed genus-two surface.

Theorem 1.2.6 follows from a special case of a more general theorem regarding train tracks for pseudo-Anosov maps on the marked disk:

Theorem C. Let ψ be a pseudo-Anosov on the marked disk. Assume that the invariant foliations of ψ have at least one k -pronged singularity away from the boundary with $k \geq 2$. Then, ψ is carried by a standard train track τ with no joints (see Section 2.2 for the definitions of standard tracks and joints).

Indeed, we use Theorem C to show that, in each of the strata $(2; 1^5; 3)$, $(1; 1^5; 4)$, and $(1; 1^5; 3^2)$ on the 5-marked disk, all pseudo-Anosovs in that stratum are carried by a single train track. Theorem 1.2.6 then follows by applying Theorem C to the stratum $(2; 1^5; 3)$, and briefly considering the geometry of the singularities under the Birman–Hilden correspondence in that case. See the end of Chapter 6 for more details.

Finally, it is worth mentioning the following very pleasing result, which follows from combining Theorem C with unreleased work of Farber–Winsor (which itself is

an application of the techniques of Chapter 6):

Theorem 1.2.7. Any pseudo-Anosov on the n -marked disk with singularity type $(n-2; 1^n; \emptyset)$ is conjugate to a map carried by a standard “interval-like” train track (i.e. a track where each vertex of a punctured monogon has valence two). In particular, any pseudo-Anosov on the punctured disk is conjugate to a map carried either by a standard track with no joints, or by an interval-like track; and which type of track is governed only by the singularity type of the map.

This carrying result could be used in tandem with the techniques of Chapters 4.2 and 5 to finish the 6-pronged boundary case of Theorem 1.2.3, obtaining a complete classification of FPF maps in genus two with non-zero fractional Dehn twist coefficient. This would complete the botany problem described in Corollary 1.2.4.

1.2.1 Applications to the Floer homology of branched covers

For a knot $K \subset S^3$, let $\Sigma_n(K)$ denote the n -fold cyclic cover of S^3 branched along K . There has been much interest recently in the Floer homology of $\Sigma_n(K)$ in terms of K . For example, Boileau–Boyer–Gordon have studied extensively in [BBG19a] and [BBG19b] the set of all integers $n \geq 2$ such that $\Sigma_n(K)$ is an L-space (see also e.g. [IT20] and [Pet09]). One question that has persisted in this area is the following:

Question 1.2.8 (Boileau–Boyer–Gordon, Moore). Can $\Sigma_n(K)$ be an L-space for K a hyperbolic L-space knot?

Combining Theorem A with ([BBG19a], Corollary 1.4) yields the following complete answer to this question for $n > 2$:

Corollary 1.2.9. If K is an L-space knot and $\Sigma_n(K)$ is an L-space for some $n > 2$, then K is either $T(2, 3)$ or $T(2, 5)$. In particular, K is not hyperbolic.

1.2.2 Applications to instanton Floer theory

For a 3-manifold Y , let $R(Y) = \text{Hom}(\pi_1(Y), SU(2))$ denote the $SU(2)$ -representation variety. We say that a 3-manifold Y is $SU(2)$ -abelian if $R(Y)$ contains no irreducibles. The name is motivated by the fact that Y is $SU(2)$ -abelian if and only if every $\rho \in R(Y)$ has abelian image.

Following work initiated by Kronheimer–Mrowka in their proof of the Property P conjecture [KM10], Baldwin–Li–Sivek–Ye [BLSY21], Baldwin–Sivek [BS21], and Kronheimer–Mrowka [KM] proved that r -surgery $S_r^3(K)$ on a nontrivial knot $K \subset S^3$ is not $SU(2)$ -abelian for all slopes $r \in [0, 3] \cup [4, 5)$ with prime power numerator, and for some additional slopes $r \in [3, 4)$.

The key theory which facilitates most of these results is the instanton Floer homology of the surgered manifold $S_r^3(K)$ (and related techniques arising from this theory, as in [KM]). Combining Theorem B with ([BLSY21], Proposition 2.4) allows us to prove an analogue of Theorem A for instanton Floer homology:

Corollary 1.2.10. The torus knot $T(2, 5)$ is the only genus-two instanton L-space knot in S^3 , i.e. the only genus-two knot $K \subset S^3$ for which $\dim I^\#(S_r^3(K)) = |H_1(S_r^3(K))|$ for some $r > 0$.

Now, as described in ([BLSY21], Section 1.3), Corollary 1.2.10 completes the set of slopes r for which $S_r^3(K)$ is not $SU(2)$ -abelian, to all rational numbers $r \in [0, 5)$ with prime power numerator:

Corollary 1.2.11. Let $K \subset S^3$ be a nontrivial knot, and $r \in [0, 5)$ a rational number with prime power numerator. Then, $S_r^3(K)$ is not $SU(2)$ -abelian.

1.2.3 Applications to Khovanov homology

Khovanov homology is another algebraic invariant of links in S^3 , which has many connections to Heegaard Floer homology. Often, detection results in one theory are

related to detection results in the other. In [BHS21], Baldwin–Hu–Sivek proved that Khovanov homology with coefficients in $\mathbb{Z}/2\mathbb{Z}$ detects $T(2, 5)$. Combining Theorem A with previous work of Baldwin–Dowlin–Levine–Lidman–Sazdanovic ([BDL⁺21], Corollary 2), we can improve Baldwin–Hu–Sivek’s result from $\mathbb{Z}/2\mathbb{Z}$ -coefficients to \mathbb{Q} -coefficients:

Corollary 1.2.12. Let K be a knot in S^3 . If $Kh(K; \mathbb{Q}) \cong Kh(T(2, 5); \mathbb{Q})$ as bi-graded \mathbb{Q} -vector spaces, then $K = T(2, 5)$.

We also obtain detection results in annular Khovanov homology. One may think of $T(2, 5)$ as the lift of the braid axis for the 5-braid $B = \sigma_1\sigma_2\sigma_3\sigma_4$ in S^3 , seen as the double-branched cover over \widehat{B} under the Birman–Hilden correspondence. From this perspective, techniques of Binns–Martin in ([BM20], Theorems 10.2, 10.4, 10.7) imply that annular Khovanov homology detects this braid closure:

Corollary 1.2.13. Let $L \subset A \times I$ be an annular link with $AKh(L; \mathbb{Q}) \cong AKh(\widehat{B}; \mathbb{Q})$. Then, L is isotopic to \widehat{B} in $A \times I$.

1.3 Outline

In Chapter 2, we review the necessary background and setup to understand the rest of this thesis. In particular, if you are not familiar with some of the concepts or notation in this outline, check there first. Within Chapter 2, in subsection 2.1.3, we also prove Theorem A from Corollary 1.2.2, and Corollary 1.2.2 from Theorem B. Both proofs are quick, so the bulk of this thesis is dedicated to proving Theorem B, which is broken down into four smaller results: Theorems B1 — B4 contained in Chapters 3 — 5. The proof also relies intimately on Theorem C, which is proved in Chapter 6; but, the work in Chapter 6 requires developing new technology which we will not need in great detail just to prove Theorem B. So, we reserve it for the end.

Here, we will describe how the results of Chapters 3 — 5 together prove Theorem B, and then we will briefly summarize the main idea of Chapter 6.

1.3.1 Reducing Theorem B into Theorems B1 — B4

Let K be a hyperbolic, genus-two, fibered knot in S^3 or \mathcal{P} with fractional Dehn twist coefficient $c(K) \neq 0$. Suppose for the sake of contradiction that K is FPF—the goal will be to show that no such K exists. Let (S, h) be the open book decomposition associated to K , thought of as a fibered knot. By assumption, we know that h is freely isotopic to a pseudo-Anosov map $\psi_h : S \rightarrow S$, that $c(h) \neq 0$, and that ψ_h has no fixed points in the interior of S , where S is the genus-two surface with one boundary component.

Because S^3 and \mathcal{P} are both L-spaces, we know by [HM18] that $|c(h)| < 1$. So, because $c(h) \neq 0$, it follows that $c(h) \notin \mathbb{Z}$. In particular, the invariant foliations of ψ_h have more than one prong on ∂S . By Theorem 2.3.1, we then know h is symmetric, and hence projects to a 5-braid β , thought of as a mapping class on the marked disk D_5 . We can see that β is pseudo-Anosov, since h is, and in fact the invariant foliations of the pseudo-Anosov representative ψ_β lift to the invariant foliations for ψ_h in a controlled manner. Specifically, the number of prongs on the boundary, and at each marked point, double in the lift. It follows that the invariant foliations for ψ_h have an even number of prongs at each marked point and on ∂S .

The Euler–Poincaré formula (see e.g. [FLP12]) then implies that the singularity type of ψ_h is one of: $(6; \emptyset; \emptyset)$, $(4; \emptyset; 4)$, $(4; 4; \emptyset)$, $(4; \emptyset; 3^2)$, $(2; \emptyset; 4^2)$, $(2; 4^2; \emptyset)$, $(2; 4; 4)$, or $(2; \emptyset; 3^4)$. The options $(4; \emptyset; 4)$, $(4; 4; \emptyset)$, and $(2; 4; 4)$ can all be eliminated immediately: the unique interior and/or marked 4-pronged singularity must be fixed by ψ_h , so ψ_h has at least one interior fixed point. The option $(2; 4^2; \emptyset)$ can also be eliminated easily: the two 4-pronged marked points must be swapped, so ψ_β must swap the projections of these two marked points on the disk. But, then β also swaps these

marked points, so the closure $\widehat{\beta}$ is not connected (i.e. not a *knot*). So, the double branched cover over $\widehat{\beta}$ is not S^3 or \mathcal{P} .

The remaining four singularity types are then: $(6; \emptyset; \emptyset)$, $(4; \emptyset; 3^2)$, $(2; \emptyset; 4^2)$, and $(2; \emptyset; 3^4)$. These cases are the subject of our analysis in Theorems B1 — B4: we will show that there are no pseudo-Anosov maps meeting the necessary criteria in each case. Combining these four theorems with the analysis presented in this outline completes the proof of Theorem B. We will present a brief summary of the techniques used in each case.

1.3.2 The case $(6; \emptyset; \emptyset)$

For the singularity type $(6; \emptyset; \emptyset)$, our arguments are significantly different from the other three cases. Here, our analysis relies on two key facts, one of which is quite special to the stratum $(6; \emptyset; \emptyset)$. The first fact, due to Masur–Smilie [MS93], is that for any pseudo-Anosov map with singularity type $(6; \emptyset; \emptyset)$, the invariant foliations are necessarily orientable. The second fact is an interpretation of the Lefschetz Fixed Point Theorem by Laneeau–Thiffeault [LT11]: roughly, the Lefschetz index of a pseudo-Anosov map at a fixed singular point can be understood in terms of how the map rotates the separatrices at that point.

Because the invariant foliations of ψ_h are orientable, we can conclude that the characteristic polynomial $\chi(\psi_{h*})$ of the action $\psi_{h*} : H_1(S) \rightarrow H_1(S)$ on homology contains the dilatation $\lambda(\psi_h)$ as a root. Laneeau–Thiffeault’s index calculation then allows us to precisely pin down $\chi(\psi_{h*})$, and then conclude that $\lambda(\psi_h) = \lambda_2$, the minimal dilatation for any pseudo-Anosov in genus two. Laneeau–Thiffeault also showed that the pseudo-Anosov realizing λ_2 as its dilatation is essentially unique, and Ham–Song [HS07] found a 5-braid α which realizes this dilatation.

After some work, we can then conclude that, in fact, ψ_h must be conjugate to the lift of α (up to inversion, reversal, and adding Dehn twists about the boundary), and

then we can show that no such map yields an open book for S^3 or \mathcal{P} . In the middle of our argument, we need to resolve a special case of a general problem of interest: if two symmetric mapping classes are conjugate, are their projections to the marked disk conjugate as braids? We resolve this question in the affirmative for braids of braid index at most 6.

1.3.3 The remaining three singularity cases

For the next three singularity types, $(2; \emptyset; 4^2)$, $(4; \emptyset; 3^2)$, and $(2; \emptyset; 3^4)$, we use broadly similar arguments, so we can describe the ideas in parallel. This is where the theory of train tracks becomes crucial, and in particular where we need to apply our Theorem C. We work with the 5-braid β on D_5 , and the corresponding singularity types of the braids in each case are $(1; 1^5; 4)$, $(2; 1^5; 3)$, and $(1; 1^5; 3^2)$, respectively. In each stratum, we are able to apply Theorem C to find a single train track that carries all pseudo-Anosov braids with the right singularity type. For the strata $(1; 1^5; 4)$ and $(2; 1^5; 3)$, this is essentially immediate. In the case of $(1; 1^5; 3^2)$, however, we need to do a bit more work, and in fact our argument requires us to examine the structure of the *folding automaton* for train tracks in that stratum.

In each case, once we pin down a unique track τ carrying all pseudo-Anosovs, we perform an extensive combinatorial analysis of train track maps carried by the canonical track. The key idea is to examine the image $\psi_\beta(\tau)$ immediately before collapsing the image back onto τ . This idea is crucial, because it allows us to understand train track maps that are actually induced by homeomorphisms, and are not just abstract graph-maps. The general problem of understanding when a train track map is induced by a homeomorphism is hard, but on a case-by-case basis, there are many ways to rule out maps that are *not* induced by any homeomorphism.

From the image $\psi_\beta(\tau)$ immediately before collapsing, we can actually understand the fixed points of the lift ψ_h , in terms of the trace of the transition matrix $M(f_\beta)$ for

the train track map $f_\beta : \tau \rightarrow \tau$ induced by ψ_β . The key result is Lemma 2.3.2, which lies at the heart of our proof technique, and is used repeatedly throughout this paper. The upshot is that, because ψ_h is assumed to be FPF, we know that the transition matrix $M(f_\beta)$ must have trace 0 (except in the final singularity type case—there, the analysis is slightly more complicated, but follows the same general principle). Our case analysis results in a complete list of pseudo-Anosov 5-braids which lift to FPF maps in the cover (these are precisely the braids appearing in Theorem 1.2.3), and then we can show that none of the lifted maps yield an open book decomposition for S^3 or \mathcal{P} . This last step involves analyzing the candidate braids, using a quick fractional Dehn twist coefficient consideration and basic techniques from knot theory, to show that none of the braids close up to the unknot or $T(3, 5)$.

1.3.4 The main idea of Chapter 6

Finally, we will say a few words about the techniques used in Chapter 6, in which we prove Theorem C. The main idea is to define a tool, which we call *tight splitting*, that preserves the conjugacy class of a pseudo-Anosov map, but produces a new train track that carries it. The repeated application of tight splitting operations is what allows us to find the desired train tracks that carry all pseudo-Anosovs with a fixed singularity type, as in Theorem C: we keep performing tight splits until we end up with a jointless track.

One can think of tight splitting as a special case of the more general operation of *splitting*, which produces a new train track from an old one. Splitting is, roughly, inverse to *folding*, and tight splitting specifically can be seen as walking backwards along the folding automaton (see Chapter 5, or [HS07] or [KLS02] for more details). The problem tight splitting solves is that, after a general splitting operation, if you naively carry the split through from the level of tracks to the level of train track maps, the map may no longer be *tight*, i.e. it may not actually be carried by the new train

track. Tight splitting is then a way to identify when a split is tight, i.e. when the new map is actually carried by the new track obtained from the split.

To develop the theory of tight splitting for our use case, the key idea is to examine how a train track map induced by a homeomorphism behaves near the vertices of a track, in order to understand when one can tightly split at a vertex. Specifically, we show that you can always tightly split at a vertex of maximal valence (Corollary 6.2.9). Theorem C then follows by showing that for any map in one of the relevant strata on the punctured disk, you can always tightly split at the vertex with the most joints to produce (possibly after several tight splits) a conjugate map carried by a track with one less joint. Repeated application then removes all joints.

Chapter 2

Background and setup

2.1 Pseudo-Anosov maps, three manifolds, fibered knots, and Floer theory

In this section, we will review the basic setup to understand most of the Outline (Section 1.3), and to prove Theorem A from Theorem B. See the next two subsections 2.2 and 2.3 for a review of the theory of train track maps and how we will use them in this paper.

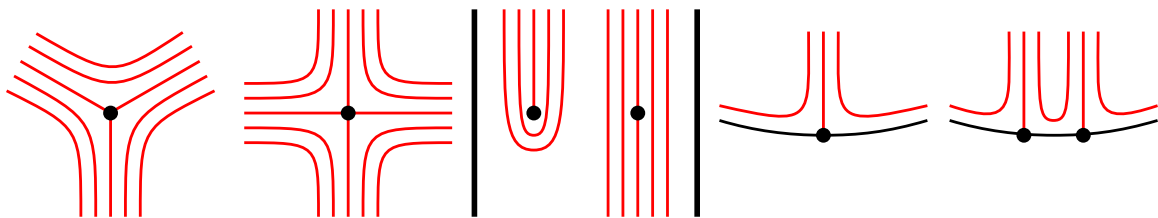


Figure 2.1: The allowable singularities in the invariant foliations of a pseudo-Anosov map. Non-marked interior singularities must have at least 3 prongs. Left: a 3-pronged and a 4-pronged singularity. Center: a 1-pronged and a 2-pronged singularity at a marked point. Right: a 1-pronged and a 2-pronged boundary component.

2.1.1 Mapping classes, pseudo-Anosovs, and singularity types

Let S be a compact surface, possibly with boundary and/or with marked points. The *mapping class group* $\text{Mod}(S)$ is the group of isotopy classes of homeomorphisms $h : S \rightarrow S$ which fix ∂S pointwise and permute the set of marked points. A *mapping class* is an element of the mapping class group, and an *n -braid* is a mapping class on the n -marked disk.

A map $\psi : S \rightarrow S$ is *pseudo-Anosov* if there is a constant $\lambda > 1$ and a pair of transverse, measured, singular foliations (\mathcal{F}_u, μ_u) and (\mathcal{F}_s, μ_s) such that:

- $\psi(\mathcal{F}_u, \mu_u) = (\mathcal{F}_u, \lambda\mu_u)$
- $\psi(\mathcal{F}_s, \mu_s) = (\mathcal{F}_s, \lambda^{-1}\mu_s)$

and the singularities of \mathcal{F}_u and \mathcal{F}_s are as described in Figure 2.1. We require that non-marked interior singular points have at least 3 prongs, and that boundary components consist of some number $k \geq 1$ of 1-pronged singularities, which we often think of collectively as a “ k -pronged boundary.”

Locally, one should think of a pseudo-Anosov map ψ as stretching S in the direction of \mathcal{F}_u and shrinking S in a transverse direction described by \mathcal{F}_s . The constant $\lambda > 1$ is called the *dilatation* of ψ , and records how much ψ stretches/shrinks S in each direction. Because the invariant foliations are set-wise preserved by ψ , note that ψ always permutes the set of singular points with a given number of prongs.

It will be convenient to refer to the *singularity type* of a pseudo-Anosov map ψ , by which we mean the tuple recording the number of prongs at each singularity of \mathcal{F}_u and \mathcal{F}_s . We will denote the singularity type of ψ by the tuple $(b_1, \dots, b_r; m_1, \dots, m_n; k_1, \dots, k_s)$ where the i^{th} boundary component of ψ has b_i prongs; the i^{th} marked point has m_i prongs; and the i^{th} non-marked interior singularity has k_i prongs. We will use \emptyset if there are no singularities of a certain type, and we will use exponents to denote

multiple singularities of the same type with the same number of prongs. For example, the tuple $(3; 1^5; \emptyset)$ indicates that \mathcal{F}_u and \mathcal{F}_s have a 3-pronged singularity at the unique boundary component of S ; five 1-pronged singularities at marked points; and no non-marked interior singularities. The tuple $(2^3; 2, 4; 3^2)$ indicates that \mathcal{F}_u and \mathcal{F}_s have 2-pronged singularities on each of the three boundary components; a 2-pronged singularity at one marked point, and a 4-pronged singularity at the other; and two 3-pronged singularities at non-marked interior points.

When S has non-empty boundary, pseudo-Anosov maps never fix ∂S point-wise, and hence do not represent well-defined mapping classes. Nonetheless, the Nielsen–Thurston classification demonstrates the ubiquity of pseudo-Anosov maps in the study of mapping classes:

Theorem 2.1.1 ([Thu88]). Let S be a compact surface, possibly with marked points. Any mapping class $h \in \text{Mod}(S)$ is freely isotopic rel. marked points to a unique homeomorphism $\psi_h : S \rightarrow S$ satisfying one of the following:

- $\psi_h^n = \text{id}$ for some power n .
- There is a collection of disjoint simple closed curves C on S for which $\psi_h(C)$ is isotopic to C .
- ψ_h is pseudo-Anosov

We call ψ_h the *geometric representative* of h , and we say that ψ_h is *periodic* in the first case, and *reducible* in the second. These first two cases are not mutually exclusive, but the pseudo-Anosov case does not overlap with either of them. We will also refer to the mapping class $h \in \text{Mod}(S)$ as periodic, reducible, or pseudo-Anosov according to the Nielsen–Thurston type of ψ_h .

Remark 2.1.2. Note the use of *free* isotopy in the theorem statement: when S has non-empty boundary, there are infinitely many mapping classes with the same

geometric representative, which are all freely isotopic but non-isotopic rel. boundary. Two mapping classes have the same geometric representative exactly when they differ by a product of Dehn twists about components of ∂S .

2.1.2 Fibered knots and fractional Dehn twists

When ∂S is connected, and for any mapping class $h \in \text{Mod}(S)$, we may associate to h a *fibered knot* K in a 3-manifold Y . First, define $Y \cong S \times [0, 1] / \sim$ where the relation \sim is defined by:

- $(x, 0) \sim (h(x), 1)$ for all $x \in S$
- $(x, s) \sim (x, t)$ for all $x \in \partial S$ and all $s, t \in [0, 1]$

Then, define $K \subset Y$ to be the image of ∂S in the quotient. Note that in this construction, the knot exterior Y_K is homeomorphic to the mapping torus M_h . Moreover, any copy of S in the quotient Y is naturally a Seifert surface for K , of minimal genus. Starting from a knot instead, we say that a knot $K \subset Y$ is *fibered* if its exterior is the mapping torus of a homeomorphism on a Seifert surface.

The pair (S, h) of surface and mapping class is called an *open book decomposition* of the 3-manifold Y , or simply an *open book*. Many properties of the open book (S, h) and its geometric representative ψ_h can be interpreted in terms of the fibered knot $K \subset Y$. For example, Thurston's geometrization of fibered 3-manifolds relates the geometry of the knot exterior Y_K to the Nielsen–Thurston type of ψ_h :

Theorem 2.1.3 ([Thu98]). Let $K \subset Y$ be a fibered knot with associated open book (S, h) . Then, the exterior $Y_K \cong M_h$ is:

- Seifert-fibered exactly when ψ_h is periodic
- Toroidal exactly when ψ_h is reducible

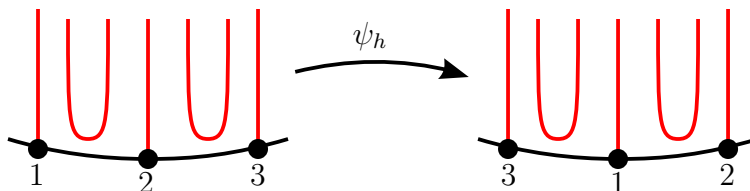


Figure 2.2: An example where ψ_h acts as a $1/3$ rotation on the boundary singular points. The fractional part of $c(h)$ is $1/3$.

- Hyperbolic exactly when ψ_h is pseudo-Anosov

One dynamical aspect of ψ_h which is important to the geometry of K is described by the *fractional Dehn twist coefficient* $c(h)$. Roughly, $c(h)$ measures how the geometric representative ψ_h behaves near ∂S . When ψ_h is pseudo-Anosov, we define $c(h) := n + m/k$, where h acts as n full twists near ∂S ; the invariant foliations of ψ_h have k singular points on ∂S ; and ψ_h acts as a m/k rotation on the cyclically-ordered set of singular points on ∂S . An example is shown in Figure 2.2.

Note that when the invariant foliations of ψ_h have a single prong on ∂S , we have $c(h) \in \mathbb{Z}$, since there is no “fractional part.” Conversely, if $c(h) \in \mathbb{Z}$ then we can conclude that ψ_h does not rotate the boundary singularity. Here are some well-known properties of fractional Dehn twist coefficients:

Theorem 2.1.4 ([IK17][HKM07]). Let S be a compact surface, possibly with marked points, and let $h \in \text{Mod}(S)$ be a mapping class.

- $c(h)$ is preserved under conjugation within $\text{Mod}(S)$
- $c(\text{id}) = 0$ and $c(D_{\partial S}^n \circ h^k) = n + kc(h)$
- If h admits a factorization into positive Dehn twists and half twists, then $c(h) \geq 0$. If h is also pseudo-Anosov, then $c(h) > 0$.
- If S has no marked points and the open book (S, h) supports a tight contact structure, then $c(h) \geq 0$. If h is also pseudo-Anosov, then $c(h) > 0$.

Given a fibered knot K , we can define $c(K) := c(h)$ where (S, h) is the open book associated to K . The first property above implies that this definition is well-defined, because isotopy of K amounts to isotopy and/or conjugation of h .

2.1.3 Floer theory, and Theorem A from Theorem B

Heegaard Floer homology, defined by Ozsváth–Szabó in [OS04d], is an invariant $\widehat{HF}(Y)$ of a closed, oriented 3-manifold Y , and it takes the form of a graded vector space over $\mathbb{F} = \mathbb{Z}/2\mathbb{Z}$. The vector space decomposes over spin^c -structures on Y , and satisfies $\chi(\widehat{HF}(Y)) = |H_1(Y; \mathbb{Z})|$ when Y is a rational homology S^3 . In particular, we have $\dim \widehat{HF}(Y) \geq |H_1(Y; \mathbb{Z})|$ for any rational homology sphere Y . When equality is achieved, we call Y an *L-space*. For some concrete examples, S^3 , \mathcal{P} , and lens spaces are all L-spaces.

A knot $K \subset Y$ which admits a non-trivial surgery to an L-space is called an *L-space knot*, and in this case the geometry of K is quite constrained. For example, combining results of [Tan11], [OS04b], [Ni07], and [Ni22], we have:

Theorem 2.1.5. Suppose that Y is an integer homology sphere L-space, and let $K \subset Y$ be an L-space knot with irreducible exterior. Then, we have:

- Every coefficient of the Alexander polynomial of K is 0 or ± 1 , the non-zero coefficients alternate in sign, and the top two coefficients are non-zero
- K is fibered and the open book decomposition (S, h) for K supports a tight contact structure
- If K is hyperbolic, then ψ_h has no interior fixed points

Corollary 1.2.2 now follows directly from Theorem B by applying Theorem 2.1.5:

proof of Corollary 1.2.2 from Theorem B. Let K be a genus-two, hyperbolic L-space knot in S^3 or \mathcal{P} . Note that S^3 and \mathcal{P} are both integer homology sphere L-spaces,

so Theorem 2.1.5 applies. We can thus conclude that K is fibered and FPF. Let (S, h) be the open book associated to K , as a fibered knot. Since K is hyperbolic by assumption, we know $h \in \text{Mod}(S)$ is a pseudo-Anosov mapping class by Theorem 2.1.3. We also know that (S, h) supports a tight contact structure by Theorem 2.1.5. It follows that $c(K) = c(h) > 0$ by Theorem 2.1.4. But, then K is a genus-two FPF knot with $c(K) \neq 0$, and no such knot exists by Theorem B. \square

And, we can now see how Theorem A follows quickly from Corollary 1.2.2.

proof of Theorem A from Corollary 1.2.2. Let K be a genus-two L-space knot in S^3 or \mathcal{P} which is *not* any of $T(2, 5) \subset S^3$, $\mathcal{K} \subset \mathcal{P}$, or $T(2, 5) \subset B^3 \subset \mathcal{P}$.

First suppose K has irreducible exterior. Our goal is to show that K is hyperbolic, so that we can apply Corollary 1.2.2 and conclude that no such knot exists. Any irreducible knot exterior in \mathcal{P} or S^3 is hyperbolic, Seifert-fibered, or toroidal. And, $T(2, 5) \subset S^3$ and $\mathcal{K} \subset \mathcal{P}$ are the unique genus-two knots in S^3 and \mathcal{P} , respectively, with Seifert-fibered exterior. So, K must have either hyperbolic or toroidal exterior.

Suppose for the moment that K has toroidal exterior. It then follows from Theorem 2.1.3 that the mapping class $h \in \text{Mod}(S)$ is reducible. Thinking of the Alexander polynomial $\Delta_K(t)$ of K as the characteristic polynomial of the action $h_* : H_1(S) \rightarrow H_1(S)$, we can see that $\Delta_K(t)$ is reducible (because the action of h_* fixes a nontrivial subspace corresponding to the fixed multicurve of ψ_h). However, one can quickly compute using the constraints of Theorem 2.1.5 that $\Delta_K(t) = t^4 - t^3 + t^2 - t + 1$, which is irreducible. So, such a K does not exist.

In particular, if K has irreducible exterior, then K must be hyperbolic. But, there are no hyperbolic L-space knots in S^3 or \mathcal{P} , by Corollary 1.2.2. So, we've shown that the only genus-two L-space knots in S^3 or \mathcal{P} with irreducible exterior are $T(2, 5) \subset S^3$ and $\mathcal{K} \subset \mathcal{P}$. And, because any knot in S^3 has irreducible exterior, we may conclude that in fact $T(2, 5)$ is the only genus-two L-space knot in S^3 . So, what about L-space knots with reducible exterior in \mathcal{P} , then?

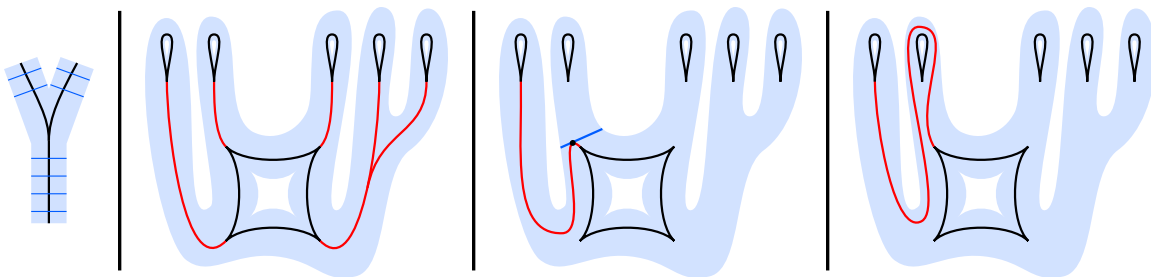


Figure 2.3: Left: leaves of a fibered neighborhood near a switch. Center left: a fibered neighborhood of a track τ . Center right: the image of the red edge is not transverse to the leaves. Right: the image of the red edge is transverse to the leaves, and ready to be collapsed onto τ .

Suppose, for the sake of contradiction, that $K \neq T(2, 5) \subset B^3 \subset \mathcal{P}$ is a genus-two L-space knot in \mathcal{P} with reducible exterior. Recall that any knot in S^3 has irreducible exterior, so we know immediately that $K \subset \mathcal{P}$. And, because \mathcal{P} is itself irreducible, we can conclude that K must in fact be contained in a 3-ball: $K \subset B^3 \subset \mathcal{P}$. If K has surgery to an L-space Y , we may write $Y = \mathcal{P} \# Y'$, where Y' is surgery on K thought of as a knot in $B^3 \subset S^3$. Since Y is an L-space, Y' must be an L-space as well. In this case, K is isotopic in $B^3 \subset S^3$ to a genus-two L-space knot, and the only such knot in S^3 is $T(2, 5)$, as demonstrated above. \square

2.2 Train tracks and maps, and standard tracks

2.2.1 Train tracks carrying mapping classes

Our eventual goal will be to classify fixed-point-free pseudo-Anosov maps in certain strata on the genus-two surface with one boundary component, in the spirit of Theorems B and 1.2.3. To do that, we will use the theory of train tracks, which may be thought of as a combinatorial perspective on the geometry of mapping classes.

A *train track* $\tau \subset S$ is a branched 1-manifold embedded in the interior of a compact surface S . We will refer to the non-manifold points of τ as *switches*. Thinking of τ as a graph whose vertices are its switches, there is a natural cyclic ordering on the

edges adjacent to any given switch. We say that two edges of τ form a *cusp* if they are adjacent at a switch, share a common tangent direction, and are adjacent in the natural cyclic ordering.

A *train path* on a train track τ is a smooth immersion $\gamma : [0, 1] \rightarrow \tau$ such that $\gamma(0)$ and $\gamma(1)$ are switches. For example, any edge of τ is a train path. A *train track map* $f : \tau \rightarrow \tau$ is a surjection such that for any train path $\gamma : [0, 1] \rightarrow \tau$, the composition $f \circ \gamma$ is also a train path. Fix an enumeration e_1, \dots, e_n of the edges of τ ; the *transition matrix* $M(f)$ is the matrix whose (i, j) entry is the number of times that the train path $f(e_i)$ passes through e_j .

A *fibred neighborhood* $F(\tau) \subset S$ is a tubular neighborhood of τ which is foliated by intervals transverse to τ , away from the switches. The intervals are called *leaves*. A geometric map $\psi_h : S \rightarrow S$ is *carried by* τ if $\psi_h(\tau)$ can be isotoped into $F(\tau)$ so that the image is everywhere transverse to the leaves of the foliation. We say that a mapping class $h \in \text{Mod}(S)$ is carried by τ if its geometric representative is. See Figure 2.3 for some local pictures, and then look at Figure 2.5 for an image of the entirety of $\psi_h(\tau) \subset F(\tau)$.

When a mapping class h is carried by τ , it induces a train track map $f_h : \tau \rightarrow \tau$, determined by the image $\psi_h(\tau)$ under the geometric representative. For an edge e of τ , we define $f_h(e)$ to be the train path that the image $\psi_h(e) \subset F(\tau)$ collapses onto under the natural deformation retraction $F(\tau) \rightarrow \tau$. The induced train track map f_h completely determines ψ_h :

Theorem 2.2.1 ([BH95]). Let $h, g \in \text{Mod}(S)$ be two mapping classes with geometric representatives ψ_h, ψ_g . Suppose that h and g are carried by the same train track τ , and induce maps $f_h, f_g : \tau \rightarrow \tau$. If $f_h = f_g$, then h and g are freely isotopic and $\psi_h = \psi_g$.

Corollary 2.2.2. Let $\alpha, \beta \in \text{Mod}(D_n)$ be two n -braids which are carried by the same track τ and induce the same train track map $f_\alpha = f_\beta : \tau \rightarrow \tau$. Then, we have

$\psi_\alpha = \psi_\beta$ and $\alpha = \Delta^{2k}\beta$ for some $k \in \mathbb{Z}$, where $\Delta^2 = (\sigma_1 \dots \sigma_{n-1})^n$ is a full twist about ∂D_n .

Given a mapping class $h \in \text{Mod}(S)$, we define the *geometric data* of h to be a tuple (h, ψ_h, τ, f_h) where ψ_h is the geometric representative of h , τ carries h , and $f_h : \tau \rightarrow \tau$ is the induced train track map. It should be noted that any mapping class h is always carried by many different train tracks. But, if τ is a train track which carries h , then the induced train track map f_h is well-defined.

Train tracks which carry mapping classes, and train track maps which are induced by mapping classes, are somewhat special. There are many train tracks which do not carry any mapping classes. And, on any given train track, it is easy to produce train track maps which are not induced by any mapping class. Indeed, the geometry of a mapping class is determined by the geometry of a train track which carries it. For example, when the mapping class is pseudo-Anosov, we have:

Proposition 2.2.3 ([BH95]). Let h be a pseudo-Anosov mapping class carried by τ . If N is a connected interior (resp. peripheral) component of $S \setminus \tau$, then τ has p cusps along ∂N if and only if ψ_h has a p -pronged singularity in the interior of N (resp. a p -pronged boundary in N).

For example, the train track in Figure 2.3 carries maps in the stratum $(1; 1^5; 4)$: the peripheral region has 1 cusp; each marked point lies in a monogon region; and there is a unique non-marked interior region, which has 4 cusps. We will often refer to a train track as belonging to a certain stratum, by which we mean it carries maps in that stratum.

When a train track map is induced by a mapping class, much of the interesting geometric information of the mapping class can be read from the train track map. For example:

Proposition 2.2.4 ([BH95][Los10][CC09]). Let (h, ψ_h, τ, f_h) be the geometric data of a mapping class. Then, the transition matrix $M(f_h)$ is Peron–Frobenius iff the mapping class is pseudo-Anosov. In this case, the dilatation $\lambda(\psi_h)$ is the largest eigenvalue of $M(f_h)$, and the number of fixed points of ψ_h is bounded in terms of the trace of $M(f_h)$:

$$\frac{1}{2}\mathrm{tr}(M(f_h)) \leq |\mathrm{Fix}(\psi_h)|$$

2.2.2 Real and infinitesimal edges

Given a geometric map ψ_h , Bestvina–Handel in [BH95] construct a train track τ which carries ψ_h . The key object of the Bestvina–Handel construction is an *efficient fibered surface* associated to ψ_h . The fibered surface $F \subset S$ is a deformation retract of S which is decomposed into *strips* and *junctions* determined by ψ_h . Roughly, the junctions are disks which record the periodic pieces of S under the action of ψ_h , and the strips are rectangles foliated by lines parallel to the junctions.

Given a fibered surface F for a geometric ψ_h , we obtain a graph G by collapsing each junction to a vertex and each strip to an edge. Bestvina–Handel explain how to insert *infinitesimal* edges into each junction according to the geometry of ψ_h , so that collapsing strips to edges and junctions to their infinitesimal edges forms a train track τ which carries ψ_h . The edges of τ formed by strips are called *real* edges.

The structure of the real and infinitesimal edges of τ is crucial to the fidelity of Bestvina–Handel’s construction. As the infinitesimal edges were inserted into periodic pieces of the fibered surface, it follows that ψ_h sends infinitesimal edges to infinitesimal edges. In particular, the train track map $f_h : \tau \rightarrow \tau$ induced by ψ_h sends infinitesimal edges to infinitesimal edges.

Moreover, the cusp structure of the infinitesimal edges in a given junction is preserved under ψ_h . An *infinitesimal polygon* is a connected component of $S \setminus \tau$ whose boundary is a union of infinitesimal edges. By the Bestvina–Handel construction, ψ_h

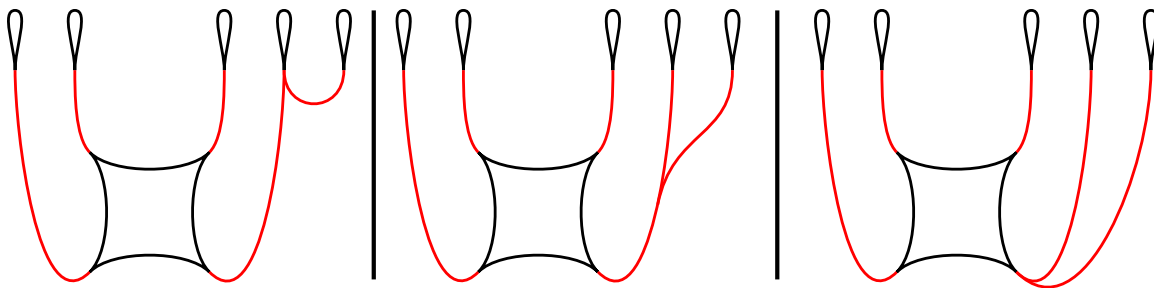


Figure 2.4: Some train tracks in the stratum $(1; 1^5; 4)$. Left: a standard track with a joint. Center: a non-standard track (with no joints). Right: a standard, jointless track.

and f_h send infinitesimal polygons of τ to other infinitesimal polygons with the same number of cusps.

For the rest of the paper, we will restrict our attention to train tracks which carry pseudo-Anosov maps. And, we will implicitly presuppose the structure of real and infinitesimal edges of τ , as imposed by an arbitrary map carried by τ . The infinitesimal edges will always be drawn in black, and the real edges in color. For example, in the tracks in Figures 2.3 and 2.4, the real edges are shown in red and the infinitesimal edges in black.

2.2.3 Standard and jointless tracks, and a carrying theorem

We say that a train track $\tau \subset D_n$ on an n -marked disk D_n is *standard* if:

- Every non-peripheral component of $S \setminus \tau$ is an infinitesimal polygon
- The switches of τ are precisely the vertices of the infinitesimal polygons
- At each switch, all adjacent infinitesimal edges are tangent to each other, all adjacent real edges are tangent to each other, and no real edge is tangent to an infinitesimal edge
- For each marked point p of D_n , there is a single edge of an infinitesimal polygon vertically above p , and no other edge of τ is vertically above p .

See Figure 2.4 for an example of a standard train track. The idea of standard tracks originally appeared in [KLS02] (and later [CH08] and [HS07]) as a tool to study dilatations of pseudo-Anosov braids. In their terminology, a track satisfying the first three properties is *standardly embedded* and a track satisfying the third is in *standard position*.

Standard tracks are useful, because they help us restrict our attention to a specific collection of tracks, which we can enumerate. The key result that facilitates this perspective is:

Proposition 2.2.5 ([KLS02]). Every pseudo-Anosov map on a marked disk is carried by a standard train track.

So, if we want to understand pseudo-Anosov maps in a particular stratum, we can instead study train track maps on standard tracks in that stratum. By further considering the singularity structure of a stratum, we can dramatically improve this enumeration.

A *joint* of a standard train track τ is a switch of an infinitesimal monogon surrounding a marked point, which has more than one adjacent real edge. See Figure 2.4. Theorem C says that, in most strata on the marked disk, all pseudo-Anosovs are conjugate to maps carried by tracks with no joints. This result will be central to the techniques used in Chapters 3 — 5. However, it requires technology that lies outside the scope of the proof of Theorem B, so we save it for the end, in Chapter 6.

2.3 Branched covers and lifting train track maps

2.3.1 Braids and the Birman–Hilden correspondence

We will be interested in studying fibered knots and mapping classes under branched coverings. The Birman–Hilden correspondence describes the relevant operation in our

setting. We may view the n -marked disk D_n as the quotient of a surface S via the action of a fixed hyperelliptic involution $\iota : S \rightarrow S$. When a map $h : S \rightarrow S$ commutes with ι , it projects to an n -braid $\beta : D_n \rightarrow D_n$. In this case, we say that h is *symmetric*. Every n -braid lifts to a symmetric map on a surface S of genus $\lfloor \frac{n-1}{2} \rfloor$ with 1 boundary component if n is odd, and 2 boundary components if n is even.

Here is how to interpret the correspondence from the perspective of knots and 3-manifolds. Suppose β lifts to h , where (S, h) is an open book decomposition for Y describing the fibered knot $K \subset Y$. Then, Y is the double cover over S^3 branched along the braid closure $\widehat{\beta}$. And, K is the lift to Y of the unknotted braid axis for β in S^3 under this covering.

For example, S^3 is the double branched cover over the unknot, so the 3-braid $\sigma_1\sigma_2$, which closes up to an unknot, lifts to a genus-one open book decomposition for S^3 : the binding of this open book is the trefoil in S^3 . Similarly, the 5-braid $(\sigma_1\sigma_2\sigma_3\sigma_4)^3$ closes up to $T(3, 5)$, so this braid lifts to a genus-two open book for \mathcal{P} (thought of as the double cover branched over $T(3, 5)$): the binding of this open book is the order-three Seifert fiber \mathcal{K} from Theorem A. It will be helpful to note that the unknot is the unique knot in S^3 whose double branched cover is again S^3 ; and $T(3, 5)$ is the unique knot in S^3 whose double branched cover is \mathcal{P} .

The Nielsen–Thurston class is preserved under the Birman–Hilden correspondence, i.e. ψ_β is pseudo-Anosov (resp. periodic, reducible) iff ψ_h is (resp. periodic, reducible). In the case that ψ_h and ψ_β are pseudo-Anosov, the invariant foliations can be tracked through the lift, as well. Specifically, the number of prongs of the foliations at the marked points double in the lift. For example, 1-pronged marked points of ψ_β lift to regular points of ψ_h ; and 2-pronged marked points of ψ_β lift to 4-pronged marked points of ψ_h . The number of boundary prongs double in a similar manner. Away from the boundary, however, each non-marked singularity of ψ_β lifts to two singularities of ψ_h with the same number of prongs. So, for example, ψ_β has

singularity type $(1; 1^5; 4)$ exactly when ψ_h has singularity type $(2; \emptyset; 4^2)$. Analyzing how ψ_β and ψ_h twist near the boundary leads also to a relationship between fractional Dehn twist coefficients: we always have $c(\beta) = 2c(h)$.

Baldwin–Hu–Sivek in [BHS21] showed that, in genus two, most FPF pseudo-Anosovs are symmetric:

Theorem 2.3.1 (Baldwin–Hu–Sivek). Let $h \in \text{Mod}(S)$ be a pseudo-Anosov mapping class on the genus-two surface with one boundary component. If the pseudo-Anosov representative ψ_h is FPF and the invariant foliations for ψ_h have more than one prong on ∂S , then h is symmetric.

It will be useful to note that, when $c(h) \notin \mathbb{Z}$, we know that ψ_h has more than one boundary prong. It follows that Theorem 2.3.1 applies for any FPF pseudo-Anosov mapping class h with $c(h) \notin \mathbb{Z}$.

2.3.2 Lifting standard tracks, and the trace lemma

Let $(\beta, \psi_\beta, \tau, f_\beta)$ be the geometric data of a pseudo-Anosov n -braid. We will explicitly construct related data $(h, \psi_h, \tilde{\tau}, f_h)$ for the lift h of β under the Birman–Hilden correspondence. For simplicity, assume that τ is standard (though a similar construction will work for non-standard tracks), and start by lifting τ to obtain two copies of τ on S . Because we assumed τ to be standard, the two copies of τ in the lift together produce a train track away from the marked points. But, near the marked points, we see two copies of the infinitesimal polygons surrounding each marked point, which we need to paste together coherently. To do this, simply replace each pair of infinitesimal p -gons surrounding a marked point with a single infinitesimal $2p$ -gon, as in Figure 2.6. If $p = 1$, instead replace the pair of monogons with a smooth point. See Figure 2.5 for an example of a full lifted track $\tilde{\tau}$.

This construction produces a train track $\tilde{\tau}$ for which edges come in pairs e_1, e_2 of lifts of a single real edge e of τ ; the pairs satisfy $\iota(e_1) = e_2$. Moreover, any train path

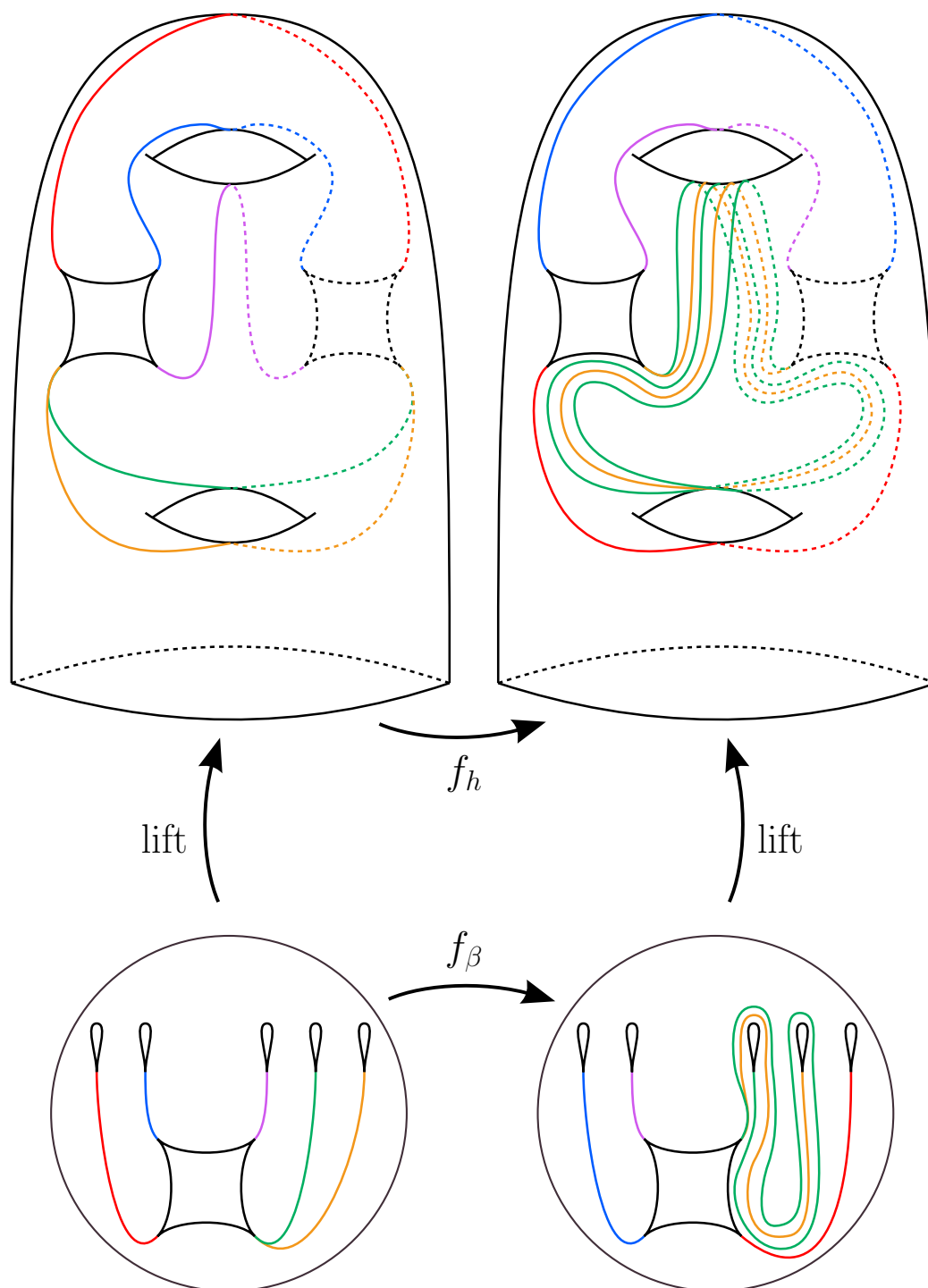


Figure 2.5: Lifting a train track and train track map from D_5 to S . Dashed edges indicate the back side of the surface.

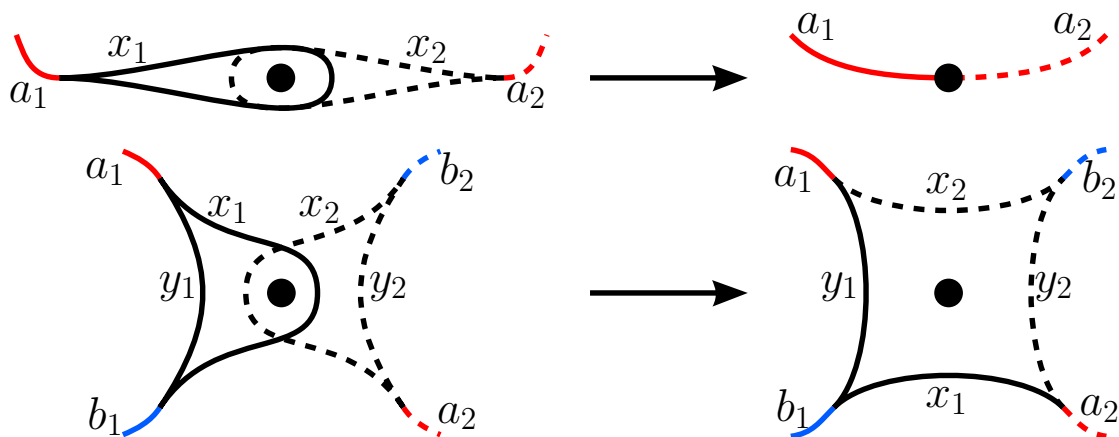


Figure 2.6: Smoothing infinitesimal polygons near a marked point. Top: smoothing monogons to a regular point. Bottom: smoothing bigons to a rectangle. In both images, the involution ι is a 180° rotation about the marked point, and the side-swapping edge in τ is x , which lifts to x_1, x_2 in $\tilde{\tau}$.

$e(1)\dots e(n)$ in τ always lifts to exactly two train paths $e(1)_1\dots e(n)_{n_i}$ and $e(1)_2\dots e(n)_{n_j}$ in $\tilde{\tau}$. These two train paths are distinguished by which “side” of $\tilde{\tau}$ the paths start on. Now, for an arbitrary real edge e of τ , let $f_\beta(e) = e(1)\dots e(n)$. To construct $f_h : \tilde{\tau} \rightarrow \tilde{\tau}$, simply define $f_h(e_i) = e(1)_{i_1}\dots e(n)_{i_n}$ to be the unique lift of $f_\beta(e)$ which starts on the same side of $\tilde{\tau}$ as $\psi_h(e_i)$ does. An example of a lifted train track map is shown in Figure 2.5.

The explicit construction of f_h from f_β allows us to examine fixed point properties of ψ_h in terms of the transition matrix $M(f_\beta)$. Recall that a standard track on the marked disk has a unique edge of an infinitesimal polygon above each marked point. For the statement and proofs of the next two lemmas we will refer to these edges as *side-swapping edges*: their key feature is that when a train path runs over a side-swapping edge, it swaps to the “other side” of $\tilde{\tau}$. See Figure 2.6. The following lemma will be crucial for our analysis.

Lemma 2.3.2 (The trace lemma). Let $(\beta, \psi_\beta, \tau, f_\beta)$ be the data of a pseudo-Anosov braid with lift $(h, \psi_h, \tilde{\tau}, f_h)$ on S . Suppose that τ is standard and that ψ_h has no interior fixed points on S . Then, for any real edge e of τ , and between any two occurrences of e in $f_\beta(e)$, the image path $f_\beta(e)$ must contain an even number of

side-swapping edges.

Proof. Because ψ_h has no interior fixed points, we know $M(f_h)$ must be traceless, by Proposition 2.2.4. In particular, for any real edge $e_i \in \tilde{\tau}$, we know that e_i does not appear in $f_h(e_i)$.

Now, note that every time $f_\beta(e)$ passes over a side-swapping edge, the image $f_h(e_i)$ of either lift of e crosses over to the other side of $\tilde{\tau}$. So, if e appears in $f_\beta(e)$ with an odd number of side-swapping edges between adjacent appearances, then both lifts e_1 and e_2 appear in the image $f_h(e_1)$ (and same for $f_h(e_2)$). \square

The following is a special case of the trace lemma as stated above. Because the train tracks relevant to this paper will always have jointless monogons at all marked points, it will be a very useful simplification.

Corollary 2.3.3 (The trace lemma for jointless monogons). Retain the same notation and assumptions as in the previous lemma. If e is a real edge of τ which is incident to a jointless monogon at a marked point, then e does not appear in $f_\beta(e)$.

Proof. Suppose that e does appear in $f_\beta(e)$. Because e is adjacent to a jointless monogon, either there are two adjacent appearances of e , or $f_\beta(e)$ ends on e . The first case is not allowed by the previous lemma, and the second case produces a fixed point in the lift, at the end of $f_h(e_i)$. \square

Chapter 3

The stratum $(6; \emptyset; \emptyset)$

The rest of this thesis will be devoted to proving Theorem B, as explained in the outline (Section 1.3). From the argument in the outline, it suffices to consider pseudo-Anosov maps in just four strata: $(6; \emptyset; \emptyset)$, $(2; \emptyset; 4^2)$, $(4; \emptyset; 3^2)$, and $(2; \emptyset; 3^4)$. Our argument for the first of these strata, $(6; \emptyset; \emptyset)$, will be a little different from the next three. Instead of performing a careful combinatorial analysis of train track maps, we will instead use more general geometric methods specific to this stratum. Our goal is to prove:

Theorem B1. Let $h \in \text{Mod}(S)$ be a pseudo-Anosov mapping class with geometric representative ψ_h . Suppose that $c(h) \neq 0$, and that ψ_h is FPF and has singularity type $(6; \emptyset; \emptyset)$. Then, (S, h) is not an open book decomposition for S^3 or \mathcal{P} .

Before turning to the proof of Theorem B1, it will be helpful to recall the Lefschetz fixed point theorem for compact surfaces, which will be a key ingredient in our proof:

Theorem 3.0.1 (Lefschetz fixed point theorem). Let S be a compact surface and $f : S \rightarrow S$ a homeomorphism. Let $f_* : H_1(S; \mathbb{Z}) \rightarrow H_1(S; \mathbb{Z})$ denote the induced map on first homology. Then, we have:

$$2 - \text{tr}(f_*) = \sum_{p=f(p)} \text{Ind}(f, p).$$

We will apply the Lefschetz fixed point theorem to read off information about the action of a pseudo-Anosov on homology, from its dynamical properties. The relevant result in this vein is an index calculation due to Lanneau–Thiffeault in [LT11]:

Proposition 3.0.2 (Lanneau–Thiffeault). Let $\psi : S \rightarrow S$ be pseudo-Anosov with orientable invariant foliations, and let p be a fixed k -prong singularity of ψ . Denote by $\psi_* : H_1(S) \rightarrow H_1(S)$ the action on homology, and denote by $\rho(\psi_*)$ the leading eigenvalue of this action, i.e. the eigenvalue with greatest absolute value.

1. If $\rho(\psi_*) < 0$ then $\text{Ind}(\psi, p) = 1$; that is, every fixed point of ψ has index 1.
2. If $\rho(\psi_*) > 0$ then either:
 - (a) ψ fixes each prong and $\text{Ind}(\psi, p) = 1 - k < 0$, or
 - (b) ψ cyclically permutes the prongs and $\text{Ind}(\psi, p) = 1$.

We can now use Lanneau–Thiffeault’s calculation to restrict the dilatation of the pseudo-Anosov representative of a potential FPF knot K in Theorem B1:

Proposition 3.0.3. Let (S, h) be an open book decomposition for an integer homology sphere Y . Suppose that $c(h) \notin \mathbb{Z}$, and that the pseudo-Anosov representative ψ_h has singularity type $(6; \emptyset; \emptyset)$ and is FPF. Then, ψ_h achieves the minimal dilatation λ_2 among pseudo-Anosovs in genus two.

Proof. Let (S, h) be such an open book decomposition. Because ψ_h has singularity type $(6; \emptyset; \emptyset)$ by assumption, we may cap-off ψ_h to a pseudo-Anosov $\widehat{\psi}_h$ on the closed genus-two surface \widehat{S} and extend the foliations preserved by ψ_h over the capping disk. For this stratum on \widehat{S} , Masur–Smillie ([MS93]) prove that the foliations preserved by $\widehat{\psi}_h$, and therefore by ψ_h , are necessarily orientable. We will use this fact to apply the

Lefschetz fixed point theorem and determine completely the Alexander polynomial of the knot K corresponding to the open book (S, h) .

Because K is a fibered knot by construction, the Alexander polynomial Δ_K is equal to the characteristic polynomial $\chi(\psi_{h*})$ of the action of ψ_h on homology. Because K is a genus-two fibered knot in an integer homology sphere, Δ_K is a monic, degree-four, palindromic polynomial satisfying $\Delta_K(1) = \pm 1$. Moreover, because the fractional Dehn twist coefficient $c(h) \notin \mathbb{Z}$ by assumption, we know $\widehat{\psi}_h$ rotates the separatrices of the 6-prong singularity p formed by the capped boundary component, so that $\text{Ind}(\widehat{\psi}_h, p) = 1$ regardless of the sign of $\rho(\psi_{h*})$. And, because p is the unique fixed point of $\widehat{\psi}_h$ by assumption, it follows from the Lefschetz fixed point theorem that $\text{tr}(\psi_{h*}) = \text{tr}(\widehat{\psi}_{h*}) = 1$.

From the discussion above, we conclude that the coefficients of t^4 and t^0 in $\Delta_K(t)$ are 1, while the coefficients of t^3 and t are $-\text{tr}(\psi_{h*}) = -1$. Now, using the fact that $\Delta_K(1) = \pm 1$, we can see $\Delta_K(t) = t^4 - t^3 \pm t^2 - t + 1$. Because the foliations preserved by ψ_h are orientable, the dilatation $\lambda(\psi_h)$ is a root of Δ_K . The polynomial $t^4 - t^3 + t^2 - t + 1$, however, has no real roots. So it must be the case that $\Delta_K(t) = t^4 - t^3 - t^2 - t + 1$. Finally, note that this polynomial has a single root λ_2 greater than 1, which is the minimal dilatation achieved by any pseudo-Anosov on the genus-two surface, see e.g. [LT11]. \square

We will also need the following lemma for the proof of Theorem B1:

Lemma 3.0.4. Let $h, h' \in \text{SMod}(S)$ be the lifts of 5-braids $\beta, \beta' \in \text{Mod}(D_5)$. Suppose that the capped-off maps \widehat{h} and \widehat{h}' on \widehat{S} are conjugate in $\text{Mod}(\widehat{S})$. Then, β is conjugate to $\Delta^{2k}\beta'$ for some $k \in \mathbb{Z}$.

Proof. Because \widehat{h} and \widehat{h}' are conjugate in $\text{Mod}(\widehat{S})$, and the hyperelliptic involution ι on \widehat{S} is in the center of $\text{Mod}(\widehat{S})$, we may quotient the conjugating homeomorphism in $\text{Mod}(\widehat{S})$ to the mapping class group of the punctured sphere $\text{Mod}(S_{0,6})$. It follows that

β and β' are conjugate after capping-off to $\text{Mod}(S_{0,6})$. In particular, β is conjugate to $\Delta^{2k}\beta'$ for some $k \in \mathbb{Z}$. \square

Though we will not need the following corollary for our larger purpose, it follows quickly from Lemma 3.0.4 and we believe it to be helpful in many other contexts.

Corollary 3.0.5. Let $h, h' \in \text{SMod}(S_g^r)$ be the lifts of braids β, β' , for $g, r \in \{1, 2\}$. Then, h and h' are conjugate in $\text{Mod}(S_g^r)$ if and only if β and β' are conjugate as braids.

Proof. For simplicity, suppose $g = 2$ and $r = 1$, though the same proof works for the other cases, with minor adjustments. If β and β' are conjugate, it is clear that h and h' are conjugate, too: we may simply lift the conjugating map to S . On the other hand, suppose h and h' are conjugate in $\text{Mod}(S)$. It follows that the capped-off maps \widehat{h} and \widehat{h}' are conjugate in $\text{Mod}(\widehat{S})$. Lemma 3.0.4 now implies that β is conjugate to $\Delta^{2k}\beta'$ for some $k \in \mathbb{Z}$. Because h and h' are conjugate in $\text{Mod}(S)$, we know that $c(h) = c(h')$ (see Theorem 2.1.4). It follows that $c(\beta) = 2c(h) = 2c(h') = c(\beta')$, whereas $c(\Delta^{2k}\beta') = c(\beta') + k$, so we must have that β and β' are conjugate as braids. \square

Returning to our main objective of proving Theorem B1, we need one last proposition before we can complete the proof.

Proposition 3.0.6. Let (S, h) be an open book decomposition with $c(h) \notin \mathbb{Z}$ and h symmetric. Suppose the pseudo-Anosov representative ψ_h has singularity type $(6; \emptyset; \emptyset)$ and dilatation $\lambda(\psi_h) = \lambda_2$. Then, (S, h) is not an open book decomposition for S^3 or \mathcal{P} .

Proof. Because ψ_h has singularity type $(6; \emptyset; \emptyset)$, we may cap-off ψ_h to a pseudo-Anosov on \widehat{S} with singularity type $(\emptyset; \emptyset; 6)$. Lanneau and Thiffeault [LT11] show that the pseudo-Anosov on \widehat{S} with foliation type $(\emptyset; \emptyset; 6)$ and dilatation λ_2 is unique, up to

conjugacy in $\text{Mod}(\widehat{S})$, inverse, and composition with the hyperelliptic involution ι on \widehat{S} . Note that the pseudo-Anosov representative ψ_α of the 5-braid $\alpha = \sigma_1\sigma_2\sigma_3\sigma_4\sigma_1\sigma_2$ studied by Ham–Song in [HS07] achieves dilatation $\lambda(\psi_\alpha) = \lambda_2$. In particular, the pseudo-Anosov representative ψ_A of the lift A of α to S achieves minimal dilatation $\lambda(\psi_A) = \lambda_2$ with the proper singularity type. It follows that $\widehat{\psi}_h$ is conjugate in $\text{Mod}(\widehat{S})$ to one of $\widehat{\psi}_A^{\pm 1}$ or $\widehat{\psi}_A^{\pm 1} \circ \iota$. This further implies that \widehat{h} is conjugate in $\text{Mod}(\widehat{S})$ to one of $\widehat{A}^{\pm 1}$ or $\widehat{A}^{\pm 1} \circ \iota$.

Because ι is freely isotopic to the lift of the 5-braid Δ^2 , we can see that $A^{\pm 1} \circ \iota$ is freely isotopic to the lift of $\Delta^2\alpha^{\pm 1}$. Since h is symmetric by assumption, it is the lift of a braid β . A is symmetric by construction, so Lemma 3.0.4 implies that β is conjugate as a braid to $\Delta^{2k}\alpha^{\pm 1}$ for some $k \in \mathbb{Z}$. In particular, if (S, h) is an open book decomposition for S^3 or \mathcal{P} , we can see that $\Delta^{2k}\alpha^{\pm 1}$ has closure either the unknot or $T(3, 5)$ for some $k \in \mathbb{Z}$.

Because S^3 and \mathcal{P} are both L-spaces, we must have $|c(\Delta^{2k}\alpha^{\pm 1})| < 2$, by [HM18]. We may deduce that $0 < c(\alpha) < 1$ because α is a positive pseudo-Anosov braid, and $\Delta^{-2}\alpha$ is a negative pseudo-Anosov braid (see Theorem 2.1.4). In particular, $k < c(\Delta^{2k}\alpha) < k + 1$. So, it suffices to check that none of the braids α , $\Delta^2\alpha^{-1}$, $\Delta^2\alpha$, or $\Delta^4\alpha^{-1}$ close up to the unknot or $T(3, 5)$. For all except α , one can use a self-linking number computation to confirm this, and one can easily perform an isotopy to see that $\widehat{\alpha} = T(2, 3)$. \square

Proof of Theorem B1. Let h be as in the statement of the theorem. Recall that since ψ_h is FPF by assumption, h is symmetric (see Theorem 2.3.1). Since (S, h) is an open book decomposition for S^3 or \mathcal{P} , both of which are L-spaces, we know $|c(h)| < 1$. So if $c(h) \neq 0$, then $c(h) \notin \mathbb{Z}$. Proposition 3.0.3 then implies that the dilatation of ψ_h is $\lambda(\psi_h) = \lambda_2$, but this contradicts Proposition 3.0.6. \square

In the stratum $(6; \emptyset; \emptyset)$, we may additionally lift the assumption that $c(h) \neq 0$:

Proposition 3.0.7. Let (S, h) be an open book decomposition for S^3 or \mathcal{P} . If $c(h) = 0$ and the pseudo-Anosov representative ψ_h has singularity-type $(6; \emptyset; \emptyset)$, then ψ_h is not FPF.

Proof. Suppose that ψ_h has no fixed points in the interior of S . As in the proof of Theorem B1, we may cap-off ψ_h to a pseudo-Anosov $\widehat{\psi}_h$ on \widehat{S} and extend the foliations preserved by ψ_h . Again, we have that these foliations are orientable. Note that if $\rho(\psi_{h*}) < 0$, then an argument identical to that of Theorem B1 will apply.

So, assuming that $\rho(\psi_{h*}) > 0$, the Lefschetz fixed point theorem then yields $\text{tr}(\widehat{\psi}_{h*}) = 2 - (-5) = 7$, because the unique fixed point p given by the boundary 6-prong singularity is unrotated (since $c(h) \in \mathbb{Z}$). Consider the Markov matrix M for a train track representative of $\widehat{\psi}_h$. It follows from a theorem of Rykken [Ryk99] that any eigenvalue of $\widehat{\psi}_{h*}$ is also an eigenvalue of M (counting multiplicity) except for possibly eigenvalues of 0 or roots of unity. Note here that a train track representative of $\widehat{\psi}_h$ has 8 real edges, so that M is an 8×8 matrix, while $\widehat{\psi}_{h*}$ is 4×4 . In particular, M has at most four more eigenvalues than $\widehat{\psi}_{h*}$, and each has absolute value at most one. Hence:

$$\text{tr}(M) \geq \text{tr}(\widehat{\psi}_{h*}) - 4 = 7 - 4 = 3.$$

On the other hand, a well-chosen train track carrying $\widehat{\psi}_h$ also carries ψ_h . In particular, by Theorem 2.2.4, we can see that $\text{tr}(M) = 0$ because ψ_h is assumed to be fixed-point-free in the interior of S , which is a contradiction. \square

Chapter 4

The strata $(2; \emptyset; 4^2)$ and $(4; \emptyset; 3^2)$

4.1 The stratum $(2; \emptyset; 4^2)$

We will need to perform some train track map analysis in this stratum. However, this case is much simpler than the next two. So, we'll also build up some notation here, and introduce the ideas that we'll develop further in the next two strata. Our goal for this section is to prove:

Theorem B2. Every pseudo-Anosov map in the stratum $(2; \emptyset; 4^2)$ has an interior fixed point.

By the discussion in the outline (section 1.3), if $h \in \text{Mod}(S)$ is a pseudo-Anosov mapping class with FPF geometric representative ψ_h , then h is the lift of a 5-braid β . If ψ_h has singularity type $(2; \emptyset; 4^2)$ then ψ_β has singularity type $(1; 1^5; 4)$, by the discussion in Section 2.3. So, Theorem B2 reduces to the following:

Proposition 4.1.1. Let β be a pseudo-Anosov 5-braid whose geometric representative ψ_β has singularity type $(1; 1^5; 4)$. Then, the lift $\psi_h : S \rightarrow S$ has an interior fixed point.

The proposition will follow from an analysis of train track maps on a special train track in the stratum $(1; 1^5; 4)$. In this stratum, there is a unique jointless standard

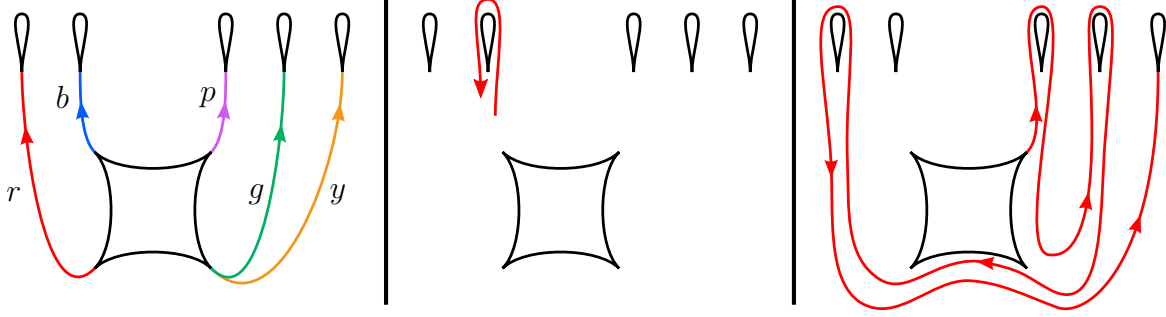


Figure 4.1: Left: the jellyfish track, with labeled edges. Center: b^+ appears in $f_\beta(r)$. Right: $f_\beta(r) = p^- g^- r^+ y^o$.

train track (up to isotopy): the “Jellyfish” track, shown in Figure 4.1. So, by Theorem C, it suffices to check braids carried by this canonical track.

For the rest of this section, τ will denote the Jellyfish track shown in 4.1. The real edges are labeled r , b , p , g , and y as in the figure, and each is oriented toward the marked points. The data $(\beta, \psi_\beta, \tau, f_\beta)$ will describe a pseudo-Anosov braid carried by τ , which lifts to a map $(h, \psi_h, \tilde{\tau}, f_h)$ on S . Note that every real edge e of τ ends at a jointless 1-marked monogon. In particular, Corollary 2.3.3 applies, so if ψ_h is FPF then e never appears in $f_\beta(e)$ for any real edge e .

For any real edge e , we may write

$$f_\beta(e) = e(1) \cdot \overline{e(1)} \cdot e(2) \cdot \overline{e(2)} \cdot \dots \cdot e(l-1) \cdot \overline{e(l-1)} \cdot e(l)$$

where each $e(i)$ is a real edge of τ , and $\overline{e(i)}$ denotes $e(i)$ with orientation reversed. To simplify and specify our notation to the relevant analysis, we will instead write

$$f_\beta(e) = e(1)^\pm e(2)^\pm \dots e(l-1)^\pm e(l)^\circ$$

Here, the \pm in $e(i)^\pm$ describes which way the image $\psi_\beta(e)$ traverses $e(i)$, as in the center of Figure 4.1, and $e(l)^\circ$ simply means that $f_\beta(e)$ ends at $e(l)$. See the right of Figure 4.1 for an example of this notation. We will also write, e.g., $f_\beta(b) = \dots r^{+\circ} \dots$ to

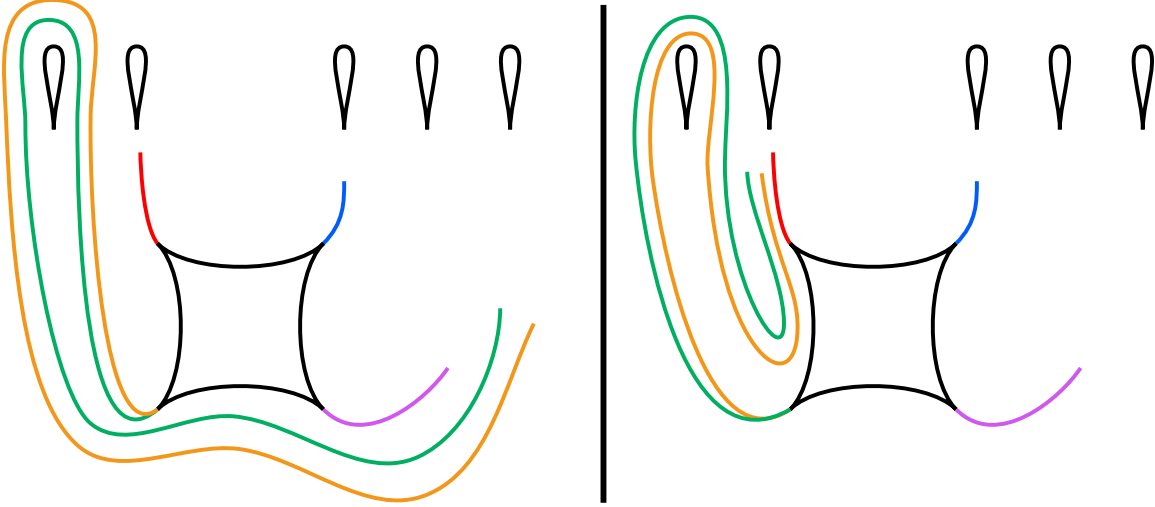


Figure 4.2: Visual aids for the proof of Lemma 4.1.2.

indicate that, at that particular instance of r in $f_\beta(b)$, we aren't sure whether $f_\beta(b)$ passes r on the right or stops there.

To begin our analysis, note that the interior infinitesimal quadrilateral of τ must rotate: if it doesn't, then, for example $f_\beta(r)$ would start at r , immediately violating the trace lemma. This rotation is determined by the first letter in $f_\beta(r)$. First, suppose that $f_\beta(r)$ starts at b .

Lemma 4.1.2. If ψ_h is FPF and $f_\beta(r)$ starts at b , then $f_\beta(g)$ does not start with r^+ and $f_\beta(y)$ does not start with r^- .

Proof. First, if $f_\beta(g)$ starts with r^+ , then so does $f_\beta(y)$. The next letter in each of $f_\beta(g)$ and $f_\beta(y)$ must be either g or y , as in the left of Figure 4.2. We know that $f_\beta(g) \neq r^+g^{\pm\circ}\dots$ by trace, so we must have $f_\beta(g) = r^+y^{\pm\circ}\dots$, but then $f_\beta(y) = r^+y^{\pm\circ}\dots$

Next, if $f_\beta(y)$ starts with r^- , then so does $f_\beta(g)$. The next letter in both $f_\beta(g)$ and $f_\beta(y)$ is b , as in the right of Figure 4.2. We can see that if $f_\beta(g) = r^-b^{+\circ}\dots$, or if $f_\beta(g) = r^-b^-r^{\pm\circ}\dots$ then $f_\beta(r) = b^+r^{\pm\circ}\dots$. A similar argument holds for $f_\beta(y)$, so we must have $f_\beta(g) = r^-b^-p^{\pm\circ}\dots$ and $f_\beta(y) = r^-b^-p^{\pm\circ}\dots$. The same type of argument holds for all of the following letters in $f_\beta(g)$ and $f_\beta(y)$, so it must be that both $f_\beta(g)$ and $f_\beta(y)$ start with $r^-b^-p^-$ and then traverse either g or y next. From here, it's

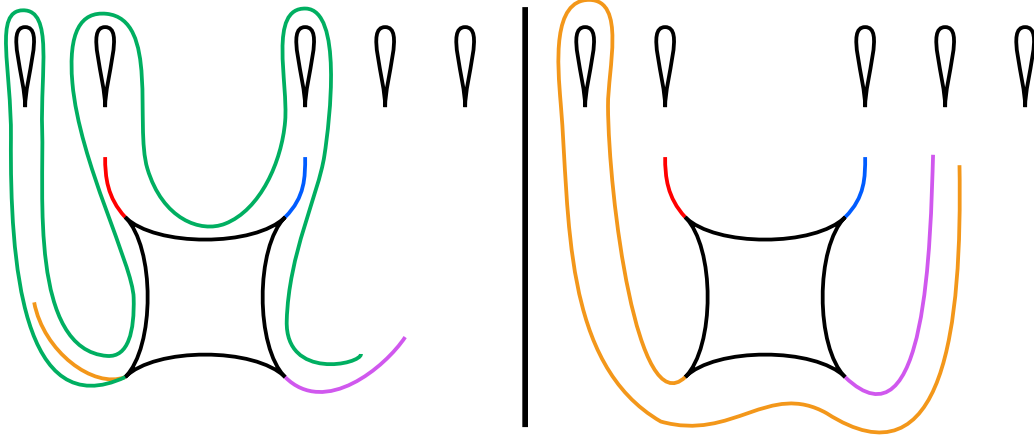


Figure 4.3: Visual aids for the proof of Lemma 4.1.3.

easy to see that either $f_\beta(g)$ passes over g or $f_\beta(y)$ passes over y . \square

Lemma 4.1.3. If ψ_h is FPF and $f_\beta(r)$ starts at b , then $f_\beta(g)$ does not start with r^- and $f_\beta(y)$ does not start with r^+ .

Proof. If $f_\beta(g)$ starts with r^- , then a very similar argument to that of the previous lemma shows that $f_\beta(g) = r^-b^-p^-y^{\pm\circ} \dots$. Note that we must have $f_\beta(g) = r^-b^-p^-y^-r^{\pm\circ} \dots$, because otherwise $f_\beta(p)$ passes over p . So, we must have $f_\beta(g) = r^-b^-p^-y^-r^-b^-p^- \dots$, as depicted on the left of Figure 4.3. But, now, $f_\beta(g)$ either eventually passes over g , or continues to spiral around the track.

If $f_\beta(y)$ starts with r^+ , then we must have $f_\beta(y) = r^+g^{\pm\circ} \dots$, as shown on the right of Figure 4.3. If $f_\beta(y) = r^+g^- \dots$ then $f_\beta(p) = g^-r^-b^{\pm\circ} \dots$. The argument here is now similar to the previous ones: if $f_\beta(p) = g^-r^-b^+ \dots$ or passes r next, then $f_\beta(r)$ passes over r . So, we must have $f_\beta(p) = g^-r^-b^-p^{\pm\circ} \dots$

It follows that $f_\beta(y) = r^+g^+p^{\pm\circ}$. A very similar argument applies for the next few letters, so $f_\beta(y) = r^+g^+p^+b^+r^+ \dots$ and either eventually stops at y or continues to spiral around the outside of the track. \square

We can conclude from the lemmas above that $f_\beta(r)$ cannot start at b : if it did, then we would have $f_\beta(g) = f_\beta(y) = r^\circ$, but both $f_\beta(g)$ and $f_\beta(y)$ cannot end at

r . The next cases for where $f_\beta(r)$ starts are almost identical. For example, if $f_\beta(r)$ starts at p , then $f_\beta(g)$ and $f_\beta(y)$ both start at b . One can then apply the analogous arguments as above to show that in this case $f_\beta(g) = f_\beta(y) = b^\circ$.

4.2 The stratum $(4; \emptyset; 3^2)$

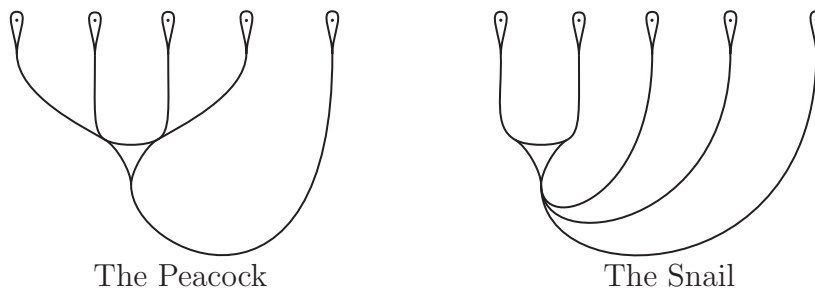


Figure 4.4: The two train track classes with no joints in the stratum $(2; 1^5; 3)$.

The goal of this section is to prove the following theorem:

Theorem B3. Let $h \in \text{Mod}(S)$ be a pseudo-Anosov mapping class with geometric representative ψ_h . Suppose that ψ_h is FPF and has singularity type $(4; \emptyset; 3^2)$. Then, (S, h) is not an open book decomposition for S^3 or for \mathcal{P} .

The first step in proving Theorem B3 is to observe the following consequence of Theorem C, which we prove at the end of Section 6:

Theorem 4.2.1. Let ψ_β be a pseudo-Anosov map on D_5 with singularity type $(2; 1^5; 3)$. Then, ψ_β is conjugate to a map carried by the Peacock train track shown in Figure 4.4.

Now, to prove Theorem B3, it suffices by Theorem 4.2.1 to look at pseudo-Anosovs carried by the lift of the Peacock track. See Figure 2.5 for an image of the lifted track. We will perform a careful analysis of train track maps on this track, together with topological arguments to study a family of braids β_n inducing a special collection of

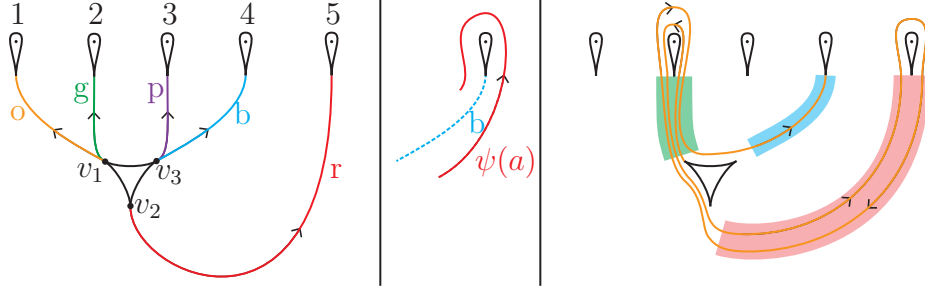


Figure 4.5: **Left:** The Peacock train track with edge labels and orientations. **Center:** $f(a)$ passes b on the right. **Right:** $f(o) = g^+r^-g^-b^o$.

train track maps. We present the relevant family of braids β_n and their corresponding train track maps in subsection 4.2.1. Then, in subsection 4.2.2, we study train track maps on the Peacock.

4.2.1 A family of braids lifting to fixed-point-free maps

For the remainder of this section, τ will be the Peacock train track depicted on the left in Figure 4.5, with edges and vertices labeled as in the figure (with edges oriented towards the punctures); β will be an arbitrary 5-braid with pseudo-Anosov data (ψ_β, τ, f) ; and h will be the lift of β to S , with pseudo-Anosov data $(\psi_h, \tilde{\tau}, \tilde{f})$, where $\tilde{\tau}$ and \tilde{f} are constructed as in subsection 2.3. An image of $\tilde{\tau}$ in this case is shown in Figure 2.5. We will use the decorations $\{+, -, \circ\}$ and other notation for the images of real edges under f_β similarly to the previous section. See the right of Figure 4.5 for an example.

Here is the family of braids which we will study:

Proposition 4.2.2. Set $\beta_n = \sigma_1^{n+2}\sigma_2\sigma_3\sigma_4\sigma_1\sigma_2\sigma_3\sigma_4^2$ for $n \geq 0$. Then, β_n is pseudo-Anosov, and the lift of $\Delta^2\beta_n^{\pm 1}$ to S is FPF. Moreover, β_n^{-1} is conjugate to a braid

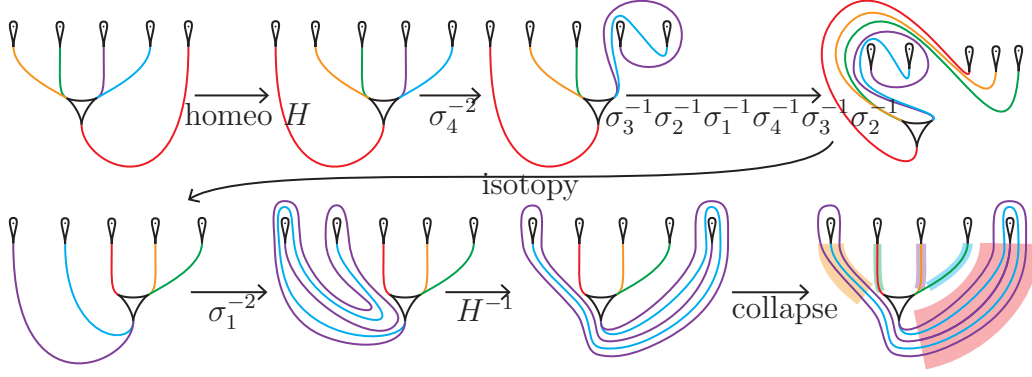


Figure 4.6: The train track map induced by $H\beta_n^{-1}H^{-1}$, where H is an orientation-preserving homeomorphism which swings r around the rest of the track.

carried by τ , which induces the train track map $f_n : \tau \rightarrow \tau$ defined by:

$$\begin{aligned}
 f_n(o) &= p^\circ & f_n(g) &= b^\circ & f_n(r) &= g^\circ \\
 f_n(p) &= \begin{cases} (r^- o^-)^{\frac{n}{2}+1} r^\circ & n \text{ even} \\ (r^- o^-)^{\frac{n+1}{2}} r^- o^\circ & n \text{ odd} \end{cases} & f_n(b) &= \begin{cases} (r^- o^-)^{\frac{n}{2}} r^- o^\circ & n \text{ even} \\ (r^- o^-)^{\frac{n+1}{2}} r^\circ & n \text{ odd} \end{cases}
 \end{aligned}$$

Proof. Figure 4.6 verifies that $H\beta_0^{-1}H^{-1}$ is carried by τ and induces the train track map $f_0 : \tau \rightarrow \tau$, where the orientation-preserving homeomorphism H is given by swinging the real edge r around the train track to the other side. For $n \geq 1$, note that $\beta_n = \sigma_1 \beta_{n-1}$, and the additional σ_1 simply adds more twists between the left-most edges before composing with H^{-1} in the last step. This additional twisting adds words of the form $(r^- o^-)$ to $f_n(p)$ and $f_n(b)$, and swaps which edges p and b end on, as in the map in the proposition statement.

We can then check that the transition matrix M_n associated to the train track map f_n is Perron–Frobenius, which will imply that $H\beta_n^{-1}H^{-1}$ is pseudo-Anosov, and hence β_n is, too. When determining the matrix M_n from the map f_n given above, it may be helpful to recall that, for real edges a, b of τ , each instance of b^\pm in $f(a)$ records the word $b\bar{b}$, and each instance of b° records just b . Regardless of the parity of n , the transition matrix is:

$$M_n = \begin{pmatrix} 0 & 0 & n+2 & n+1 & 0 \\ 0 & 0 & 0 & 0 & 1 \\ 1 & 0 & 0 & 0 & 0 \\ 0 & 1 & 0 & 0 & 0 \\ 0 & 0 & n+3 & n+2 & 0 \end{pmatrix}$$

It is straightforward to check that M_n^7 is strictly positive for all $n \geq 0$, so M_n is Perron-Frobenius.

Finally, one can check that the lift of $\Delta^2\beta_n^{\pm 1}$ to S is FPF, by using the fixed point computation of Los or Cotton-Clay in terms of train track maps in [Los10][CC09]. The point is simply that the transition matrix for the lift is traceless, the lift of Δ^2 swaps the pair of 3-prong singular points of the lift of $\beta_n^{\pm 1}$, and there are no fixed regular points arising from what Cotton-Clay calls “flips.” \square

It follows from Proposition 4.2.2 that any braid inducing the train track map $f_n : \tau \rightarrow \tau$ must be conjugate to β_n^{-1} within the mapping class group of the punctured sphere. In subsection 4.2.2, we’ll prove the following:

Proposition 4.2.3. If a pseudo-Anosov braid β is carried by τ and lifts to a FPF map h in the cover, then β is conjugate to β_n for some n , up to powers of Δ^2 .

Assuming Proposition 4.2.3, we can conclude the proof of Theorem B3:

proof of Theorem B3. Suppose for contradiction there were such an h . We can conclude that h is symmetric, and projects to a 5-braid β which is carried by the Peacock track, by Theorem 4.2.1. We can compute that, as a braid, $c(\Delta^{2k}\beta_n^{\pm 1}) = k \pm \frac{1}{2}$. Because S^3 and \mathcal{P} are both L-spaces, we know $c(h) < 1$ by [HM18], and therefore $c(\beta) < 2$. So, we can conclude that β must be conjugate to one of $\beta_n^{\pm 1}$, $\Delta^{\pm 2}\beta_n^{\mp 1}$, $\Delta^{\pm 2}\beta_n^{\pm 1}$, or $\Delta^{\pm 4}\beta_n^{\mp 1}$. Moreover, because (S, h) is an open book decomposition for S^3

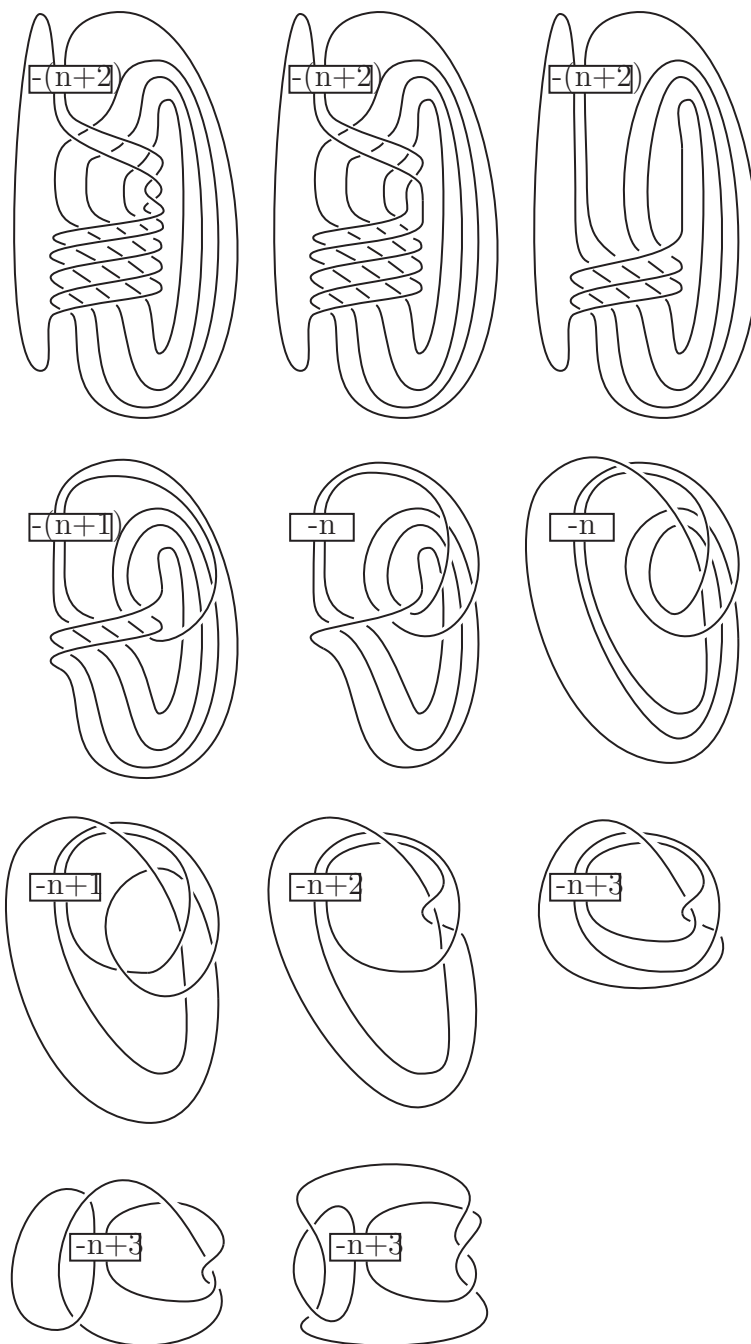


Figure 4.7: Isotopies of $\widehat{\Delta^2 \beta_n^{-1}}$ to $P(3, 3 - n, -2)$

or \mathcal{P} , we know that, as a knot, $\widehat{\beta}$ is either the unknot or $T(3, 5)$. So, it suffices to check that none of β_n , $\Delta^2\beta_n^{-1}$, $\Delta^2\beta_n$, or $\Delta^4\beta_n^{-1}$ close up to the unknot or $T(3, 5)$.

The closure $\widehat{\beta}_n$ is easily seen to be the torus knot $T(2, n + 7)$. And, figure 4.7 verifies that the closure $\widehat{\Delta^2\beta_n^{-1}}$ is the 3-stranded pretzel knot $P(3, 3 - n, -2)$. None of these knots are isotopic to the unknot or $T(3, 5)$. For $\Delta^2\beta_n$, we may simply compute the self-linking number: $sl(\Delta^2\beta_n) = 25 + n$ is greater than the maximal self-linking number $\overline{sl}(T(3, 5)) = 7$ of $T(3, 5)$ and of the unknot $\overline{sl}(\text{unknot}) = -1$. And, for $\Delta^4\beta_n^{-1}$, note that $\det \widehat{\Delta^4\beta_n^{-1}} \neq 1$: if the determinant were 1, then $\det \widehat{\beta_n^{-1}} = 1$, too, but instead $\det \widehat{\beta_n^{-1}} = \det T(2, n + 7) = n + 7 > 1$. \square

So, our goal for the remainder of this chapter will be to prove Proposition 4.2.3.

4.2.2 Train track maps on the Peacock

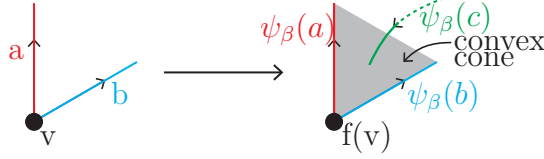
In this subsection, we will prove 4.2.3 through an extensive combinatorial analysis of train track maps on the Peacock track. We begin with some helpful lemmas to simplify the case analysis. It will be helpful to review the Trace Lemma, Lemma 2.3.2 from Section 2.3, since we will use it very frequently in this section. It will be the main tool for our case analysis.

We can start by applying the Trace Lemma to constrain the rotation of the infinitesimal triangle in the Peacock track:

Lemma 4.2.4. If ψ_h is fixed-point-free, then $f_\beta(v_i) \neq v_i$ for $i = 1, 2, 3$.

Proof. If $f_\beta(v_i) = v_i$ for some i , then $f_\beta(r)$ immediately crosses r , which is forbidden by the Trace Lemma. \square

The above lemma implies that $f_\beta(v_1) \in \{v_2, v_3\}$, and this choice also determines the images $f_\beta(v_i)$ for $i = 2, 3$. Note that there is a natural horizontal symmetry of τ induced by reversing the orientation of the disk. Composing with this symmetry takes a braid to its reverse inverse, and a braid lifts to a fixed-point-free map if and

Figure 4.8: c will be absorbed into $f(v)$.

only if its reverse inverse does. Hence, it suffices to choose either one of the images $f_\beta(v_1)$ as above. Therefore, without loss of generality, $f_\beta(v_1) = v_3$.

Lemma 4.2.5. Let a, b be any two real edges of τ with a and b adjacent at initial vertex v . Then, for any real edge c of τ , $\psi_\beta(c)$ does not intersect the convex cone determined by the initial segments of $\psi_\beta(a)$ and $\psi_\beta(b)$. See Figure 4.8 for reference.

Proof. By injectivity of ψ_β , we know that $\psi_\beta(c)$ may not cross $\psi_\beta(b)$ or $\psi_\beta(a)$. If $\psi_\beta(c)$ enters the convex cone X on the initial segments of $\psi_\beta(a)$ and $\psi_\beta(b)$, then $\psi_\beta(c)$ must either have its endpoint inside X or must leave X . The first case is not possible because c ends at a vertex of an infinitesimal monogon by assumption. Therefore $\psi_\beta(c)$ must enter and leave X . Let A and B denote the strips of the fibered surface F that collapse onto a and b , respectively. The arc $\psi_\beta(c)$ lies transverse to the fibers of F . Assume without loss of generality that $\psi_\beta(c)$ enters X along A . Since it must exit X , $\psi_\beta(c)$ must subsequently traverse either A or B . Neither case is possible, however, since a and b form a cusp: the arc $\psi_\beta(c)$ is forced to be non-smooth. \square

When a situation as in Lemma 4.2.5 arises, we say that the edge c is *absorbed into* $f_\beta(v)$. In practice, an edge being absorbed into a vertex is much easier to spot visually than by formal definition: the typical picture is the one depicted in Figure 4.8.

For the following arguments, recall that we assume without loss of generality that $f_\beta(v_1) = v_3$. The figures provided in each proof below are single scenarios appearing in each main case, not exhaustive images of every possibility. We *strongly* encourage

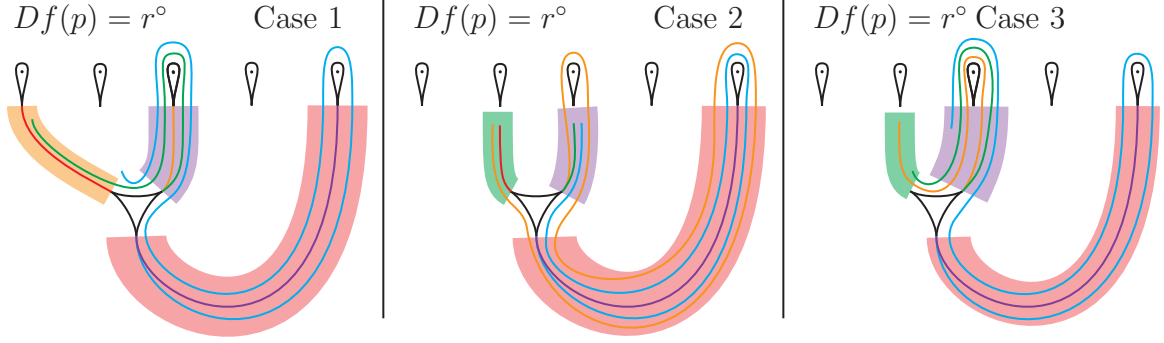


Figure 4.9: Cases for the proof of Lemma 4.2.7.

the reader to draw by hand the train track maps which are written in words, as they read through each argument.

Lemma 4.2.6. If ψ_h is fixed-point-free, then $f_\beta(r)$ does not start with o^+ or g^+ .

Proof. If $f_\beta(r)$ starts with o^+ , then we must have $f_\beta(r) = o^+r^{\pm o} \dots$, which is forbidden by the Trace Lemma. The same argument applies to g^+ . \square

Lemma 4.2.7. If ψ_h is fixed-point-free, then $f_\beta(p)$ starts with r^- .

Proof. First suppose that $f_\beta(p)$ starts with r^+ . Then, the second letter in $f_\beta(p)$ is either p or b . The former is not allowed by trace. In the latter case, note that then $f_\beta(b) = r^+b^{\pm o} \dots$, which is again ruled out by trace.

Now, suppose that $f_\beta(p) = r^o$. Note that then $f_\beta(b)$ starts with r^+ , and this further implies by trace that $f_\beta(b) = r^+p^{\pm o} \dots$. It then follows that $f_\beta(o)$ starts with $p^{\pm o}$, so we will check these three possible cases individually. See Figure 4.9.

Case 1: $f_\beta(o) = p^o$. In this case, $f_\beta(b) = r^+p^+ \dots$ and $f_\beta(g)$ starts with p^+ . By trace, it follows that $f_\beta(g) = p^+o^{\pm o} \dots$, and this in turn forces $f_\beta(r)$ to start at o . By Lemma 4.2.6, we know $f_\beta(r)$ does not start with o^+ , so $f_\beta(r)$ starts with o^- or o^c . If $f_\beta(r)$ starts with o^o , then the real edges o , p , and r are permuted, implying that the transition matrix of f is not Perron-Frobenius. Finally, if $f_\beta(r)$ starts with o^- , we can see that $f_\beta(r) = o^-p^-r^{\pm o} \dots$, which is ruled out by trace.

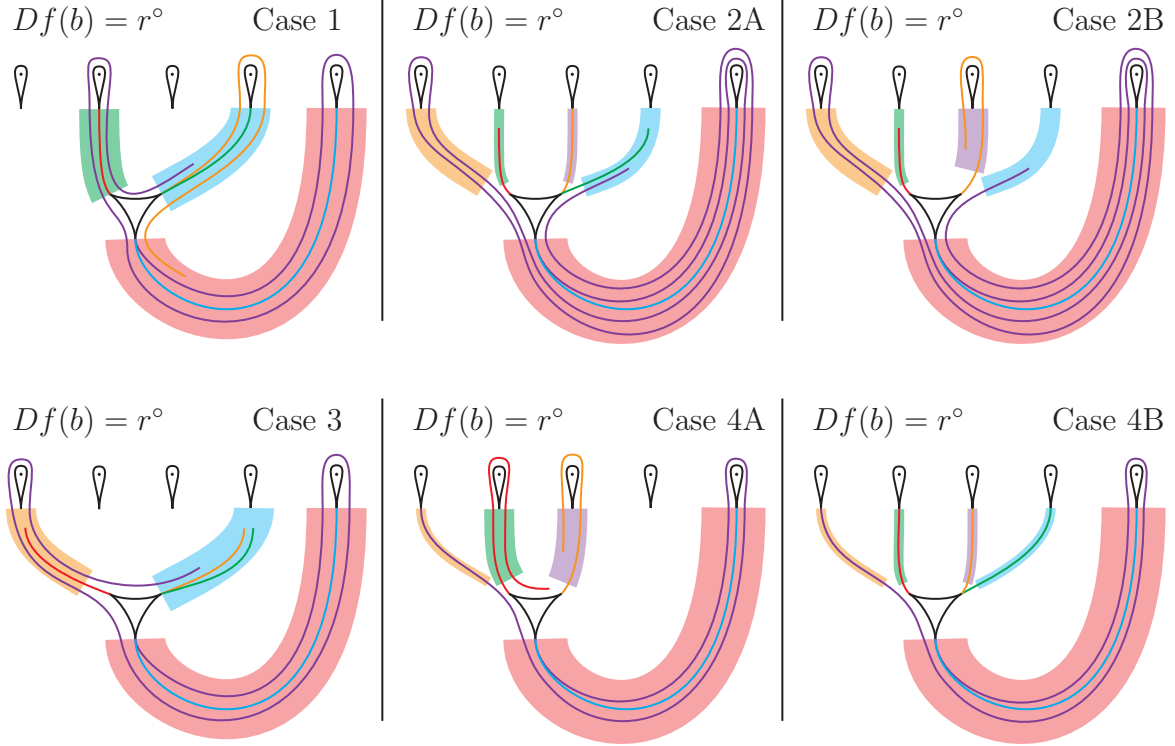


Figure 4.10: Cases for the proof of Lemma 4.2.8.

Case 2: $f_\beta(o)$ starts with p^- . In this case, we must have $f_\beta(o) = p^- r^- g^{\pm o} \dots$ by trace (or else $f_\beta(o)$ is absorbed into either $f_\beta(v_3)$ or $f_\beta(v_1)$, if it goes “inside” b or g , respectively). This further implies that $f_\beta(g) = p^- r^- g^{\pm o} \dots$, which is ruled out by trace.

Case 3: $f_\beta(o)$ starts with p^+ . Here, we have $f_\beta(o) = p^+ g^{\pm o} \dots$, and therefore $f_\beta(b) = r^+ p^+ g^{\pm o} \dots$. In particular, this forces $f_\beta(g) = p^+ g^{\pm o} \dots$, which is ruled out by trace. \square

Lemma 4.2.8. If ψ_h is fixed-point-free, then $f_\beta(b)$ starts with r^- .

Proof. By Lemma 4.2.7, we may assume $f_\beta(p)$ starts with r^- . Note that $f_\beta(b)$ cannot start with r^+ , because then one of b or p will be absorbed into $f_\beta(v_3)$.

So, suppose $f_\beta(b) = r^-$. We branch along cases for the second letter in $f_\beta(p)$. Note that if $f_\beta(p) = r^- g^+ \dots$, then $f_\beta(r)$ starts with g^+ , which contradicts Lemma 4.2.6. So, there are four cases left to consider, shown in Figure 4.10.

Case 1: $f_\beta(p) = r^-g^-...$ In this case, we must have $f_\beta(p) = r^-g^-b^{\pm\circ}...$, because otherwise p is absorbed into $f_\beta(v_3)$ (if it follows r next) or contributes trace (if it follows p next). Now note that $f_\beta(o)$ starts at b . If $f_\beta(o)$ starts with b^+ or b° , then $f_\beta(g) = b^+g^{\pm\circ}...$, which is ruled out by trace. So, $f_\beta(o)$ starts at b^- and we must have $f_\beta(o) = b^-r^-g^{\pm\circ}...$ by trace. Note that $f_\beta(g)$ does not start with b^+ by Lemma 4.2.5, so $f_\beta(g)$ must start with b^- or b° . If $f_\beta(g)$ starts with b^- , then we have $f_\beta(g) = b^-r^-g^{\pm\circ}...$, which is ruled out by trace. So, $f_\beta(g)$ starts with b° . Finally, consider cases for $f_\beta(r)$. We know $f_\beta(r)$ starts at g , and by Lemma 4.2.6, we must have that $f_\beta(r)$ starts with g^- or g° . If $f_\beta(r)$ starts with g° , then the transition matrix is not Perron-Frobenius. If $f_\beta(r)$ starts with g^- , then $f_\beta(r) = g^-b^-r^{\pm\circ}...$, which is ruled out by trace.

Case 2: $f_\beta(p) = r^-o^+...$ In this case, $f_\beta(p) = r^-o^+r^+b^{\pm\circ}...$ by trace and, by Lemma 4.2.6, it follows that $f_\beta(r)$ starts with g^- . Now, look at cases for $f_\beta(o)$.

If $f_\beta(o)$ starts with b^+ or b° then $f_\beta(g) = b^+g^{\pm\circ}...$, which is ruled out by trace. And, if $f_\beta(o)$ starts with b^- then $f_\beta(o) = b^-r^-o^{\pm\circ}...$, also ruled out by trace. If $f_\beta(o)$ starts with p^- then similarly $f_\beta(o) = p^-r^-o^{\pm\circ}...$, which is again ruled out by trace. There are two remaining subcases to consider:

Subcase 2A: $f_\beta(o)$ starts with p° . Here, consider cases for $f_\beta(g)$: $f_\beta(g)$ starts with either p^+ or $b^{\pm\circ}$. If $f_\beta(g)$ starts with p^+ then $f_\beta(g) = p^+g^{\pm\circ}...$ which is ruled out by trace. We cannot have $f_\beta(g)$ starts with b^+ because then g is absorbed into $f_\beta(v_1)$. Finally, we cannot have $f_\beta(g)$ starts with b^- or b° because then either p is absorbed into $f_\beta(v_1)$ (if $f_\beta(g)$ starts with b° or b^- , with p outside g) or g is absorbed into $f_\beta(v_3)$ (if $f_\beta(g)$ starts with b^- , and g is outside p).

Subcase 2B: $f_\beta(o)$ starts with p^+ . Here, consider cases for $f_\beta(r)$: $f_\beta(r)$ starts with either g° or g^- , by Lemma 4.2.6. If $f_\beta(r)$ starts with g° then o will be absorbed into $f_\beta(v_3)$. If $f_\beta(r)$ starts with g^- , then either o is inside r , in which case $f_\beta(r) = g^-p^-r^{\pm\circ}...$ (which is ruled out by trace); or, r is inside o , in which case o will be

absorbed into $f_\beta(v_3)$.

Case 3: $f_\beta(p) = r^- o^- \dots$. In this case, we must have $f_\beta(p) = r^- o^- b^{\pm\circ} \dots$ (otherwise p will be absorbed into $f_\beta(v_3)$ or contribute trace), which forces $f_\beta(o)$ and $f_\beta(g)$ to both start at b . If $f_\beta(o)$ starts with b^+ , then either $f_\beta(o) = b^+ o^{\pm\circ} \dots$ (which is ruled out by trace), or $f_\beta(o) = b^+ g^{\pm\circ} \dots$ in which case $f_\beta(g) = b^+ g^{\pm\circ} \dots$, too (which is again ruled out by trace). And, if $f_\beta(o)$ starts with b^- , then $f_\beta(o) = b^- r^- o^{\pm\circ} \dots$, which is ruled out by trace.

So, we must have $f_\beta(o) = b^\circ$. Note here that $f_\beta(r)$ must start with o^- or o° , by Lemma 4.2.6, and $f_\beta(g)$ must start with b^+ . Now, look at r : if $f_\beta(r)$ starts with o^- , then $f_\beta(r) = o^- b^- r^{\pm\circ} \dots$ which is ruled out by trace. Finally, if $f_\beta(r)$ starts with o° , then either g is inside p , in which case g is absorbed into $f_\beta(v_3)$, or p is inside g , in which case p will be absorbed into $f_\beta(v_1)$.

Case 4: $f_\beta(p) = r^- o^\circ$. In this case, note that $f_\beta(r)$ starts with either g^- or g° by Lemma 4.2.6, so consider subcases for $f_\beta(r)$.

Subcase 4A: $f_\beta(r)$ starts with g^- . Here, consider cases for $f_\beta(o)$. If $f_\beta(o)$ starts with b^+ or b° then $f_\beta(g) = b^+ g^{\pm\circ} \dots$, which is ruled out by trace. If $f_\beta(o)$ starts with b^- then $f_\beta(o) = b^- r^- o^- \dots$, again ruled out by trace. If $f_\beta(o)$ starts with p^- or p° then $f_\beta(r) = g^- p^- r^{\pm\circ} \dots$, ruled out by trace. And finally, if $f_\beta(o)$ starts with p^+ then either o is inside r in which case $f_\beta(r) = g^- p^- r^{\pm\circ} \dots$ (which is ruled out trace), or o is outside r in which case it will be absorbed into $f_\beta(v_3)$.

Subcase 4B: $f_\beta(r)$ starts with g° . Look first at $f_\beta(o)$. If $f_\beta(o)$ starts with p^+ or b^+ then o will be absorbed into $f_\beta(v_3)$. If $f_\beta(o)$ starts with p^- or b^- then $f_\beta(o) = p^- r^- o^{\pm\circ} \dots$ or $f_\beta(o) = b^- r^- o^{\pm\circ} \dots$, both of which are ruled out trace. So, we must have $f_\beta(o) = p^\circ$ or $f_\beta(o) = b^\circ$, and then it follows that $f_\beta(g) = b^\circ$ or $f_\beta(g) = p^\circ$, respectively, as well, after some simple analysis on $f_\beta(g)$. But, note that $f_\beta(o) = b^\circ$ and $f_\beta(g) = p^\circ$ is not possible, since ψ_β is orientation-preserving. And, $f_\beta(o) = p^\circ$ and $f_\beta(g) = b^\circ$ is not possible, because then the transition matrix is not

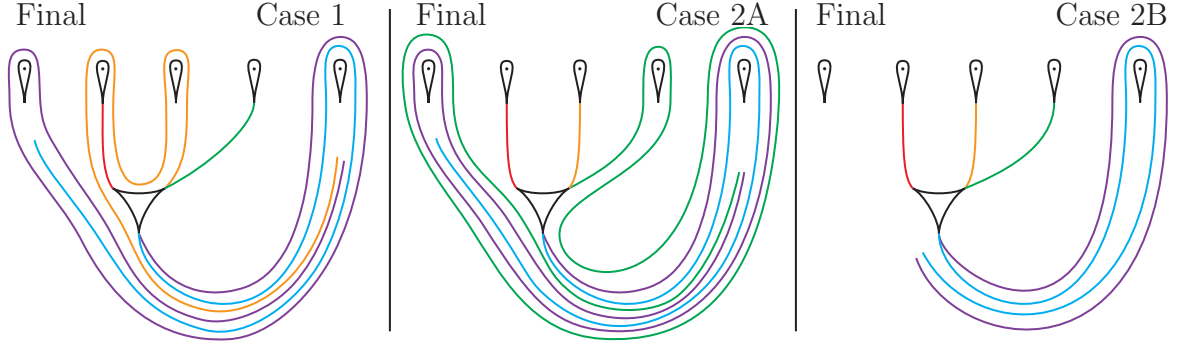


Figure 4.11: Cases for the proof of Proposition 4.2.3. In this figure, we have chosen to omit the shaded collapsing regions for readability.

Perron-Frobenius. □

Lemma 4.2.9. If ψ_h is fixed-point-free, then $f_\beta(r)$ starts with g^- or g° .

Proof. By Lemma 4.2.6, we know that $f_\beta(r)$ does not start with g^+ or r^+ , so we just need to show that $f_\beta(r)$ does not start with o^- or o° . Suppose otherwise, i.e. $f_\beta(r)$ does start with o^- or o° . By Lemmas 4.2.7 and 4.2.8, we know that $f_\beta(p)$ and $f_\beta(b)$ both start with r^- , and then because $f_\beta(r)$ starts with o^- or o° by assumption, it follows that $f_\beta(p) = r^- o^- \dots$ and $f_\beta(b) = r^- o^- \dots$. From here, we must have $f_\beta(b) = r^- o^- p^{\pm\circ} \dots$ by trace, but then $f_\beta(p) = r^- o^- p^{\pm\circ}$, which is ruled out by trace. □

We are finally ready to prove Proposition 4.2.3.

Proof of Proposition 4.2.3. Note by the discussion after Lemma 4.2.4, it suffices to assume $f_\beta(v_1) = v_3$. By Lemmas 4.2.7 and 4.2.8, we know $f_\beta(p)$ and $f_\beta(b)$ both start with r^- , and by Lemma 4.2.9 we know $f_\beta(r)$ starts with g^- or g° . From here, we branch along cases for $f_\beta(o)$. The cases where $f_\beta(o)$ starts at b can be ruled out quickly as follows.

If $f_\beta(o)$ starts with b^+ , then $f_\beta(o) = b^+ g^{\pm\circ} \dots$ by trace. But, then $f_\beta(g) = b^+ g^{\pm\circ} \dots$, which is ruled out by trace. If $f_\beta(o) = b^\circ$, then $f_\beta(g) = b^+ g^{\pm\circ} \dots$ because $f_\beta(r)$ starts with g^- or g° , and this is ruled out by trace. Finally, if $f_\beta(o)$ starts with b^- , then $f_\beta(o) = b^- r^- g^{\pm\circ} \dots$ by trace. Because $f_\beta(r)$ starts with g^- or g° , it follows that

$f_\beta(p) = r^-g^- \dots$ and $f_\beta(b) = r^-g^- \dots$. From here, we must have $f_\beta(b) = r^-g^-p^{\pm\circ} \dots$ by trace. But, then $f_\beta(p) = r^-g^-p^{\pm\circ}$, too, which is ruled out by trace.

And, note that if $f_\beta(o)$ starts with p^- , then $f_\beta(o) = p^-r^-g^{\pm\circ} \dots$ by trace. Here, we must have $f_\beta(p) = r^-g^-p^{\pm\circ} \dots$ because $f_\beta(r)$ starts with g^- or g° , which is ruled out by trace. So, we have two cases left to consider, shown in Figure 4.11.

Case 1: $f_\beta(o)$ starts with p^+ . In this case, we have $f_\beta(o) = p^+g^{\pm\circ} \dots$ by trace. If $f_\beta(o) = p^+g^{-\circ} \dots$ then $f_\beta(r)$ is either absorbed into $f_\beta(v_1)$ or passes over r . So $f_\beta(o) = p^+g + r^{\pm\circ} \dots$

Next, consider $f_\beta(g)$. If $f_\beta(g)$ starts with b^+ then g is absorbed into $f_\beta(v_1)$, and the case where $f_\beta(g)$ starts with p^+ is ruled out quickly by trace. So, $f_\beta(g)$ must start with b^- or b° . In either case, note that for both of $f_\beta(p)$ and $f_\beta(b)$, the second letter is in the set $\{o^{\pm\circ}, g^-\}$ because $f_\beta(r)$ starts with g^- or g° . If $f_\beta(p) = r^-g^- \dots$ then $f_\beta(p) = r^-g^-p^{\pm\circ} \dots$, which is ruled out by trace. So, $f_\beta(p) = r^-o^{\pm\circ} \dots$

Similarly, if $f_\beta(b) = r^-g^- \dots$ then either b is outside o , in which case b will be absorbed into $f_\beta(v_1)$, or o is outside b , in which case o will be absorbed into $f_\beta(v_3)$. So, we must have $f_\beta(b) = r^-o^{\pm\circ} \dots$, too.

Now, if $f_\beta(p) = r^-o^{+\circ} \dots$ then $f_\beta(b) = r^-o^+r^+b^{\pm\circ} \dots$ which is ruled out by trace. So, we must have $f_\beta(p) = r^-o^-r^{\pm\circ} \dots$. And, if $f_\beta(p) = r^-o^-r^{-\circ} \dots$ then $f_\beta(o) = b^+g^+r^-o^{\pm\circ} \dots$, which is ruled out by trace. So, we have instead $f_\beta(p) = r^-o^-r^+g^-p^{\pm\circ} \dots$ because $f_\beta(r)$ starts with g^- or g° , which is again ruled out by trace.

Case 2: $f_\beta(o) = p^\circ$. Here, we branch along subcases for $f_\beta(g)$. Note that if $f_\beta(g)$ starts with b^+ then g is absorbed into $f_\beta(v_1)$, and if $f_\beta(g)$ starts with p^+ then $f_\beta(g) = p^+g^{\pm\circ} \dots$, which is ruled out by trace. So we have two remaining subcases to consider:

Subcase 2A: $f_\beta(g)$ starts with b^- . Because $f_\beta(r)$ starts with either g^- or g° , note that if $f_\beta(p) = r^-g^- \dots$ then p is absorbed into $f_\beta(v_1)$. A similar argument applies to $f_\beta(b)$, so we must have both $f_\beta(p) = r^-o^{\pm\circ} \dots$ and $f_\beta(b) = r^-o^{\pm\circ} \dots$. Now, if

$f_\beta(b) = r^- o^+ \dots$ then either b is absorbed into $f_\beta(v_3)$, or $f_\beta(b) = r^- o^+ r^+ b^{\pm\circ}$, which is ruled out by trace. So, either $f_\beta(b) = r^- o^- r^{\pm\circ} \dots$ or $f_\beta(b) = r^- o^\circ$.

In the first case, note that if $f_\beta(b) = r^- o^- r^+ \dots$, then either b is absorbed into $f_\beta(v_3)$, absorbed into $f_\beta(v_1)$, or $f_\beta(b) = r^- o^- r^+ o^+ r^+ b^{\pm\circ} \dots$, which is ruled out by trace. So, we must have either $f_\beta(b) = r^- o^- r^- \dots$ or $f_\beta(b) = r^- o^- r^\circ$.

We can then see that $f_\beta(b) = (r^- o^-)^k r^- o^\circ$ or $f_\beta(b) = (r^- o^-)^{k+1} r^\circ$ for some $k \geq 0$. The argument that follows will not depend on k (with large k , all remaining strands will just turn more times along r and o), so for simplicity suppose either $f_\beta(b) = r^- o^\circ$ or $f_\beta(b) = r^- o^- r^\circ$.

First, suppose $f_\beta(b) = r^- o^\circ$. Then, we must have $f_\beta(p) = r^- o^- r^{\pm\circ} \dots$ and $f_\beta(g) = b^- r^- o^- \dots$. Note here that if $f_\beta(p) = r^- o^- r^+ \dots$ then g will be absorbed into $f_\beta(v_3)$. But, if $f_\beta(p) = r^- o^- r^- \dots$, then p will be absorbed into $f_\beta(v_3)$. This same argument will work for arbitrary k after several twists around r and o .

Next, suppose $f_\beta(b) = r^- o^- r^\circ$. The argument is very similar in this case. We must have $f_\beta(p) = r^- o^- r^- o^{\pm\circ} \dots$ and $f_\beta(g) = b^- r^- o^- r^- o^{\pm\circ} \dots$. If $f_\beta(p) = r^- o^- r^- o^- \dots$ then g will be absorbed into $f_\beta(v_3)$. And, if $f_\beta(p) = r^- o^- r^- o^+$ then either g will be absorbed into $f_\beta(v_3)$ or p will be absorbed into $f_\beta(v_1)$. As before, the same argument will work for arbitrary k after several additional twists around r and o .

Subcase 2B: $f_\beta(g) = b^\circ$. We can see that $f_\beta(r)$ cannot start with g^- , since then r will be absorbed into $f_\beta(v_1)$. So, we must have $f_\beta(r) = g^\circ$. From here, note that $f_\beta(b) = r^- o^- \dots$ because otherwise b will be absorbed into either $f_\beta(v_1)$ or $f_\beta(v_3)$. In either case, it follows that $f_\beta(p) = r^- o^- r^- \dots$ because otherwise p will be absorbed into either $f_\beta(v_1)$ or $f_\beta(v_3)$. Iterating the same argument, it is now easy to see that $f_\beta(b) = (r^- o^-)^{\frac{n}{2}} r^- o^\circ$ or $f_\beta(b) = (r^- o^-)^{\frac{n+1}{2}} r^\circ$, and $f_\beta(p) = (r^- o^-)^{(\frac{n}{2}+1)} r^\circ$ or $f_\beta(p) = (r^- o^-)^{\frac{n+1}{2}} r^- o^\circ$ for some $n \geq 0$.

One may observe that these final train track maps match identically with the ones given in Proposition 4.2.2. Proposition 4.2.2 and the subsequent discussion then

implies that the braid β is conjugate to β_n^{-1} for some n , within the mapping class group of the punctured sphere. □

Chapter 5

The stratum $(2; \emptyset; 3^4)$

There is one more stratum to consider for the proof of Theorem B. This last stratum will be a bit more challenging, so we will need to consider some additional geometry mixed into our train track analysis. Here is what we will prove:

Theorem B4. Let $h \in \text{Mod}(S)$ be a pseudo-Anosov mapping class with geometric representative ψ_h . Suppose that ψ_h is FPF and has singularity type $(2; \emptyset; 3^4)$. Then, (S, h) is not an open book decomposition for S^3 or \mathcal{P} .

Together with Theorems B1—B3, Theorem B4 will complete the proof of Theorem B, as explained in the outline (section 1.3). Note that any h from Theorem B4 is the lift of a pseudo-Anosov braid in the stratum $(1; 1^5; 3^2)$. We will show that there is a canonical track that carries all pseudo-Anosov maps in this stratum, and then check train track maps on that track.

Proposition 5.0.1. Any pseudo-Anosov map (or its reverse) in the stratum $(1; 1^5; 3^2)$ is conjugate to one carried by the Camel track on the right in Figure 5.2.

Proof. By Theorem C, any pseudo-Anosov in this stratum is carried by a jointless track. The only jointless tracks in this stratum are those shown in Figure 5.2: the Enoki pair and the Camel pair. Note that the tracks shown in pairs are related by a

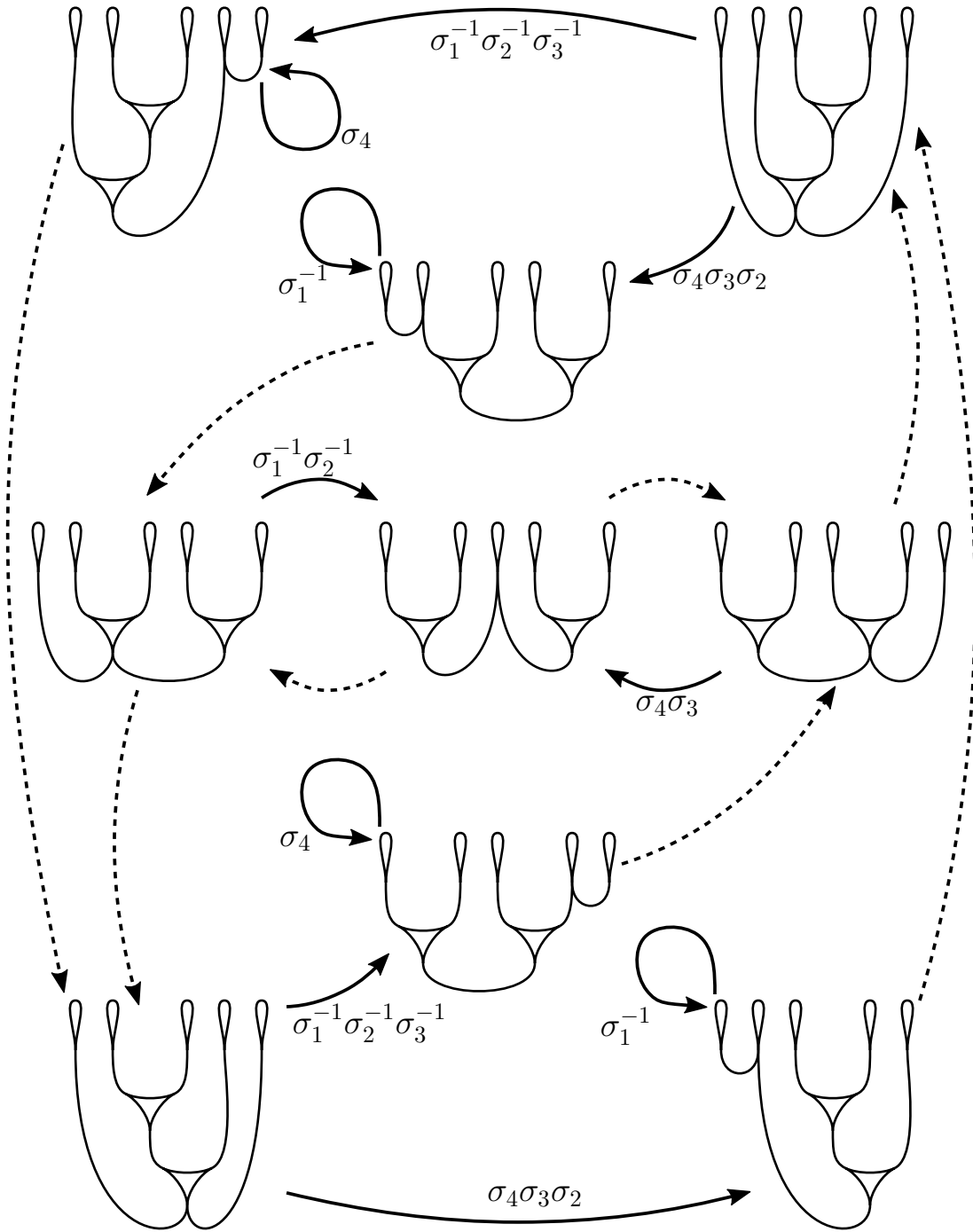


Figure 5.1: The folding automaton for the stratum $(1; 1^5; 3^2)$ on D_5 . The dashed edges induce trivial braid words. Any circuit around the outside of the automaton yields a reducible braid.

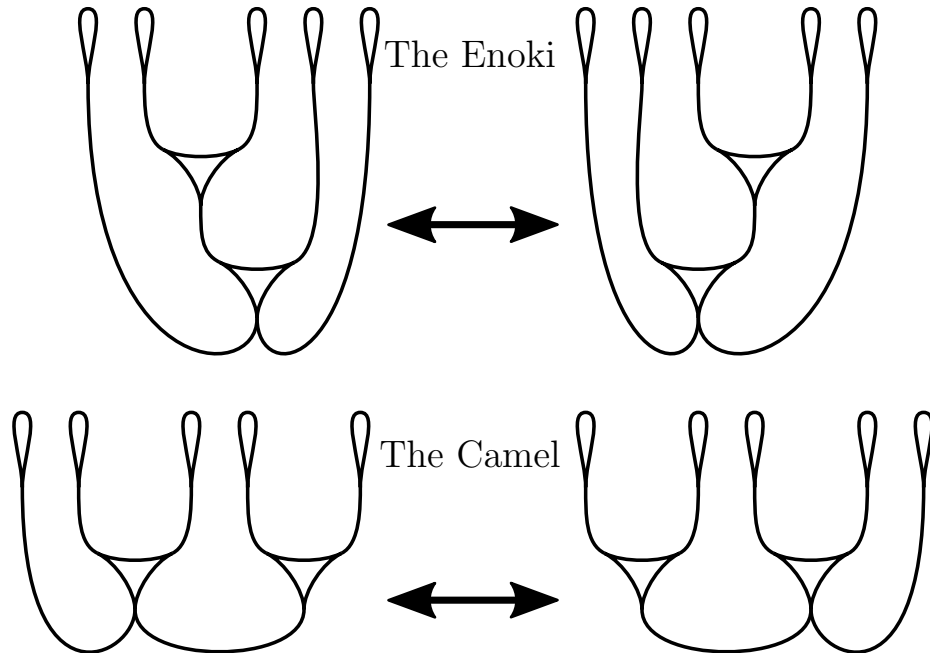


Figure 5.2: The two pairs of jointless tracks in the stratum $(1; 1^5; 3^2)$. Each pair is preserved under a horizontal reflection of the plane. Every pseudo-Anosov map is carried by one of the Camel tracks.

horizontal reflection on the disk. In particular, if a map is carried by one track from a pair, then its reverse is carried by the partner track. So, it suffices to show that any pseudo-Anosov map is carried by one of the two Camel tracks.

Ham and Song in [HS07] compute the folding automaton for train tracks in the stratum $(1; 1^5; 3^2)$. This automaton is depicted in Figure 5.1. The key fact for our proof is that any pseudo-Anosov is represented by a loop in the automaton, and a map ψ_β is carried by a track τ if and only if τ appears in the automaton loop representing ψ_β . From this perspective, changing the starting track of such a loop amounts to conjugating β .

Now, let $\beta(a, b) = \sigma_4^a \sigma_3 \sigma_2 \sigma_1^{-b} \sigma_2^{-1} \sigma_3^{-1}$. The braid $\beta(a, b)$ is given by an “outside” loop in the folding automaton, which only passes through the tracks in the corners. Note that any loop starting at one of the Enoki tracks which doesn’t pass through either Camel track is given by a product of $\beta(a, b)$ ’s. But, $\beta(a, b)$ is reducible: it is conjugate to $(\sigma_3^{-1} \sigma_4^a \sigma_3)(\sigma_2 \sigma_1^{-b} \sigma_2^{-1})$, which fixes the isotopy class of a curve sur-

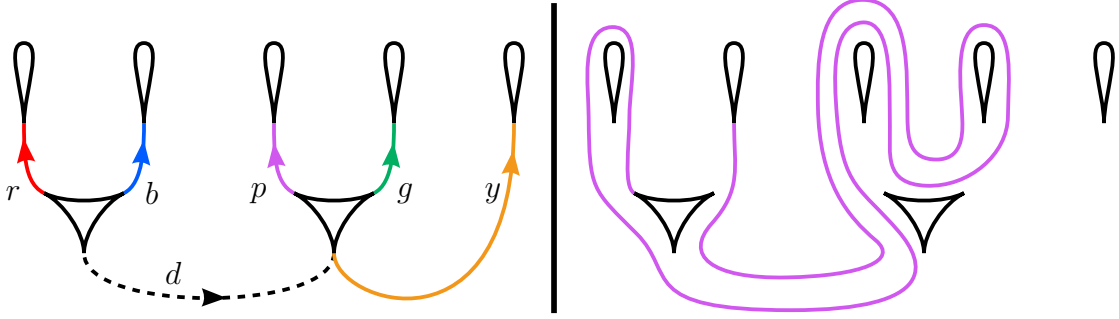


Figure 5.3: Left: the Camel track. Right: $f_\beta(p) = r^+ dp^- g^+ p^+ \bar{d}b^\circ$

rounding only the second and fourth marked points. Similarly, any braid of the form $\beta(a_1, b_1)\beta(a_2, b_2)\dots\beta(a_n, b_n)$ is reducible, where $a_i, b_i, n \geq 0$ for all i . It follows that any pseudo-Anosov in this stratum is carried by one of the Camel tracks, up to conjugation. \square

5.1 Analyzing the candidate braids

This singularity type does lead to some FPF maps ψ_h , but we will show that none of the corresponding mapping classes h describe open book decompositions for S^3 or \mathcal{P} . First, we introduce the candidates.

Proposition 5.1.1. The braids

$$\beta_1 = (\sigma_4\sigma_3)^2(\sigma_2\sigma_1)^{-2}$$

$$\beta_2 = \sigma_1^{-3}\sigma_2^{-1}\sigma_3^{-1}\sigma_2(\sigma_3\sigma_4)^2$$

$$\beta_3 = (\sigma_4\sigma_3\sigma_1^{-1}\sigma_2^{-1})^2$$

are all pseudo-Anosov and carried by τ . The images $\beta_i(\tau)$ are shown in Figure 5.4 immediately before collapsing onto τ . The braids $\Delta^{4k+2}\beta_i$ lift to FPF maps on S , for any $i \in \{1, 2, 3\}$ and any $k \in \mathbb{Z}$.

Proof. A routine isotopy rel. marked points certifies that the images $\beta_i(\tau)$ depicted

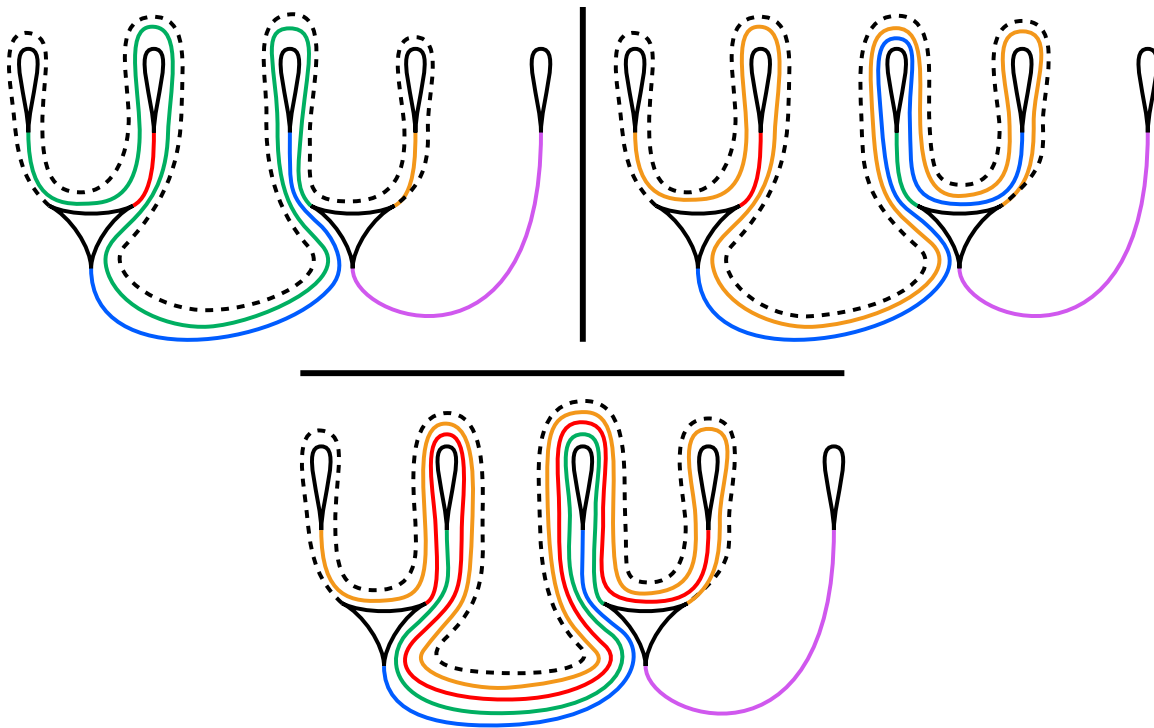


Figure 5.4: The images $\beta_i(\tau)$ before collapsing. Left: β_1 . Right: β_2 . Bottom: β_3 .

in Figure 5.4 are correct. From there, it is immediate that all three β_i are carried by τ : the images are transverse to the leaves of an appropriate fibered neighborhood of τ . To check that the braids are pseudo-Anosov, one may compute their transition matrices $M(f_{\beta_i})$ from the images depicted. The matrices are all Perron–Frobenius, so the braids are pseudo-Anosov by Proposition 2.2.4. The fact that the braids $\Delta^2\beta_i$ lift to FPF maps can be verified by e.g. XTrain [Bri00]. \square

Remark 5.1.2. The braids β_i themselves do not lift to FPF maps, since their lifts fix all four 3-pronged singularities. Composition with Δ^2 lifts to composition with the hyperelliptic involution $\iota : S \rightarrow S$, which swaps the 3-pronged singularities in pairs.

Proposition 5.1.3. If a pseudo-Anosov braid β is carried by τ and lifts to a FPF map h in the cover, then β is conjugate to some β_i , up to powers of the full twist Δ^2 .

Assuming Proposition 5.1.3, we will prove Theorem B4:

proof of Theorem B4. Suppose for the sake of contradiction that there is such an h .

Because ψ_h is fixed-point-free and the invariant foliations of ψ_h have $2 \geq 1$ boundary prongs, we can conclude that h is symmetric and projects to a pseudo-Anosov 5-braid β , by Theorem 2.3.1. It then follows that $\widehat{\beta}$ is the unknot or $T(3, 5)$, since the double branched cover over $\widehat{\beta}$ is S^3 or \mathcal{P} . And, since S^3 and \mathcal{P} are both L-spaces, we know that $|c(h)| < 1$ by [HM18], and therefore $|c(\beta)| < 2$. By Proposition 5.0.1, we know β (or its reverse) is conjugate to a map carried by the Camel track from Figure 5.2. By Proposition 5.1.3, we know β is conjugate to $\Delta^{2k}\beta_i^{\pm 1}$ for some $i, k \in \mathbb{Z}$. We can easily compute $c(\Delta^{2k}\beta_i^{\pm 1}) = k$, so we know β is conjugate to $\beta_i^{\pm 1}$ or $\Delta^2\beta_i^{\pm 1}$ for some i . It thus suffices to check that none of those braids close up to the unknot or $T(3, 5)$. For each, a determinant computation will work: their determinants are all either 5 or 9, but the determinants of the unknot and of $T(3, 5)$ are both 1. \square

The rest of this section will be devoted to proving Proposition 5.1.3. We will do that by an argument similar to that of Section 4, by carefully analyzing the possible train track maps on the canonical track τ .

5.2 Setup for the case analysis

For the rest of this section, τ will denote the Camel track shown in Figure 5.3. Denote the real edges of τ by r, b, g, p, y all oriented upward, and d (for dashed) oriented to the right. As in the previous chapter, we will simplify notation to write $e\bar{e}$ as just e for any $e \neq d$. The edge d , on the other hand, never appears in a train path twice in a row, and the orientation of d or \bar{d} will be an important consideration later. The decorations $+$, $-$, and \circ over a real edge $e \neq d$ will notate passing e on the right or left or ending there, respectively, as in Chapter 4. For d , we will only use \circ to denote ending on d . An example of this notation is shown in Figure 5.3.

Next, we will interpret the Trace Lemma (Lemma 2.3.2) on τ , and see how it interacts with the singularity type of the lifted map. Note that every real edge besides

d ends at a 1-marked monogon, so if β lifts to a FPF map under the Birman–Hilden correspondence, then e does not appear in $f_\beta(e)$ for $e \neq d$. For d , we know there are an even number of letters between any two occurrences of d or \bar{d} in $f_\beta(d)$.

To further restrict the behavior of $f_\beta(d)$, we may examine the interaction of the infinitesimal triangles with the lift ψ_h of ψ_β to the surface S . Each infinitesimal triangle contains a 3-pronged singularity, which lifts to two 3-pronged singularities in the lift. Note that h commutes with a hyperelliptic involution $\iota : S \rightarrow S$, by construction. Denote the four 3-pronged singularities in the lift by p_1, \dots, p_4 , and suppose $\iota(p_1) = p_3$, and $\iota(p_2) = p_4$. Because ψ_h permutes the set of p_i , ψ_h and ι commute, and ψ_h is FPF: it follows that there are only a few possibilities for $\psi_h(p_1), \dots, \psi_h(p_4)$. The following table lists all the possibilities.

	Case A	Case B	Case C	Case D
$\psi_h(p_1)$	p_3	p_2	p_4	p_2
$\psi_h(p_2)$	p_4	p_1	p_1	p_3
$\psi_h(p_3)$	p_1	p_4	p_2	p_4
$\psi_h(p_4)$	p_2	p_3	p_3	p_1

The upshot of this analysis is that the infinitesimal triangles in τ downstairs are fixed by f_β if and only if their lifts are sent by f_h to the other side of $\tilde{\tau}$ (case A). Conversely, the infinitesimal triangles in τ downstairs are swapped by f_β if and only if at least one of their lifts is sent to the same side of $\tilde{\tau}$ (case B: both are sent to the same side; cases C and D: one is sent to the same side, one to the opposite side).

We can then conclude by the Trace Lemma (2.3.2) that in case A (the triangles are fixed by f_β), every occurrence of d or \bar{d} in $f_\beta(d)$ occurs after an even number of preceding letters. In cases B, C, and D (the triangles are swapped by f_β), that at least one of $f_\beta(d)$ or $f_\beta(\bar{d})$ passes over d or \bar{d} after an odd number of letters.

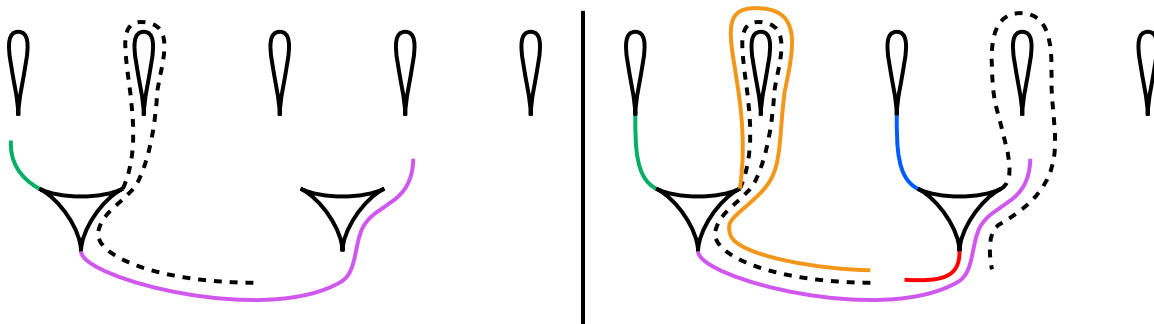


Figure 5.5: Visual aids for the proof of Lemma 5.3.1.

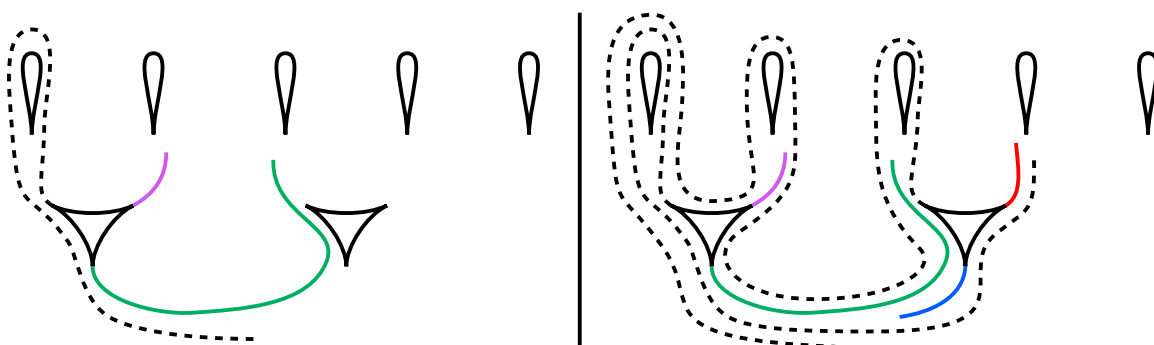


Figure 5.6: Visual aids for the proof of Lemma 5.3.2.

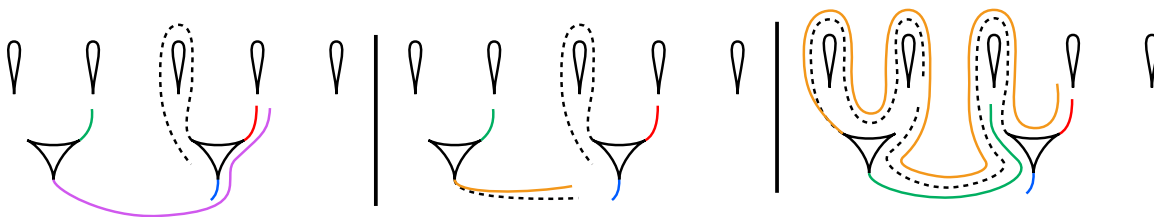


Figure 5.7: Visual aids for the proof of Lemma 5.3.3.

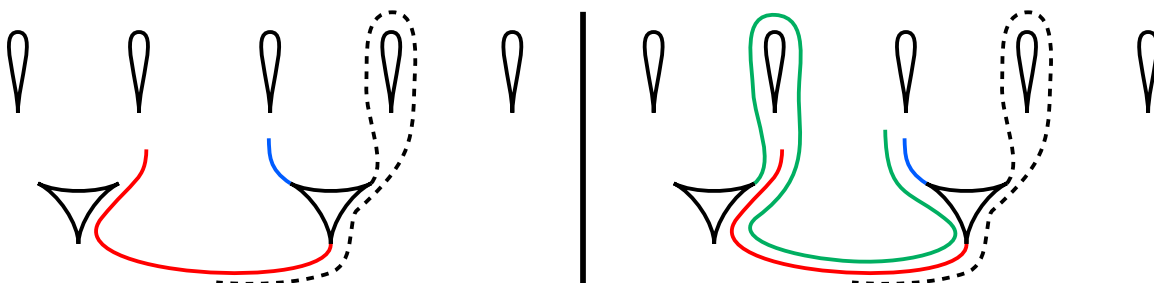


Figure 5.8: Visual aids for the proof of Lemma 5.3.4.

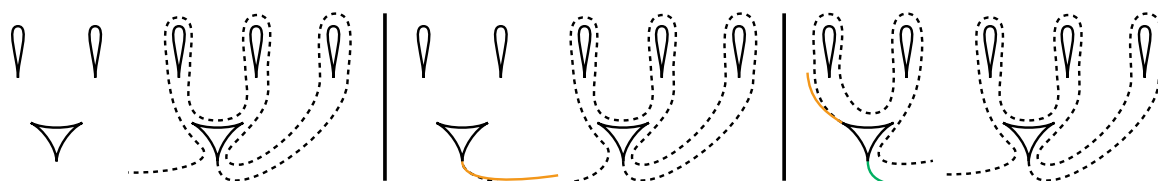


Figure 5.9: Visual aids for the proof of Lemma 5.3.5.

5.3 Cases B, C, D

Our analysis begins with cases B,C, and D above, when the triangles are swapped by f_β . In these cases, we know that at least one of $f_\beta(d)$ or $f_\beta(\bar{d})$ passes over d or \bar{d} after an odd number of letters. We will build our case analysis around which of $f_\beta(d)$ or $f_\beta(\bar{d})$ satisfies this property. In what follows, we *strongly* encourage the reader to grab some colored writing implements and draw the maps described in each proof: the symbols can only help so much.

First, assume that $f_\beta(\bar{d})$ passes over d after an odd number of letters. We know that $f_\beta(\bar{d})$ starts at b , r , or d because the triangles are swapped by f_β . But, $f_\beta(\bar{d})$ cannot start at d , because by assumption it passes over d after an odd number of letters. So, it must be that $f_\beta(\bar{d})$ starts at either b or r .

Lemma 5.3.1. If $f_\beta(\bar{d})$ starts at b , then ψ_h has a fixed point.

Proof. Because $f_\beta(\bar{d})$ starts at b , we must have that $f_\beta(g)$ starts at r and $f_\beta(p)$ starts at d . Now, note that $f_\beta(p) = dg^{\pm\circ} \dots$ by trace. It follows that either $f_\beta(g) = r^\circ$, or $f_\beta(g) = r^+b^{\pm\circ} \dots$ by trace. Note that $f_\beta(\bar{d}) = b^-d \dots$ (possibly after some initial twisting over r and b), and then it's easy to see that $f_\beta(g) = r^\circ$ or $f_\beta(g) = r^-b^-dp^{\pm\circ} \dots$. We're now in the situation pictured on the left of Figure 5.5 (with some extra information about $f_\beta(g)$ not yet shown).

From here, look at the other triangle. We don't know where each edge starts on the right triangle, so consider which edge starts at g . If $f_\beta(r)$ starts at g , then either $f_\beta(r)$ will pass over r or $f_\beta(p)$ will pass over p . We reach a similar conclusion if $f_\beta(b)$ starts at g .

The slightly harder case is if $f_\beta(d)$ starts at g . In this case, look at $f_\beta(b)$: we know it starts at p . If $f_\beta(b)$ starts with p^+ then it will pass over b . On the other hand, if $f_\beta(b)$ starts with p^- then either $f_\beta(b)$ will pass over b or $f_\beta(p)$ will pass over p . It follows that $f_\beta(b) = p^\circ$. From there, we can quickly conclude that $f_\beta(g) = r^\circ$.

Next, follow $f_\beta(\bar{d})$ and $f_\beta(y)$. We must have $f_\beta(\bar{d}) = b^-dp^-g^- \dots$ and then $f_\beta(\bar{d})$ must spiral around the track some (possibly 0) number of times before eventually passing over y . This situation is pictured on the right in Figure 5.5. Finally, note that $f_\beta(y)$ follows all of $f_\beta(\bar{d})$ to that point, so $f_\beta(y)$ passes over y . \square

Lemma 5.3.2. If $f_\beta(\bar{d})$ starts at r , then ψ_h has a fixed point.

Proof. In this case, because $f_\beta(\bar{d})$ passes over d after an odd number of letters, we must have $f_\beta(\bar{d}) = r^+d \dots$ (possibly after some initial twisting on r and b). Also, we know g starts at d , so we must have $f_\beta(g) = dp^{\pm o} \dots$ by trace. It is easy to see from here that either $f_\beta(p) = b^o$ or $f_\beta(p) = b^+r + dg^{\pm o} \dots$. This situation is pictured on the left of Figure 5.6.

Now, consider which edge starts at p ; whichever edge it is, it must start with p^+ , because otherwise $f_\beta(g)$ will be forced to pass over g . If $f_\beta(b)$ starts at p , we know $f_\beta(b) = p^+\bar{d}b^{\pm o} \dots$ and if $f_\beta(r)$ starts at p , we know $f_\beta(r) = p^+\bar{d}b^+r^{\pm o} \dots$. In either case, we've reached a contradiction by trace.

So, we are left to consider if $f_\beta(d)$ can start at p . Note that in this case, $f_\beta(d) = p^+\bar{d}b^+r^+d \dots$ and $f_\beta(\bar{d}) = r^+dg^{\pm o} \dots$. See the right of Figure 5.6. From here, because there must be an even number of letters between occurrences of d or \bar{d} in both $f_\beta(d)$ and $f_\beta(\bar{d})$, we can see that $f_\beta(d)$ and $f_\beta(\bar{d})$ will continue to spiral around the outside of the track and never meet. \square

This completes the casework under the assumption that $f_\beta(\bar{d})$ passes over d after an odd number of letters. Now, suppose instead that $f_\beta(\bar{d})$ passes over d after an even number of letters. From the argument in the previous subsection, we can then conclude that $f_\beta(d)$ passes over \bar{d} after an odd number of letters. In this case, $f_\beta(d)$ starts at one of p , g , or y .

Lemma 5.3.3. If $f_\beta(d)$ starts at p , then ψ_h has a fixed point.

Proof. In this case, we know $f_\beta(d)$ starts with p^+ , $f_\beta(b)$ starts with \bar{d} or $y^{\pm\circ}$, and $f_\beta(r)$ starts with $g^{\pm\circ}$. We don't know which edges start where on the left triangle, but consider cases for which edge starts at d . The options are: $f_\beta(p)$ starts at d , $f_\beta(\bar{d})$ starts at d , or $f_\beta(g)$ starts at d . If $f_\beta(p)$ starts at d , then we must have $f_\beta(p) = dg^{\pm\circ}\dots$ by trace. See the left of Figure 5.7. Then, we can see $f_\beta(b) = \bar{d}b^{\pm\circ}\dots$, so $f_\beta(p)$ can't start at d .

If instead $f_\beta(\bar{d})$ starts at d , then a similar argument works by looking at $f_\beta(\bar{d})$ and $f_\beta(b)$. See the center of Figure 5.7. We know the next letter in $f_\beta(\bar{d})$ is either p or g . If $f_\beta(\bar{d}) = dg^{\pm\circ}$, then we must have $f_\beta(b) = \bar{d}b^{\pm\circ}\dots$. On the other hand, if $f_\beta(\bar{d}) = dp^{\pm\circ}\dots$ then after a quick inspection of $f_\beta(y)$ and $f_\beta(\bar{d})$ we can conclude that $f_\beta(y) = dp^-g^{\pm\circ}\dots$. From here, we can check that either $f_\beta(y)$ passes over y , $f_\beta(r)$ passes over r , or $f_\beta(g)$ passes over g .

The last case is if $f_\beta(g)$ starts at d . Here, we know $f_\beta(g) = dp^{\pm\circ}\dots$ and $f_\beta(d) = p^+\bar{d}\dots$. Because by assumption $f_\beta(\bar{d})$ passes over d or \bar{d} after an even number of times, we must have $f_\beta(\bar{d}) = r^-b^-d\dots$ and we can quickly conclude that $f_\beta(d)$ and $f_\beta(\bar{d})$ must meet here. So, then, $f_\beta(d) = p^+\bar{d}b^+r^\circ$. We can then see that $f_\beta(y) = r^-b^-dp^-g^{\pm\circ}\dots$, as in the right of Figure 5.7. Looking at $f_\beta(r)$ now, we find $f_\beta(r) = g^\circ$. But, then $f_\beta(y)$ will continue spiraling around the outside of the track unless it eventually passes over y . □

Lemma 5.3.4. If $f_\beta(d)$ starts at g , then ψ_h has a fixed point.

Proof. Here, we know $f_\beta(d) = g^-\bar{d}\dots$ (it's possible that $f_\beta(d)$ twists over g and y some number of times before going to \bar{d} , but this won't matter for our analysis). It follows that $f_\beta(r) = \bar{d}b^{\pm\circ}\dots$. See the left of Figure 5.8. Now, consider cases for which edge starts at b ; whichever edge it is will start with b^- because otherwise $f_\beta(r)$ will pass over r .

If $f_\beta(\bar{d})$ starts with b^- , then $f_\beta(\bar{d}) = b^-d\dots$, so $f_\beta(\bar{d})$ passes over d after an odd number of letters. But we're assuming this is not the case. And, if $f_\beta(p)$ starts

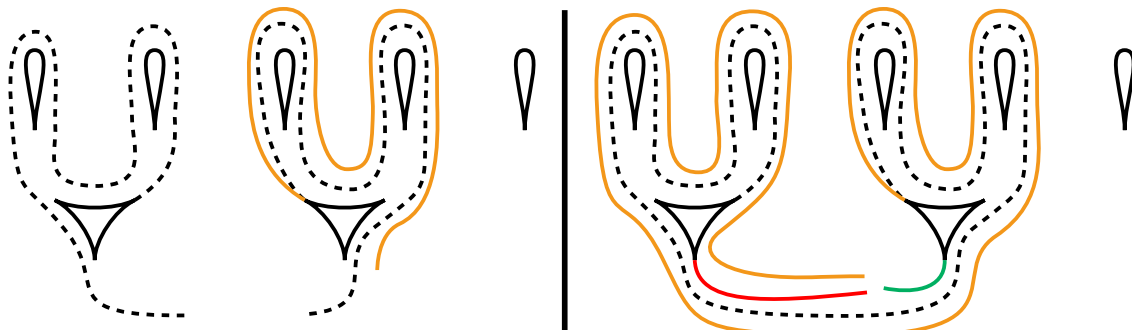


Figure 5.10: Visual aids for the proof of Lemma 5.4.1

with b^- , then it will pass over p . Finally, if $f_\beta(g)$ starts with b^- , then we must have $f_\beta(g) = b^-dp^{\pm\circ}\dots$, as in the right of Figure 5.8. From there, it is not so hard to see that either $f_\beta(b)$ passes over b or $f_\beta(g)$ passes over g . \square

Lemma 5.3.5. If $f_\beta(d)$ starts at y , then ψ_h has a fixed point.

Proof. If $f_\beta(d)$ starts at y , then we must have $f_\beta(d) = y^+g^+p^+d\dots$ (possibly after some initial twisting which will not matter for our analysis). See the left of Figure 5.9. We'll consider cases for which edge starts with d ; whichever edge it is must then continue to p afterward. In particular, we know $f_\beta(p)$ cannot start with d here.

If $f_\beta(\bar{d})$ starts with d , then we can quickly deduce that $f_\beta(d)$ and $f_\beta(\bar{d})$ must meet here, so that $f_\beta(d) = y^+g^+p^+d^\circ$. See the center of Figure 5.9. But, we then have $f_\beta(y) = dp^-g^-y^{\pm\circ}\dots$

If instead $f_\beta(g)$ starts with d , then we also know $f_\beta(\bar{d})$ and $f_\beta(y)$ both start with r . By the assumption that $f_\beta(\bar{d})$ passes over d after an even number of letters, we know $f_\beta(\bar{d}) = r^-b^-d\dots$, as in the right of Figure 5.9. We can quickly conclude that $f_\beta(d)$ and $f_\beta(\bar{d})$ must meet here, so that $f_\beta(d) = y^+g^+p^+\bar{d}b^+r^\circ$. But, then $f_\beta(y)$ will eventually pass over y . \square

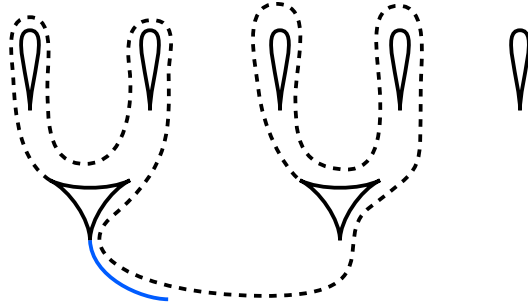


Figure 5.11: Visual aid for the proof of Lemma 5.4.2.

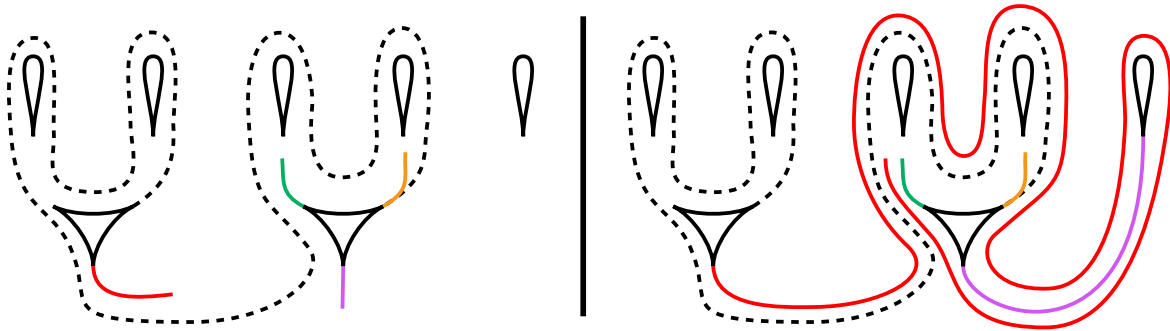


Figure 5.12: Visual aids for the proof of Lemma 5.4.3

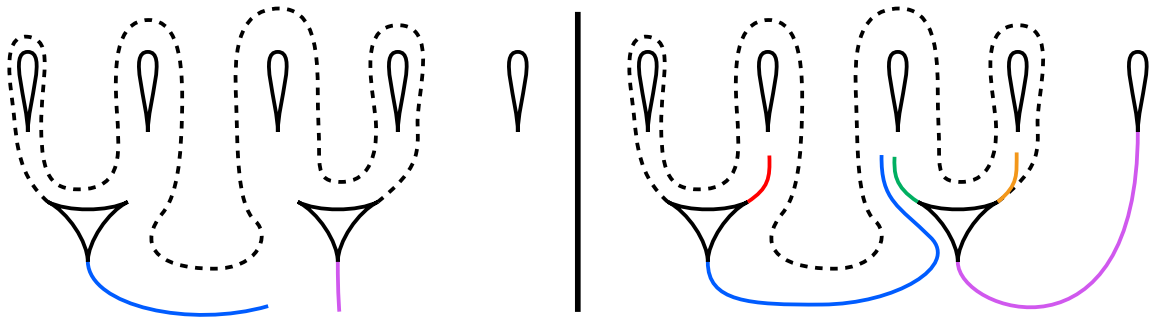


Figure 5.13: Visual aids for the proof of Lemma 5.4.4.

5.4 Case A

This is the case in which the candidate braids β_i arise, and we will see them appear at the end of this subsection. In case A, recall that we know the infinitesimal triangles of τ are fixed by f_β , and that $f_\beta(d)$ and $f_\beta(\bar{d})$ both pass over d after an even number of letters. As in cases B,C,D, we will split our argument into cases based on $f_\beta(d)$ and $f_\beta(\bar{d})$. This time, we know that $f_\beta(d)$ does not start at d and $f_\beta(\bar{d})$ does

not start at \bar{d} , because otherwise r , b , p , and g would all pass over themselves. We also know that $f_\beta(\bar{d})$ does not start at y , because then y would pass over itself.

So, we know $f_\beta(d)$ must start at r or b , and $f_\beta(\bar{d})$ must start at p or g . The four pairs of choices for $f_\beta(d)$ and $f_\beta(\bar{d})$ are the final cases to complete the proof of Proposition 5.0.1 and Theorem B4.

Lemma 5.4.1. If $f_\beta(d)$ starts at b and $f_\beta(\bar{d})$ starts at p , then ψ_h has a fixed point.

Proof. In this case, we can completely work out $f_\beta(d)$. Note that $f_\beta(d) = b^+r^+d\dots$ and $f_\beta(\bar{d}) = p^-g^-\dots$ because each needs to pass over d after an even number of letters. From here, note that $f_\beta(\bar{d}) = p^-g^-\bar{d}\dots$ because otherwise y passes over itself. This situation is pictured on the left of Figure 5.10. Now, $f_\beta(d)$ and $f_\beta(\bar{d})$ must meet here: otherwise, whichever end goes “inside” the other would have to pass over d again after an odd number of letters. For example, if $f_\beta(\bar{d})$ goes above $f_\beta(d)$ and inside it to continue towards r , then $f_\beta(\bar{d})$ will eventually be forced to pass over d after an odd number letters.

So, we must have $f_\beta(d) = b^+r^+dg^+p^\circ$. Now, note that $f_\beta(y) = p^-g^-\bar{d}r^-b^-d\dots$. From here, look at r and g . We know that $f_\beta(r)$ starts at d and $f_\beta(g)$ starts at \bar{d} . See the right of Figure 5.10. If $f_\beta(g)$ goes “above” r here, then we must have $f_\beta(g)$ will eventually pass over g . On the other hand, if $f_\beta(r)$ goes “above” g , then either $f_\beta(r)$ will pass over r , or $f_\beta(y)$ will pass over y (e.g. if $f_\beta(r) = dp^-g^-y\dots$) \square

Lemma 5.4.2. If $f_\beta(d)$ starts at r and $f_\beta(\bar{d})$ starts at p then ψ_h has a fixed point.

Proof. Just as in the previous lemma, we can completely determine $f_\beta(d)$ here. Using a very similar argument to the previous lemma, we can conclude that $f_\beta(d) = r^-b^-dg^+p^\circ$. Now, simply note that $f_\beta(b) = dg^+p^+\bar{d}b^{\pm\circ}\dots$ See Figure 5.11. \square

Lemma 5.4.3. If $f_\beta(d)$ starts at b and $f_\beta(\bar{d})$ starts at g , then ψ_h has a fixed point.

Proof. As in the previous two lemmas, we can completely determine $f_\beta(d)$: it must be $f_\beta(d) = b^+r^+dp^-b^\circ$. See the left of Figure 5.12. Next, look at $f_\beta(p)$. We must

have $f_\beta(p) = y^\circ$ by trace. From here, note that $f_\beta(r) = dp^-g^-y^-p^{\pm\circ}$... as shown on the right of Figure 5.12. To finish the proof, consider how $f_\beta(r)$ interacts with $f_\beta(g)$ and $f_\beta(y)$.

$f_\beta(r)$ must continue $f_\beta(r) = dp^-g^-y^-p^-b^{\pm\circ}$... because otherwise $f_\beta(g)$ eventually passes over g (after following $f_\beta(r)$ backwards for a while). But, in that case, $f_\beta(y)$ must eventually pass over y (note that $f_\beta(y) \neq g^\circ$, because then $f_\beta(r)$ is absorbed into the vertex of the triangle near g). \square

Lemma 5.4.4. If $f_\beta(d)$ starts at r and $f_\beta(\bar{d})$ starts at g , then either ψ_h has a fixed point, or β is conjugate (up to full twists) to one of the β_i .

Proof. By Theorem 2.2.1, it suffices to show that $f_\beta = f_{\beta_i}$ for some $i \in \{1, 2, 3\}$.

In this case, we can conclude that $f_\beta(d) = r^-b^-dp^-g^\circ$. See the left of Figure 5.13. Now, look at $f_\beta(p)$. We can quickly conclude that either $f_\beta(p) = y^\circ$ or $f_\beta(p) = \bar{d}b^{\pm\circ}$. In the latter case, $f_\beta(b) = dg^+p^+\bar{d}b^{\pm\circ}$... So, we must have $f_\beta(p) = y^\circ$, and then we also have $f_\beta(b) = dp^{\pm\circ}$. See the right of Figure 5.13.

From here, we will look at $f_\beta(b)$, $f_\beta(r)$, $f_\beta(g)$, and $f_\beta(y)$. By considering how the images of these four edges interact, we will find that f_β must be one of the train track maps induced by the β_i . To start, note that either $f_\beta(b) = dp^\circ$ or $f_\beta(b) = dp^-g^-$... (if $f_\beta(b) = dp^+$... then $f_\beta(b)$ will eventually pass over b). In the latter case, we can conclude that $f_\beta(b) = dp^-g^\circ$, because otherwise either $f_\beta(g)$ will pass over g or $f_\beta(b)$ will pass over b . So, either $f_\beta(b) = dp^\circ$ or $f_\beta(b) = dp^-g^\circ$.

If $f_\beta(b) = dp^\circ$, then $f_\beta(g) = p^+\bar{d}b^{\pm\circ}$... By looking at $f_\beta(r)$ and $f_\beta(g)$, we can conclude that either $f_\beta(g) = p^+\bar{d}b^\circ$, or $f_\beta(g) = p^+\bar{d}b^+r^\circ$. In the first case, we must then have $f_\beta(r) = b^-dp^-g^\circ$ and $f_\beta(y) = g^+p^+\bar{d}b^+r^\circ$, which is the train track map induced by β_3 . In the second case, where $f_\beta(g) = p^+\bar{d}b^+r^\circ$, we then have $f_\beta(r) = b^\circ$ and $f_\beta(y) = g^\circ$. This is the train track map for β_1 .

If instead $f_\beta(b) = dp^-g^\circ$, then $f_\beta(g) = p^\circ$ and $f_\beta(y) = g^+p^+\bar{d}b^{\pm\circ}$. Here, we must have $f_\beta(y) = g^+p^+\bar{d}b^+r^\circ$, because otherwise r will follow back along the path of $f_\beta(y)$

and get absorbed into the vertex near b . From here, we can then conclude $f_\beta(r) = b^\circ$, and this is the train track map for β_2 . \square

Chapter 6

The tight splitting

This section is devoted to developing a tool which is integral to proving Theorem C, which in turn lies at the heart of our major proof techniques. The key idea is a specialized form of “splitting,” which will allow us to determine a canonical class of train tracks carrying all pseudo-Anosovs in most strata on the marked disk. This is how we restrict our attention to pseudo-Anosovs carried only by a single track in each stratum in the previous chapters.

6.1 Splitting standardly embedded tracks

We start by adapting the following definition from Ham–Song’s notion of an elementary folding map [HS07].

Definition 6.1.1. Let $\tau, \tau_1 \hookrightarrow D_n$ be standardly embedded train tracks. A *Markov map* is a graph map $p : \tau_1 \rightarrow \tau$ that maps vertices to vertices, and is locally injective away from the preimages of vertices. An *elementary folding map* is a smooth Markov map such that for exactly one real edge α , the image $p(\alpha)$ has word length 2, while the images of all other edges have word length 1. We require that the distinguished edge α belong to a cusp (α, β) of τ_1 , and that $p(\alpha)$ be of the form

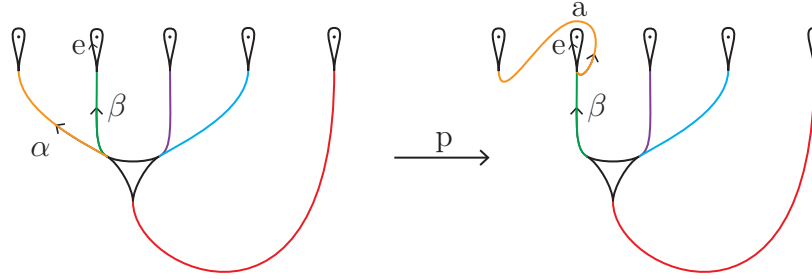


Figure 6.1: An example of an elementary folding map. The map p is the identity except at the edge α , which is mapped as a directed path to $\beta \cdot e \cdot a$.

$$p(\alpha) = p(\beta) \cdot a,$$

where a is a real edge joined to $p(\beta)$ by an infinitesimal edge.

For the purposes of this paper, an elementary folding map $p : \tau_1 \rightarrow \tau$ will be the identity map away from the distinguished real edge α . See Figure 6.1.

Remark 6.1.2. An elementary folding map in our terminology is the composition of two elementary moves in Ham-Song’s terminology [HS07].

Suppose now that (τ, ψ, f) is the data of a pseudo-Anosov ψ on D_n carried by the standardly embedded τ :

$$\begin{array}{ccc} & & \tau \\ & \nearrow f & \uparrow \text{collapse} \\ \tau & \xrightarrow{\psi} & \psi(\tau) \end{array}$$

Suppose further that $\tau_1 \hookrightarrow D_n$ is another standardly embedded train track such that there exists an elementary folding map $p : \tau_1 \rightarrow \tau$. Then there is a well-defined elementary folding map $p_\psi : \psi(\tau_1) \rightarrow \psi(\tau)$ such that the following diagram commutes:

$$\begin{array}{ccc}
 & & \tau \\
 & \nearrow f & \uparrow \text{collapse} \\
 \tau & \xrightarrow{\psi} & \psi(\tau) \\
 \uparrow p & & \uparrow p_\psi \\
 \tau_1 & \xrightarrow{\psi} & \psi(\tau_1)
 \end{array}$$

In general, we cannot expect τ_1 to carry ψ : if it did, we would then be able to complete the above commutative diagram as follows:

$$\begin{array}{ccc}
 & & \tau \\
 & \nearrow f & \uparrow \text{collapse} \\
 \tau & \xrightarrow{\psi} & \psi(\tau) \\
 \uparrow p & & \uparrow p_\psi \\
 \tau_1 & \xrightarrow{\psi} & \psi(\tau_1) \\
 & \searrow f_1 & \downarrow \text{collapse} \\
 & & \tau_1
 \end{array}$$

In this section we will discuss how to find such a τ_1 . The process of producing the data (τ_1, ψ, f_1) from (τ, ψ, f) is called *tight splitting*, or *t-splitting* for short.

Let $\tau \hookrightarrow D_n$ be standardly embedded, and let $v \in \tau$ be a switch. The *link* of v is the collection $\text{Lk}(v)$ of edges of τ incident to v . The elements of $\text{Lk}(v)$ inherit a natural counterclockwise cyclic order e_1, \dots, e_k . A subset $C \subseteq \text{Lk}(v)$ is *connected* if whenever $e_i, e_j \in C$ and $i < j$, then either

1. $e_{i+1}, \dots, e_{j-1} \in C$, or
2. $e_{j+1}, \dots, e_k, e_1, \dots, e_{i-1} \in C$.

The collections

$$R(v) = \{\text{real edges in } \text{Lk}(v)\}, \quad I(v) = \{\text{infinitesimal edges in } \text{Lk}(v)\}$$

are connected. We index the elements of $\text{Lk}(v)$ so that the real edges are e_1, \dots, e_m

under the cyclic order. In other words, from the perspective of v facing its real edges, e_1 is the real edge furthest to the right and e_m is the edge furthest to the left.

Definition 6.1.3. The *right extremal edge* of v is $r(v) = e_1$, and the *left extremal edge* is $l(v) = e_m$. If $R(v) = \{e\}$ is a singleton, then we set $e = l(v) = r(v)$.

If v is a switch at an infinitesimal loop of τ , we treat each end of the loop as a distinct element of $\text{Lk}(v)$. Hence $I(v)$ always consists of two elements, i_l and i_r . These are defined so that, under the cyclic order, we have

$$l(v) < i_l < i_r < r(v).$$

Definition 6.1.4. We denote by v_l the switch of τ at the other end of i_l from v . Similarly, we denote by v_r the switch of τ at the other end of i_r from v . In the case that v is at a loop of τ , we set $v_l = v_r = v$.

From now on, we set the convention that, for a given switch v of τ , all edges in $R(v)$ are oriented into v as paths.

Definition 6.1.5. Let $\tau \hookrightarrow D_n$ be a standardly embedded train track. Let v be a switch of τ . Fix a train track map $f : \tau \rightarrow \tau$. We say that v *splits tightly to the left* or *l-splits* if for every real edge $x \subseteq \tau$ the following two conditions hold:

1. Whenever $l(v)$ appears in the train path $f(x)$, it is followed by $\overline{r(v_l)}$, and
2. whenever $\overline{l(v)}$ appears in the train path $f(x)$, it is preceded by $r(v_l)$.

Similarly, we say that v *splits tightly to the right* or *r-splits* if for every real edge $x \subseteq \tau$ the following two conditions hold:

1. Whenever $r(v)$ appears in the train path $f(x)$, it is followed by $\overline{l(v_r)}$, and
2. whenever $\overline{r(v)}$ appears in the train path $f(x)$, it is preceded by $l(v_r)$.

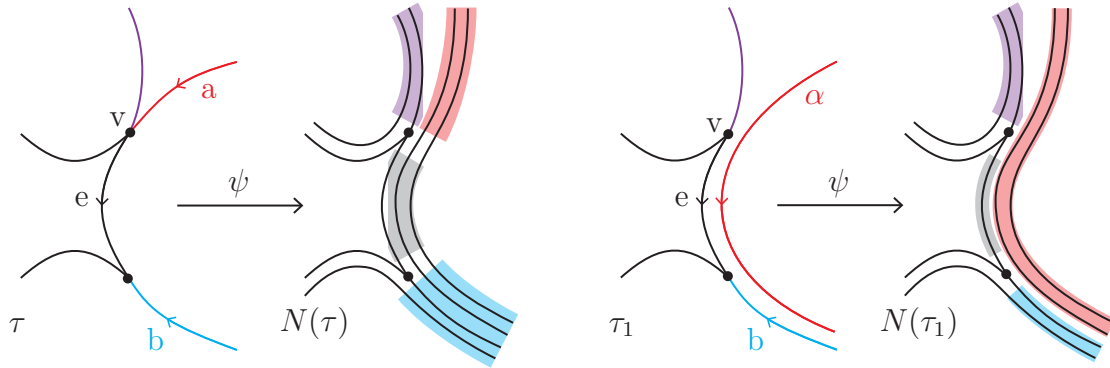


Figure 6.2: **Left:** part of a train track τ and the image of a pseudo-Anosov ψ carried by τ . Here ψ induces a train track map $f : \tau \rightarrow \tau$ for which v splits tightly to the right. **Right:** The train track τ_1 after r -splitting v , and the action of ψ on τ_1 . Note in particular that ψ has not changed, only τ and its fibered neighborhood $N(\tau)$. In each row, the highlighted regions are collapsed by a deformation retraction onto the corresponding edges.

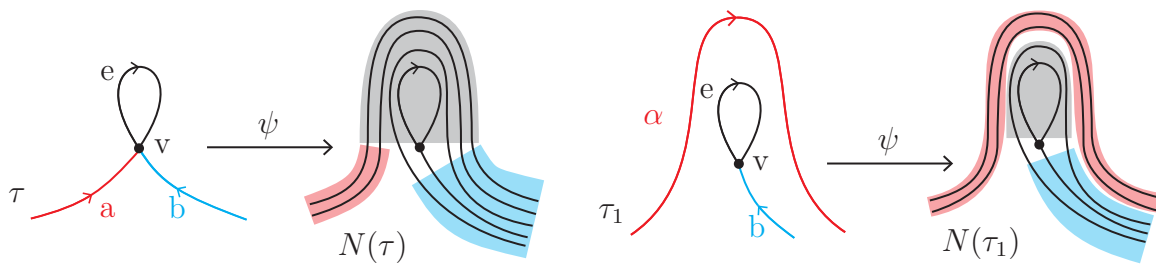


Figure 6.3: **Left:** another train track τ and map $f : \tau \rightarrow \tau$ for which v splits tightly to the right. **Right:** the train track τ_1 after r -splitting v .

In either case, we say that v *splits tightly*, or that v *t-splits*. See Figures 6.2 and 6.3.

If v splits tightly, we define a new train track that maps to τ by an elementary folding map. In this way, we view splitting as an inverse operation to folding. In what follows we will restrict our attention to the case that v tightly splits to the left: all definitions are analogous if v splits tightly to the right. To obtain these analogous statements and proofs, one need only replace all l 's with r 's and vice versa.

Suppose v l -splits. Define τ_v^l to be the standardly embedded train track obtained by deleting $l(v)$ and replacing it with a real edge α such that

1. As a directed edge, $\alpha(0) = l(v)(0)$ and $\alpha(1) = r(v_l)(1)$.
2. The edge α forms a bigon (i.e. a two-cusped disk) with the train path $l(v) \cdot \overline{r(v_l)}$, and there is an isotopy rel the punctures of D_n so that α lies transverse to the leaves of the fibered neighborhood of τ .

The standardly embedded track τ_v^l comes equipped with a natural elementary folding map $p : \tau_v^l \rightarrow \tau$, defined by

$$p(x) = \begin{cases} x & x \neq \alpha \\ l(v) \cdot \overline{r(v_l)} & x = \alpha \end{cases}$$

Definition 6.1.6. If v splits tightly to the left, then the map $p : \tau_v^l \rightarrow \tau$ is called a *tight left split* or an *l -split* of τ . We analogously define the *tight right split* or *r -split* $p : \tau_v^r \rightarrow \tau$.

Proposition 6.1.7. Suppose (τ, ψ, f) is the data of a pseudo-Anosov carried by the standardly embedded train track τ :

$$\begin{array}{ccc} & & \tau \\ & \nearrow f & \uparrow \text{collapse} \\ \tau & \xrightarrow{\psi} & \psi(\tau) \end{array}$$

If v l -splits, then τ_v^l carries ψ . Hence the above diagram may be completed to the commutative diagram

$$\begin{array}{ccc}
 & & \tau \\
 & \nearrow f & \uparrow \text{collapse} \\
 \tau & \xrightarrow{\psi} & \psi(\tau) \\
 \uparrow p & & \uparrow p_\psi \\
 \tau_v^l & \xrightarrow{\psi} & \psi(\tau_v^l) \\
 & \searrow f_v^l & \downarrow \text{collapse} \\
 & & \tau_v^l
 \end{array}$$

where f_v^l is a train track map.

Proof. Let $F \subseteq D_n$ be a fibered surface for ψ from which the Bestvina-Handel algorithm produces τ . Let L, I , and R denote the strips of F collapsing to the (unoriented) edges $l(v)$, i_l , and $r(v_l)$ of τ , respectively. Deleting L and replacing it with a strip A collapsing to α produces a new fibered surface F' from which the algorithm produces τ_v^l . The fact that F' is a fibered surface for ψ follows from the fact that v l -splits: any strip of $\psi(F)$ passing through L in fact passes through all three of L, I , and R in order, and hence after an isotopy we may arrange for the strip to pass through A instead. Furthermore, since α is isotopic to $l(v) \cdot i_l \cdot \overline{r(l_v)}$ and $\psi(L)$, $\psi(I)$, and $\psi(R)$ may be isotoped into F' , it follows that $\psi(A)$ may be isotoped into F' as well. \square

Proposition 6.1.8. Suppose that v l -splits and let M and M_v be the transition matrices of $f : \tau \rightarrow \tau$ and $f_v^l : \tau_v^l \rightarrow \tau_v^l$, respectively. Then

$$M_v = P^{-1}MP,$$

where P is the transition matrix of the elementary folding map $p : \tau_v^l \rightarrow \tau$: that is, if $l(v)$ is the j th edge and $r(v_l)$ is the i th edge, then we have

$$P = I_n + D_{i,j},$$

where τ has n real edges, I_n is the identity, and $D_{i,j}$ is the square matrix with a 1 in the (i, j) -entry and 0's elsewhere.

Proof. We will argue that we have the following commutative diagram:

$$\begin{array}{ccc} \tau_v^l & \xrightarrow{f_v^l} & \tau_v^l \\ \downarrow p & & \downarrow p \\ \tau & \xrightarrow{f} & \tau \end{array}$$

From this the claim will follow, since each of the arrows is a Markov map, and so upon passing to transition matrices we obtain the relation

$$PM_v = MP.$$

Suppose x is an edge of τ_v^l . By the definition of p we have

$$(f \circ p)(x) = \begin{cases} f(x) & x \neq \alpha \\ f(l(v)) \cdot f(\overline{r(v_l)}) & x = \alpha \end{cases}$$

On the other hand, we must understand the map $f_v^l : \tau_v^l \rightarrow \tau_v^l$ in order to analyze the composition $p \circ f_v^l$. For any edge $y \in \tau$, define $f'(y)$ to be the word obtained from the train path $f(y)$ by replacing each instance of $l(v) \cdot \overline{r(v_l)}$ with α and each instance of $r(v_l) \cdot \overline{l(v)}$ with $\bar{\alpha}$. In other words, $f'(x)$ is the unique word such that

$$p(f'(x)) = f(x).$$

If $x \neq \alpha$ is an edge of τ_v^l , then $f_v^l(x) = f'(x)$. If $x = \alpha$, then $f_v^l(x) = f_v^l(\alpha) = f'(l(v)) \cdot f'(\overline{r(v_l)})$. In either case, we obtain the formula

$$(p \circ f_v^l)(x) = \begin{cases} f(x) & x \neq \alpha \\ f(l(v)) \cdot f(\overline{r(v_l)}) & x = \alpha \end{cases}$$

This agrees with the formula for $f \circ p$, so the proof is complete. \square

Recall that by the Perron-Frobenius theorem, the dilatation of ψ is a simple eigenvalue of the transition matrix M , and there exists a positive right λ -eigenvector μ of M . For a fixed choice of μ we will denote by $\mu(x)$ the entry of μ corresponding to the real edge x .

Corollary 6.1.9. Let (τ, ψ, f) be the data of a pseudo-Anosov carried by a standardly embedded train track. Let M be the transition matrix for $f : \tau \rightarrow \tau$, and let λ be the dilatation of f . Fix a positive right λ -eigenvector μ of M . If v l -splits then $\mu_v = P^{-1}\mu$ is a positive right λ -eigenvector of M_v . Consequently,

$$\mu(l(v)) < \mu(r(v_l)).$$

Proof. Since $M_v = P^{-1}MP$, it immediately follows that $\mu_v = P^{-1}\mu$ is a right λ -eigenvector of M_v . At least one entry of μ_v is positive, since $\mu_v(\alpha) = \mu(l(v)) > 0$. Therefore μ_v is positive, since the Perron-Frobenius theorem states that λ is a simple eigenvalue of M_v and has a positive eigenvector.

To see that $\mu(l(v)) < \mu(r(v_l))$, observe that

$$0 < \mu_v(r(v_l)) = \mu(r(v_l)) - \mu(l(v)).$$

\square

Example 6.1.10. Here is an extended example of a sequence of t -splits. The maps appearing in this example are closely related to the maps studied in Section 4.2. Let

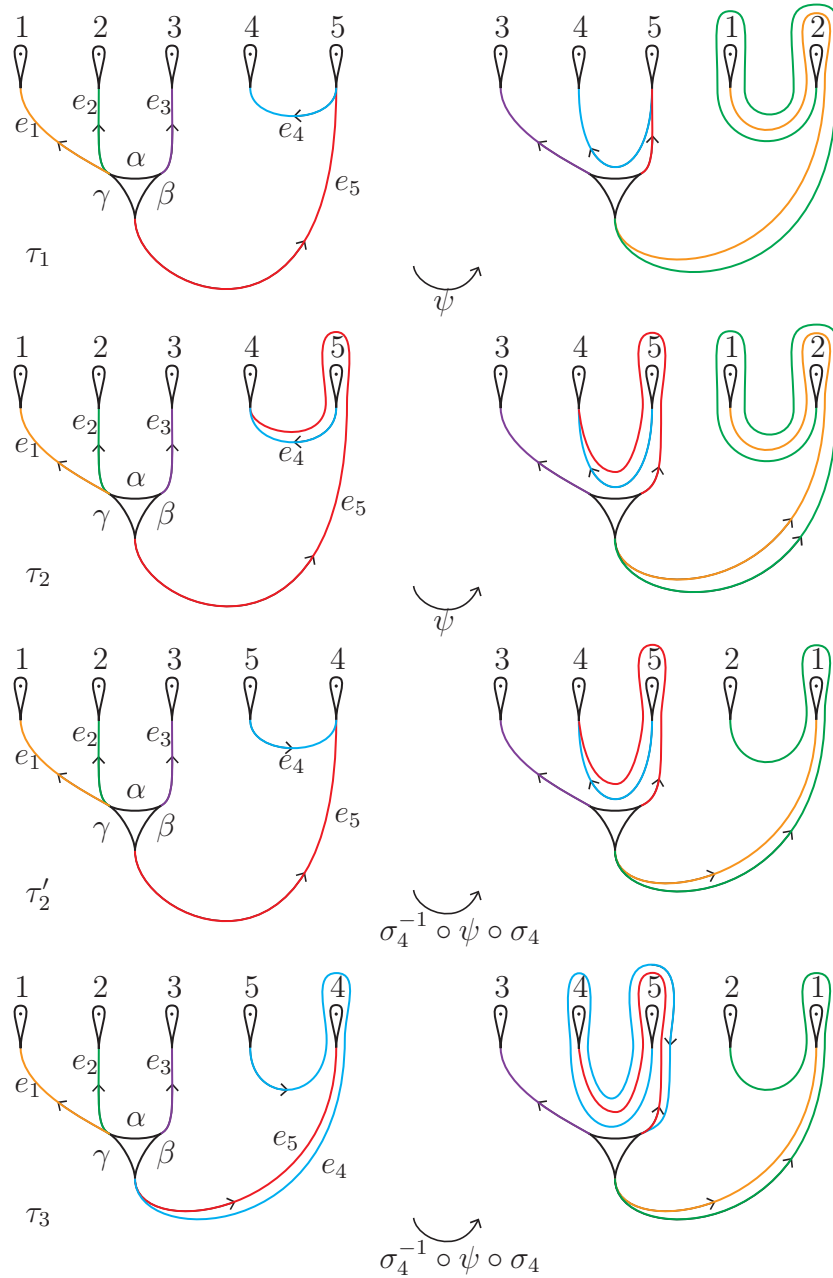


Figure 6.4: The track τ_1, τ_2 carries ψ . The track $\tau'_2 = \sigma_4^{-1}(\tau_2)$ carries $\sigma_4^{-1} \circ \psi \circ \sigma_4$. The track τ_3 carries $\sigma_4^{-1} \circ \psi \circ \sigma_4$.

(τ, ψ, f) be the data of the pseudo-Anosov represented in Figure 6.4. The transition matrix for $f : \tau \rightarrow \tau$ is

$$M_1 = \begin{pmatrix} 0 & 0 & 1 & 0 & 0 \\ 0 & 0 & 0 & 1 & 0 \\ 0 & 0 & 0 & 1 & 1 \\ 1 & 2 & 0 & 0 & 0 \\ 1 & 1 & 0 & 0 & 0 \end{pmatrix}.$$

The characteristic polynomial of M_1 is $\chi(t) = (t+1)(t^4 - t^3 - t^2 - t + 1)$. The dilatation of ψ is the root λ of this polynomial with largest absolute value. A positive right λ -eigenvector for M_1 is

$$\mu_1 = \begin{pmatrix} \mu_1(e_1) \\ \mu_1(e_2) \\ \mu_1(e_3) \\ \mu_1(e_4) \\ \mu_1(e_5) \end{pmatrix} = \begin{pmatrix} 2 + 5\lambda - \lambda^2 - \lambda^3 \\ -2 - 2\lambda + \lambda^2 + \lambda^3 \\ 1 + \lambda + 4\lambda^2 - 2\lambda^3 \\ -1 - \lambda - \lambda^2 + 2\lambda^3 \\ 3 \end{pmatrix} = \begin{pmatrix} 2.537\dots \\ 2.628\dots \\ 4.370\dots \\ 4.526\dots \\ 3 \end{pmatrix}$$

One can see that the vertex at loop 5 splits tightly to the left. Performing this l -split produces the track τ_2 , which also carries ψ . See Figure 6.4. The transition matrix of the l -split $p_1 : \tau_2 \rightarrow \tau_1$ is

$$P_1 = \begin{pmatrix} 1 & 0 & 0 & 0 & 0 \\ 0 & 1 & 0 & 0 & 0 \\ 0 & 0 & 1 & 0 & 0 \\ 0 & 0 & 0 & 1 & 1 \\ 0 & 0 & 0 & 0 & 1 \end{pmatrix} = I_5 + D_{4,5}$$

and the transition matrix for $f_2 : \tau_2 \rightarrow \tau_2$ is

$$M_2 = P_1^{-1}M_1P_1 = \begin{pmatrix} 0 & 0 & 1 & 0 & 0 \\ 0 & 0 & 0 & 1 & 1 \\ 0 & 0 & 0 & 1 & 2 \\ 0 & 1 & 0 & 0 & 0 \\ 1 & 1 & 0 & 0 & 0 \end{pmatrix}$$

which has right λ -eigenvector

$$\mu_2 = P_1^{-1}\mu_1 = \begin{pmatrix} \mu_2(e_1) \\ \mu_2(e_2) \\ \mu_2(e_3) \\ \mu_2(e_4) \\ \mu_2(e_5) \end{pmatrix} = \begin{pmatrix} \mu_1(e_1) \\ \mu_1(e_2) \\ \mu_1(e_3) \\ \mu_1(e_4) - \mu_1(e_5) \\ \mu_1(e_5) \end{pmatrix} = \begin{pmatrix} 2.537\dots \\ 2.628\dots \\ 4.370\dots \\ 1.526\dots \\ 3 \end{pmatrix}$$

We may conjugate by σ_4^{-1} to obtain the track τ'_2 , which is slightly easier to read. See Figure 6.4. This move is a standardizing braid move in the language of [KLS02]. It is not a t -split and is purely cosmetic. It does not alter the transition matrix or any other relevant dynamical information.

We can now see that the switch at loop 4 splits tightly to the right. Performing this r -split produces the track τ_3 , which also carries $\sigma_4^{-1} \circ \psi \circ \sigma_4$. See Figure 6.4. The transition matrix of the r -split $p_2 : \tau_3 \rightarrow \tau_2$ is

$$P_2 = \begin{pmatrix} 1 & 0 & 0 & 0 & 0 \\ 0 & 1 & 0 & 0 & 0 \\ 0 & 0 & 1 & 0 & 0 \\ 0 & 0 & 0 & 1 & 0 \\ 0 & 0 & 0 & 1 & 1 \end{pmatrix} = I_5 + D_{5,4}$$

and the transition matrix for $f_3 : \tau_3 \rightarrow \tau_3$ is

$$M_3 = P_2^{-1}M_2P_2 = \begin{pmatrix} 0 & 0 & 1 & 0 & 0 \\ 0 & 0 & 0 & 2 & 1 \\ 0 & 0 & 0 & 3 & 2 \\ 0 & 1 & 0 & 0 & 0 \\ 1 & 0 & 0 & 0 & 0 \end{pmatrix}$$

which has right λ -eigenvector

$$\mu_3 = P_2^{-1}\mu_2 = \begin{pmatrix} \mu_2(e_1) \\ \mu_2(e_2) \\ \mu_2(e_3) \\ \mu_2(e_4) \\ \mu_2(e_5) - \mu_2(e_4) \end{pmatrix} = \begin{pmatrix} \mu_1(e_1) \\ \mu_1(e_2) \\ \mu_1(e_3) \\ \mu_1(e_4) - \mu_1(e_5) \\ 2\mu_1(e_4) - \mu_1(e_4) \end{pmatrix} = \begin{pmatrix} 2.537\dots \\ 2.638\dots \\ 4.370\dots \\ 1.526\dots \\ 1.473\dots \end{pmatrix}$$

6.2 Switch rigidity

In this section we investigate when a t -split is possible at a given switch, identifying the essential obstruction. We call this obstruction *switch rigidity* and show that it is uncommon. Indeed, the orbit of every switch contains a switch that is t -splittable (cf. Proposition 6.2.7).

Let v be a switch of the train track τ . Recall that $\text{Lk}(v)$ is the set of edges of τ incident to v . A Markov map $f : \tau \rightarrow \tau$ induces a map $Df : \text{Lk}(v) \rightarrow \text{Lk}(f(v))$ as follows. Orient all edges in $\text{Lk}(v)$ and $\text{Lk}(f(v))$ away from v and $f(v)$, respectively. Then

$$Df(a) = b \text{ if } f(a) \text{ begins with } b.$$

As a consequence of the Bestvina-Handel algorithm, all elements of $R(v)$ belong to

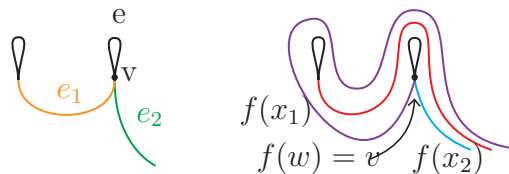


Figure 6.5: An example of a rigid switch. On the left is the switch, on the right the image of the map near the switch.

the same *gate*: that is, there exists an integer $k \geq 1$ such that $(Df)^k = D(f^k)$ is constant on $R(v)$.

Definition 6.2.1. Let $\tau \hookrightarrow D_n$ be standardly embedded, and let $f : \tau \rightarrow \tau$ be a train track map. Let v be a switch of τ such that $R(v)$ is not a singleton, and set $R(v) = \{e_1, \dots, e_k\}$. Let w be the switch of τ such that $f(w) = v$. We say that v is *rigid* if there exist $x_1, \dots, x_k \in R(w)$ such that

$$Df(x_i) = e_i \text{ for all } i.$$

Lemma 6.2.2. Let (τ, ψ, f) be the data of the pseudo-Anosov ψ on D_n carried by the standardly embedded τ . Let w be a switch of τ . Write $\alpha = r(w)$, $\beta = l(w)$, and $v = f(w)$. For any $c \in R(v)$ between $Df(\alpha)$ and $Df(\beta)$, there exists $\gamma \in R(w)$ such that $Df(\gamma) = c$. In other words, the set $Df(\text{Lk}(w)) \subseteq \text{Lk}(v)$ is connected.

Proof. Suppose $c \in R(v)$ is between $Df(\alpha)$ and $Df(\beta)$. Since ψ is pseudo-Anosov, f is surjective. Hence there exists a real edge γ such that $f(\gamma)$ collapses onto c . But since ψ is a homeomorphism, $\psi(\gamma)$ cannot intersect $\psi(\alpha \cup \beta)$, so γ must be incident to w . In other words, $c = Df(\gamma)$. \square

Definition 6.2.3. We say a switch v of τ is a *loop switch* if it is incident to an infinitesimal loop.

The next lemma says that switch rigidity is the only barrier to the existence of a t -split at a loop switch. Note that if v is a loops switch, then $v_l = v_r = v$.

Lemma 6.2.4. Let (τ, ψ, f) be the data of a pseudo-Anosov ψ on D_n carried by the standardly embedded τ . Let v be a loop switch, and suppose that $R(v)$ is not a singleton. Then exactly one of the following three possibilities is true.

1. The switch v splits tightly to the left.
2. The switch v splits tightly to the right.
3. The switch v is rigid.

Proof. Let w be the loop switch of τ such that $f(w) = v$. If either (1) or (2) holds then v cannot be rigid: for example, if v l -splits then there does not exist $x \in R(w)$ such that $Df(x) = l(v)$. On the other hand, if v is not rigid then Lemma 6.2.2 implies that at least one of $l(v), r(v)$ is not in the image $Df(\text{Lk}(w))$.

Assume without loss of generality that $l(v) \notin Df(\text{Lk}(w))$. Then any appearance of $l(v)$ in an image train path is in fact an appearance of $l(v) \cdot \bar{x}$, up to orientation. Here x is some edge in $R(v)$ that might vary. If x is always $r(v)$ then v l -splits. Otherwise, we claim that v r -splits.

Indeed, suppose that there exists a real edge $y \subseteq \tau$ such that $f(y)$ contains $l(v) \cdot \bar{x}$, up to orientation, for some real edge $x \neq r(v)$. Lemma 6.2.2 implies that $Df(\text{Lk}(w))$ is a subset of the real edges between $l(v)$ and x . In particular, $r(v) \notin Df(\text{Lk}(w))$. Let z be a real edge such that $f(z)$ contains $r(v)$, up to orientation. Since ψ is a homeomorphism and $f(z)$ is a train path, the appearance of $r(v)$ in $f(z)$ must be followed by $\overline{l(v)}$, due to the existence of $\psi(y)$. In other words, v r -splits.

Thus we have established that (1) or (2) holds if and only if (3) does not hold. It remains to show that (1) and (2) are mutually exclusive. Corollary 6.1.9 says that if v l -splits then $\mu(l(v)) < \mu(r(v))$. It follows that if (1) holds then (2) cannot. The proof is complete. \square

The same argument gives the following proposition for a switch not at a loop.

Proposition 6.2.5. Let (τ, ψ, f) be the data of a pseudo-Anosov ψ on D_n carried by the standardly embedded τ . Let v be a switch of τ , and suppose that $R(v)$ is not a singleton. Suppose additionally that $R(v_l)$ and $R(v_r)$ are singletons. Then at least one of the following three possibilities is true.

1. The switch v splits tightly to the left.
2. The switch v splits tightly to the right.
3. The switch v is rigid.

Moreover, case (3) is disjoint from cases (1) and (2).

Lemma 6.2.4 says that if we cannot split at a particular switch v , then it is rigid. The natural next step is to consider the preimage switch v_1 causing v to be rigid. If v_1 is also rigid, we look at its preimage v_2 . It might happen that we never find a splittable switch. In this case, the periodic orbit of v consists of a cycle of rigid switches.

Definition 6.2.6. A *rigid cycle* of length k is a collection of rigid switches $v_1, \dots, v_k \in \tau$ such that $f(v_j) = v_{j-1}$ for all j , where the indices are taken modulo k .

Proposition 6.2.7. Rigid cycles do not exist.

Proof. Let $v \in \tau$ be a switch. Since τ is standardly embedded, every element of $R(v)$ belongs to the same gate of v , hence there exists $k \geq 1$ such that $(Df)^k$ is constant on $R(v)$. In fact, for all $n \geq k$ we have that $(Df)^n$ is constant on $R(v)$. On the other hand, if v belonged to a rigid cycle of length n then $(Df)^n : R(v) \rightarrow R(v)$ would be the identity map, a contradiction. \square

Corollary 6.2.8. Let $v \in \tau$ be a switch such that $R(v)$ is not a singleton. Then some iterated preimage switch w of v is not rigid.

It is well-known that if (τ, ψ, f) is the data of a pseudo-Anosov, then f permutes the infinitesimal k -gons for each k (cf. [BH95]). We obtain the following corollary, which will be of central importance in the following section. The *real valence* of a switch v is the cardinality of $R(v)$.

Corollary 6.2.9. Let n_k denote the maximal real valence of a switch at an infinitesimal k -gon of τ , where $k \geq 1$. If $n_k > 1$ then there exists a switch of valence n_k at such a k -gon which is not rigid.

Proof. The infinitesimal k -gons are permuted by f . If every such maximal valence switch is rigid, then they must form a rigid cycle, since real valence cannot decrease when passing to the preimage of a rigid switch. This is impossible, since rigid cycles do not exist. \square

6.3 The proofs of Theorems 4.2.1, 1.2.6, and C

In this subsection, we will use the theory of t -splits developed in Section 6 to prove Theorems C, and see 4.2.1 as a consequence. Though Theorem D itself is more general than necessary to prove Theorem 4.2.1, we believe it has wider-reaching applications to surface dynamics.

Definition 6.3.1. Let $\tau \hookrightarrow D_n$ be a standardly embedded train track. We say a real edge e of τ is a *stem* if at least one end of e is incident to an infinitesimal k -gon, where $k \geq 2$.

Definition 6.3.2. Let $\tau \hookrightarrow D_n$ be a standardly embedded train track. We say a loop switch $v \in \tau$ is a *joint* if $|R(v)| \geq 2$.

Theorem C. Let ψ be a pseudo-Anosov on D_n with at least one k -pronged singularity away from the boundary with $k \geq 2$. Then ψ is carried by a train track τ with no joints.

The central argument in the proof of Theorem C hinges on finding a maximal-valence vertex v near a puncture, and then using Corollary 6.2.9 to tightly split at v . Before diving into the proof, we observe one crucial lemma. Although well-known to experts, the authors could not find a complete proof of Lemma 6.3.3 in the literature. For the sake of completeness, we have included a proof which arose from a helpful conversation with Karl Winsor.

Lemma 6.3.3. For any fixed n and $B > 0$, there is a finite number of Perron-Frobenius matrices of size n and spectral radius at most B . In particular, there is a finite number of Perron-Frobenius matrices of a given size with a particular Perron-Frobenius eigenvalue.

Proof. Fix $n \geq 2$, and let M be an $n \times n$ Perron-Frobenius matrix. Write $M_{i,j}$ for the (i, j) th entry of M , and $C_j(M)$ for the j th column of M . An exercise in matrix algebra shows that for each integer $k \geq 1$,

$$C_j(M^k) = \sum_{i=1}^n (M^{k-1})_{i,j} \cdot C_i(M).$$

It is well-known (cf. [Wie50]) that M^{n^2-2n+2} has all entries positive. Hence the smallest column sum of M^{n^2-2n+3} is at least the sum $\|M\|_1$ of all the entries of M . It is not hard to see that the smallest column sum of a Perron-Frobenius matrix is a lower bound on its spectral radius $\rho(M)$. We now have

$$\rho(M)^{n^2-2n+3} = \rho(M^{n^2-2n+3}) \geq \|M\|_1.$$

In particular, $\rho(M) \geq \|M\|_1^{\frac{1}{n^2-2n+3}}$. Since there are only finitely many integer-valued matrices M with $\|M\|_1$ below a given bound, the result follows. \square

Proof of Theorem C. Let $\tau_0 \hookrightarrow D_n$ be a standardly embedded train track carrying ψ . We will algorithmically produce a finite sequence of t -splits on τ_0 to produce the

desired track τ with no joints.

Let J denote the number of cusps at the loop switches of τ , i.e. $J = \sum_v (|R(v)| - 1)$, where v ranges over the loop switches of τ . If $J = 0$ then there is nothing to prove, so assume $J \geq 1$. By Corollary 6.2.9 there exists a loop switch of τ_0 of maximal valence that can be t -split. Therefore, we introduce the following simple algorithm.

1. Initialize $\tau = \tau_0$ and $\mathcal{M} = \{M_0\}$, where M_0 is the transition matrix associated to the data (τ_0, ψ, f_0) .
2. Find a loop switch of τ of maximal valence that is not rigid, and split it, obtaining the data (τ_1, ψ, f_1) with transition matrix M_1 . Set $\tau = \tau_1$.
3. If J has decreased by 1, terminate.
4. If J has not decreased, add M_1 to \mathcal{M} and repeat Steps 2 and 3.

We claim that this algorithm terminates in finitely many steps, and returns a train track τ with one fewer joint than τ_0 . Indeed, by Lemma 6.3.3 there are only finitely many possible transition matrices that can appear, hence we will eventually produce a matrix $M_j = M_i \in \mathcal{M}$. Since this matrix is Perron-Frobenius, the dilatation λ of ψ is an eigenvalue with strictly positive eigenvectors μ_i and μ_j . Moreover, λ is simple, so in fact μ_j is a scalar multiple of μ_i . According to Corollary 6.1.9, each t -split reduces one of the entries of this eigenvector, so recurring to a matrix in \mathcal{M} implies that every entry of μ has been reduced, i.e. that every real edge of τ_0 has been split over. In particular, the stems of τ_0 have been split over. Such a split necessarily decreases the joint number J , causing the algorithm to terminate.

Repeating this algorithm sufficiently many times will eventually reduce J to 0, proving the theorem. □

proof of Theorem 4.2.1. Note that in the stratum $(2; 1^5; 3)$, there are only two classes of standardly-embedded train tracks without joints: those shown in Figure 4.4. By

Theorem C, any pseudo-Anosov in this stratum is conjugate to one carried by either the Peacock or the Snail. We will argue that any pseudo-Anosov ψ carried by the Snail tightly splits to one carried by the Peacock.

First, observe that ψ must split at the unique valence-3 switch of the infinitesimal triangle in the Snail, by Corollary 6.2.9. Either a left or right split at this vertex yields a pseudo-Anosov ψ' conjugate to ψ , and carried by a track τ' with a unique two-valent vertex v at a puncture. This vertex v is again splittable by Corollary 6.2.9. At v , note that ψ' splits either to another map carried by τ' , with strictly smaller edge weight on the edge running between two punctures, or to a map carried by the Peacock. In particular, after sufficiently many splits, ψ' splits to a pseudo-Anosov carried by the Peacock. \square

proof of Theorem 1.2.6. Note that if $\psi : S \rightarrow S$ has the given singularity type, we may cap-off ψ to a pseudo-Anosov $\widehat{\psi}$ on the closed genus-two surface \widehat{S} and extend the foliations preserved by ψ along the capping disk. In this case, the 4-prong singularity p in the capping disk is the unique 4-prong singularity of $\widehat{\psi}$. In particular, $\widehat{\psi}$ commutes with the hyperelliptic involution ι on \widehat{S} and p is fixed by ι , as in e.g. Lemma 3.7 of [BHS21]. And, because p is fixed by ι , we see that ψ commutes with the hyperelliptic involution on S , as well. We may then quotient ψ to a pseudo-Anosov 5-braid β . Theorem 4.2.1 implies that β is carried by the Peacock track depicted in Figure 4.4, and we can then lift this track to S as described in section 2.3. \square

Bibliography

- [BBG19a] Michel Boileau, Steven Boyer, and Cameron McA. Gordon. Branched covers of quasi-positive links and l-spaces. *Journal of Topology*, 12(2):536–576, 2019. [6](#)
- [BBG19b] Michel Boileau, Steven Boyer, and Cameron McA. Gordon. On definite strongly quasipositive links and l-space branched covers. *Advances in Mathematics*, 357:106828, 2019. [6](#)
- [BDL⁺21] John A. Baldwin, Nathan Dowlin, Adam Simon Levine, Tye Lidman, and Radmila Sazdanovic. Khovanov homology detects the figure-eight knot. *Bulletin of the London Mathematical Society*, 53(3):871–876, 2021. [8](#)
- [BH95] M. Bestvina and M. Handel. Train-tracks for surface homeomorphisms. *Topology*, 34(1):109–140, 1995. [2](#), [22](#), [23](#), [24](#), [90](#)
- [BHS21] John A. Baldwin, Ying Hu, and Steven Sivek. Khovanov homology and the cinquefoil, 2021. [2](#), [3](#), [8](#), [28](#), [93](#)
- [BLSY21] John A. Baldwin, Zhenkun Li, Steven Sivek, and Fan Ye. Small dehn surgery and $su(2)$, 2021. [7](#)
- [BM20] Fraser Binns and Gage Martin. Knot floer homology, link floer homology and link detection, 2020. [8](#)

- [Bri00] Peter Brinkmann. An implementation of the Bestvina-Handel algorithm for surface homeomorphisms. *Experimental Mathematics*, 9(2):235 – 240, 2000. [61](#)
- [BS21] John A. Baldwin and Steven Sivek. Instantons and l-space surgeries, 2021. [7](#)
- [BS22] John A. Baldwin and Steven Sivek. Characterizing slopes for 5_2 , 2022. [1](#)
- [Cau23] Jacob Caudell. On lens space surgeries from the poincaré homology sphere, 2023. [1](#)
- [CC09] Andrew Cotton-Clay. Symplectic floer homology of area-preserving surface diffeomorphisms. *Geometry & Topology*, 13(5):2619–2674, 2009. [24](#), [45](#)
- [CH08] Jin-Hwan Cho and Ji-Young Ham. The minimal dilatation of a genus-two surface. *Experimental Mathematics*, 17(3):257 – 267, 2008. [26](#)
- [FLP12] Albert Fathi, François Laudenbach, and Valentin Poénaru. *Thurston’s Work on Surfaces (MN-48)*. Princeton University Press, Princeton, 2012. [9](#)
- [FRW22] Ethan Farber, Braeden Reinoso, and Luya Wang. Fixed point-free pseudo-anosovs and the cinquefoil, 2022. [2](#)
- [Ghi08] Paolo Ghiggini. Knot floer homology detects genus-one fibred knots. *American Journal of Mathematics*, 130(5):1151–1169, 2008. [2](#)
- [Gre13] Joshua Evan Greene. The lens space realization problem. *Annals of Mathematics*, 177(2):449–511, 2013. [1](#)
- [GS22] Paolo Ghiggini and Gilberto Spano. Knot floer homology of fibred knots and floer homology of surface diffeomorphisms, 2022. [2](#), [3](#)

- [Han23] Jonathan Hanselman. Heegaard floer homology and cosmetic surgeries in s^3 . *J. Eur. Math. Soc.*, 25:1627–1670, 2023. [1](#)
- [Hed10] Matthew Hedden. Notions of positivity and the ozsváth–szabó concordance invariant. *Journal of Knot Theory and Its Ramifications*, 19(05):617–629, 2010. [2](#), [3](#)
- [HKM07] Ko Honda, William H Kazez, and Gordana Matić. Right-veering diffeomorphisms of compact surfaces with boundary. *Invent. Math.*, 169:427–449, 2007. [18](#)
- [HM18] Matthew Hedden and Thomas E. Mark. Floer homology and fractional dehn twists. *Advances in Mathematics*, 324:1–39, 2018. [9](#), [36](#), [45](#), [62](#)
- [HS07] Ji-Young Ham and Won Taek Song. The minimum dilatation of pseudo-anosov 5-braids. *Experimental Mathematics*, 16(2):167 – 180, 2007. [2](#), [10](#), [12](#), [26](#), [36](#), [59](#), [74](#), [75](#)
- [IK17] Tetsuya Ito and Keiko Kawamuro. Essential open book foliations and fractional dehn twist coefficient. *Geometriae Dedicata*, 187:17–67, 2017. [18](#)
- [IT20] Ahmad Issa and Hannah Turner. Links all of whose cyclic branched covers are l-spaces, 2020. [6](#)
- [KLS02] Ki Hyoung Ko, Jérôme E. Los, and Won Taek Song. Entropies of braids. *Journal of Knot Theory and Its Ramifications*, 11(04):647–666, 2002. [2](#), [12](#), [26](#), [85](#)
- [KM] Peter Kronheimer and Tomasz Mrowka. Dehn surgery, the fundamental group and $su(2)$. [7](#)

- [KM10] Peter Kronheimer and Tomasz Mrowka. Knots, sutures, and excision. *Journal of Differential Geometry*, 84(2):301–364, 2010. [7](#)
- [Los10] Jérôme Los. Infinite sequence of fixed-point free pseudo-anosov homeomorphisms. *Ergodic Theory and Dynamical Systems*, 30(6):1739—1755, 2010. [24](#), [45](#)
- [LT11] Erwan Lanneau and Jean-Luc Thiffeault. On the minimum dilatation of pseudo-Anosov homeomorphisms on surfaces of small genus. *Annales de l'Institut Fourier*, 61(1):105–144, 2011. [10](#), [33](#), [34](#), [35](#)
- [MS93] Howard A. Masur and Jonathan Smillie. Quadratic differentials with prescribed singularities and pseudo-anosov diffeomorphisms. *Commentarii Mathematici Helvetici*, 68:289–307, 1993. [10](#), [33](#)
- [Ni07] Yi Ni. Knot floer homology detects fibered knots. *Inventiones mathematicae*, 170(3):577–608, 2007. [2](#), [19](#)
- [Ni20] Yi Ni. Exceptional surgeries on hyperbolic fibered knots, 2020. [4](#)
- [Ni22] Yi Ni. Knot floer homology and fixed points, 2022. [2](#), [3](#), [19](#)
- [NW15] Yi Ni and Zhongtao Wu. Cosmetic surgeries on knots in S^3 . *Journal für die reine und angewandte Mathematik (Crelles Journal)*, 2015(706):1–17, 2015. [1](#)
- [OS04a] Peter Ozsváth and Zoltán Szabó. Holomorphic disks and genus bounds. *Geom. Topol.*, 8:311–334, 2004. [1](#), [2](#)
- [OS04b] Peter Ozsváth and Zoltán Szabó. Holomorphic disks and knot invariants. *Advances in Mathematics*, 186(1):58–116, 2004. [19](#)

- [OS04c] Peter Ozsváth and Zoltán Szabó. Holomorphic disks and three-manifold invariants: Properties and applications. *Annals of Mathematics*, 159(3):1159–1245, 2004. [1](#)
- [OS04d] Peter Ozsváth and Zoltán Szabó. Holomorphic disks and topological invariants for closed three-manifolds. *Annals of Mathematics*, 159(3):1027–1158, 2004. [1](#), [19](#)
- [Pet09] Thomas Peters. On l-spaces and non left-orderable 3-manifold groups, 2009. [6](#)
- [PH22] R. C. Penner and J. L. Harer. *Combinatorics of Train Tracks. (AM-125)*. Princeton University Press, 1922. [2](#)
- [Rei23] Braeden Reinoso. Fixed-point-free pseudo-anosovs, and genus-two l-space knots in the poincare sphere, 2023. [2](#)
- [Ryk99] E. Rykken. Expanding factors for pseudo-Anosov homeomorphisms. *Michigan Math. J.*, 46(2):281–296, 1999. [37](#)
- [Tan11] Motoo Tange. On the non-existence of l-space surgery structure. *Osaka J. Math*, 48:541–547, 2011. [2](#), [3](#), [19](#)
- [Thu88] William P. Thurston. On the geometry and dynamics of diffeomorphisms of surfaces. *Bulletin (New Series) of the American Mathematical Society*, 19(2):417–431, 1988. [2](#), [16](#)
- [Thu98] William P. Thurston. Hyperbolic structures on 3-manifolds, ii: Surface groups and 3-manifolds which fiber over the circle, 1998. [17](#)
- [Wie50] Helmut Wielandt. Unzerlegbare, nicht negative Matrizen. *Math. Z.*, 52:642–648, 1950. [91](#)